NASA TECHNICAL NOTE

NASA TN D-6597

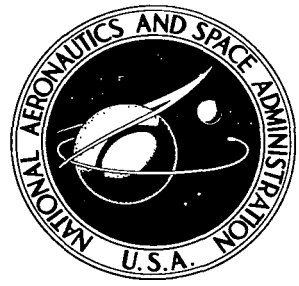

STATIC LONGITUDINAL AERODYNAMIC CHARACTERISTICS OF CLOSE-COUPLED WING-CANARD CONFIGURATIONS AT MACH NUMBERS FROM 1.60 TO 2.86

by Samuel M. Dollyhigh

Langley Research Center
Hampton, Va. 23365

NATIONAL AERONAUTICS AND SPACE ADMINISTRATION • WASHINGTON, D. C. • DECEMBER 1971

1. Report No. NASA TN D-6597	2. Government Accession No.	3. Recipient's Catalog No.
4. Title and Subtitle STATIC LONGITUDINAL AERODYNAMIC CHARACTERISTICS OF CLOSE-COUPLED WING-CANARD CONFIGURATIONS AT MACH NUMBERS FROM 1.60 TO 2.86		5. Report Date December 1971 6. Performing Organization Code
7. Author(s) Samuel M. Dollyhigh		8. Performing Organization Report No. L-7962
9. Performing Organization Name and Address NASA Langley Research Center Hampton, Va. 23365		10. Work Unit No. 760-74-01-04 11. Contract or Grant No.
12. Sponsoring Agency Name and Address National Aeronautics and Space Administration Washington, D.C. 20546		13. Type of Report and Period Covered Technical Note 14. Sponsoring Agency Code
15. Supplementary Notes		

16. Abstract An experimental investigation has been made in the Mach number range from 1.60 to 2.86 to determine the static longitudinal aerodynamic characteristics of close-coupled wing-canard configurations. Three canards, ranging in exposed planform area from 17.5 to 30.0 percent of the wing reference area, were employed in this investigation. The canards were either located in the plane of the wing or in a position 18.5 percent of the wing mean geometric chord above the wing plane. Most data obtained were for a model with a 60^{o} leading-edge-sweep wing; however, a small amount of data were obtained for a 44^{o} leading-edge-sweep wing. The model utilized two balances to isolate interference effects between wing and canard.

In general, it was determined that at angle of attack for all configurations investigated with the canard in the plane of the wing an unfavorable interference exists which causes the additional lift on the canard generated by a canard deflection to be lost on the wing due to an increased downwash at the wing from the canard. Further, this interference decreased somewhat with increasing Mach number. Raising the canard above the plane of the wing also greatly decreased the interference of the canard deflection on the wing lift. However, at Mach 2.86 the presence of the canard in the high position had a greater unfavorable interference effect at high angles of attack than the canard in the wing plane. This interference resulted in the in-plane canard having better trimmed performance at Mach 2.86 for the same center-of-gravity location. The trends shown for the trim drag polars do not account for any differences in subsonic stability level that may exist for the different canard configurations. Pitching effectiveness was not significantly affected by canard height throughout the Mach range.

17. Key Words (Suggested by Author(s)) Canard configurations Aerodynamic characteristics Supersonic experimental data	18. Distribution Statement Unclassified – Unlimited		
19. Security Classif. (of this report) Unclassified	20. Security Classif. (of this page) Unclassified	21. No. of Pages 115	22. Price* $3.00

*For sale by the National Technical Information Service, Springfield, Virginia 22151

STATIC LONGITUDINAL AERODYNAMIC CHARACTERISTICS OF CLOSE-COUPLED WING-CANARD CONFIGURATIONS AT MACH NUMBERS FROM 1.60 TO 2.86

By Samuel M. Dollyhigh
Langley Research Center

SUMMARY

An experimental investigation has been made in the Mach number range from 1.60 to 2.86 to determine the static longitudinal aerodynamic characteristics of close-coupled wing-canard configurations. Three canards, ranging in exposed planform area from 17.5 to 30.0 percent of the wing reference area, were employed in this investigation. The canards were either located in the plane of the wing or in a position 18.5 percent of the wing mean geometric chord above the wing plane. Most data obtained were for a model with a 60° leading-edge-sweep wing; however, a small amount of data were obtained for a 44° leading-edge-sweep wing. The model utilized two balances to isolate interference effects between wing and canard.

In general, it was determined that at angle of attack for all configurations investigated with the canard in the plane of the wing an unfavorable interference exists which causes the additional lift on the canard generated by a canard deflection to be lost on the wing due to an increased downwash at the wing from the canard. Further, this interference decreased somewhat with increasing Mach number. Raising the canard above the plane of the wing also greatly decreased the interference of the canard deflection on the wing lift. However, at Mach 2.86 the presence of the canard in the high position had a greater unfavorable interference effect at high angles of attack than the canard in the wing plane. This interference resulted in the in-plane canard having better trimmed performance at Mach 2.86 for the same center-of-gravity location. The trends shown for the trim drag polars do not account for any differences in subsonic stability level that may exist for the different canard configurations. Pitching effectiveness was not significantly affected by canard height throughout the Mach range.

INTRODUCTION

A continuing study (refs. 1 to 4) is being directed by the National Aeronautics and Space Administration in the area of advanced air-superiority fighter aircraft. As a part

of this program, a general research model has been constructed with which to provide basic data on the static longitudinal aerodynamic characteristics for these highly maneuverable fighters as well as to make available experimental data for use in evaluating theoretical methods. This model has been tested subsonically in both aft-tail and canard-wing configurations, with the trim drag results being reported in reference 5. The present paper provides the necessary data to extend the analysis of reference 5 for some of the canard-wing configurations to supersonic speeds.

SYMBOLS

The longitudinal results are referred to the wind-axis system. The moment reference point was located at fuselage station 59.144 cm (23.285 inches) for the 60° leading-edge-sweep wing and at fuselage station 57.165 cm (22.506 inches) for the 44° leading-edge-sweep wing.

The units used for the physical quantities of this paper are given both in the International System of Units (SI) and in the U.S. Customary Units. Measurements and calculations were made in U.S. Customary Units.

A aspect ratio

b wing span

$\bar{c}$ wing mean geometric chord

C_D drag coefficient, $\frac{\text{Drag}}{qS_w}$

C_L lift coefficient, $\frac{\text{Lift}}{qS_w}$

C_m pitching-moment coefficient, $\frac{\text{Pitching moment}}{qS_w\bar{c}}$

$\partial C_m/\partial C_L$ longitudinal stability parameter at $C_L = 0$

$\partial C_m/\partial \delta_c$ pitching effectiveness of canard at $C_L = 0$

L/D lift-drag ratio

M free-stream Mach number

q free-stream dynamic pressure

S_c reference area of canard (exposed)

S_w reference area of wing with leading and trailing edges extended to plane of symmetry

z vertical direction (positive up)

α angle of attack, deg

δ_c canard deflection angle, positive when trailing edge down, deg

Λ leading-edge sweep angle, deg

DESCRIPTION OF MODEL

A three-view drawing of the general research model is shown in figure 1 and some of the pertinent geometric characteristics are given in table I. A photograph of one of the configurations investigated is presented in figure 2. The wing and canard were closely coupled in all test configurations.

Two different untwisted wings were used on this model; however, they both had the same area, mean geometric chord, uncambered circular-arc airfoil sections, and maximum thickness (varying linearly from 6 percent of the chord at the root to 4 percent at the tip). The main difference, as seen in figure 1, was that the wing-leading-edge sweep angle was 60^o for one configuration and 44^o for the other (hereinafter, called the 60^o wing and the 44^o wing, respectively).

Three canards were used which had a leading-edge sweep angle of 52^o and an exposed area of 17.5, 24.0, and 30.0 percent of the wing reference area. The canards were tested both in the plane of the wing (planar position) and in a position 18.5 percent of the wing geometric chord above the wing plane (high position). The canards were deflected by pivoting about the canard half-root-chord.

The canards were also untwisted and had uncambered circular-arc airfoil sections that had a maximum thickness varying linearly from 6 percent of the chord at the root to 4 percent at the tip. The configuration had no vertical stabilizing surfaces.

TESTS AND CORRECTIONS

The tests were conducted in the Langley Unitary Plan wind tunnel at Mach numbers 1.60, 2.00, 2.36, and 2.86. The Reynolds number per meter (per foot) was 9.8×10^6 (3.0×10^6) for all data points except those at higher angles of attack at Mach numbers

1.60, 2.00, and 2.36 where the Reynolds number per meter (per foot) was reduced to 8.2×10^6 (2.5×10^6) and 6.6×10^6 (2.0×10^6) in order to stay within balance load limits. The dewpoint was maintained sufficiently low to prevent measurable condensation effects in the test section. The angle-of-attack range was from approximately -4^o to 24^o. In order to assure boundary-layer transition to turbulent conditions, 0.16-cm-wide (1/16-inch) transition strips of No. 50 carborundum grit (shown to be adequate in ref. 6) were placed on the body 3.05 cm (1.20 inches) aft of the nose of the model and 1.02 cm (0.40 inch) streamwise on the wings and canards.

Aerodynamic forces and moments were measured by means of two six-component strain-gage balances. One balance was housed within the forward segment of the fuselage and was rigidly attached to the rearward segment of the fuselage. This balance (called canard balance herein) measured the combined forces and moments of the canard and forward segment of the fuselage, as indicated by the shaded area in figure 1. There was a small unsealed gap between the fuselage segments to insure that they did not foul.

The second balance, housed in the rearward segment of the fuselage, was attached to a sting which in turn was rigidly fastened to the tunnel support system. This balance (called main balance herein) measured the total forces and moments on the model. Only the total load balance was used with the 44^o wing, and data were taken only at Mach 1.60 and 2.00.

Balance-chamber static pressures were measured with pressure tubes located in the vicinity of the main balance. The drag data presented herein have been corrected to the condition of free-stream static pressure in the main balance chamber. The base of the model was feathered so that no base pressure corrections were necessary. Corrections to the indicated model angles of attack have been made for both tunnel-airflow misalinement and deflection of the balance and sting under load.

PRESENTATION OF RESULTS

Most of the experimental data presented herein (figs. 3 to 14) were obtained for the 60^o wing. Unless otherwise noted by a reference to the 44^o wing (figs. 15 and 16), all results are for the 60^o wing and the word "wing" in the discussion refers to the 60^o wing.

The general format for figures 4 to 10 is to present the lift and pitching moment measured with the canard balance and the total lift and pitching moment measured with the main balance side-by-side. These plots are presented in the form of force and moment coefficients as a function of angle of attack. The variations of drag coefficient and lift-drag ratio for the total configuration as a function of lift coefficient are also presented. An exception to this format is for the configuration with the smallest canard

($S_c/S_w = 0.175$) in the high position (fig. 8) for which data on only the main balance were available; for this particular configuration, data were available at only Mach 1.60 and 2.00.

An outline of the data figure contents is as follows:

DISCUSSION

A summary of the longitudinal stability parameter and pitching effectiveness of the canards is presented in figure 3 over the Mach range for $z/\bar{c} = 0$ (from figs. 4 to 6) and $z/\bar{c} = 0.185$ (from figs. 8 to 10). These results show that increasing the canard area decreases the static margin of the configuration and increases the pitching effectiveness of the canard, as expected; increasing the canard height produces an increase in the static

margin but has little effect on the pitching effectiveness. The reasons for this phenomenon are found by looking at the data in detail.

Figures 4 to 6 show that for canards in the plane of the wing at angle of attack an unfavorable interference exists which causes the additional lift on the canard generated by a canard deflection to be lost on the wing due to an increased downwash at the wing from the canard. Furthermore, this interference between canard and wing seems to decrease somewhat as Mach number increases. Figure 7 shows the effects of adding planar canards to the body alone. This figure shows the additional lift and drag associated with the increasing canard size in the absence of any interference on a wing. This figure also documents that the canard loading is, in fact, measured by the main balance and that the interaction between canard and wing lift are as discussed.

The longitudinal aerodynamic characteristics of the canards in the high position are presented in figures 8 to 10. The most obvious change over the data for the planar canards is that now the additional lift on the canard associated with canard deflection is not offset by a comparable loss in wing lift. Also an increase in stability occurs when the canard is raised above the wing. This increase in stability results because the wing loading behind the pitch center is not appreciably altered by the interference of the canard wing.

Curves showing the effects of canard size and canard vertical position on the trimmed drag and trimmed L/D at Mach 1.60 and 2.86 are presented in figures 11 and 12, respectively. In general, at M = 1.60 (fig. 11), increasing canard size (destabilizing effect) improves trimmed drag polar shape and raises trimmed L/D. Raising the canard to the high position further improved trimmed drag polar shape and trimmed L/D due to less interference by the canard on wing loading. At Mach 2.86, the situation is changed somewhat, as shown in figure 12. Increasing the canard size has the same effects, but raising the canard vertical location results in a less desirable trimmed drag polar and lower trimmed L/D. The small canard was not tested in the high position at Mach 2.86.

Trends found in the trimmed data are explained by an examination of the significant points of the two balance measurements. Figures 13 and 14 present the effect of canard size on lift and pitching moment for the canard in the plane of the wing and then they present the effect of canard height for the two larger canards. At Mach 1.60 (fig. 13), it is seen that the canards carry the same lift in both planar and high positions, but the total lift is greater for the high position. Also, since the wing has greater lift for the canard in the high position, the static stability is greater than the planar canard. However, at Mach 2.86 (fig. 14), even though the canards carry the same lift, there tends to be more total lift at the high angle of attack for the planar canard. Further, this results in less stability for the planar canards. As stated earlier, canard height has no effect on pitching effectiveness of the canard at Mach 2.86. Hence, the improved performance which is

shown in figure 12 for the in-plane canard comes partly from increased lift and partly from the smaller canard deflection required to balance the model at $M = 2.86$.

The 44° wing configurations were tested at Mach 1.60 and 2.00 with only the main balance installed in the rearward segment of the fuselage, and the results are presented in figures 15 and 16. These configurations were tested with the smallest canard ($S_c/S_w = 0.175$) in both the planar and high positions. The center of gravity was moved forward with respect of the 60° wing so that both configurations would have the same stability level at Mach 0.70 (see discussion of tests in ref. 5), and this forward movement resulted in a more stable configuration. The effect of moving the canard to the high position was similar to that determined for the 60° wing. The Mach range was too narrow to determine Mach number effects.

CONCLUDING REMARKS

An experimental investigation has been made in the Mach number range from 1.60 to 2.86 to determine the static longitudinal aerodynamic characteristics of close-coupled wing-canard configurations. Three canards, ranging in exposed planform area from 17.5 to 30.0 percent of the wing reference area, were employed in this investigation. The canards were either located in the plane of the wing or in a position 18.5 percent of the wing mean geometric chord above the wing plane. Most data obtained were for a model with a 60° leading-edge-sweep wing; however, a small amount of data were obtained on a 44° leading-edge-sweep wing. The model utilized two balances to isolate interference effects between wing and canard.

In general, it was determined that at angle of attack for all configurations investigated with the canard in the plane of the wing an unfavorable interference exists which causes the additional lift on the canard generated by a canard deflection to be lost on the wing due to an increased downwash at the wing from the canard. Further, this interference decreased somewhat with increasing Mach number. Raising the canard above the plane of the wing also greatly decreased the interference of the canard deflection on the wing lift. However, at Mach 2.86 the presence of the canard in the high position had a greater unfavorable interference effect at high angles of attack than the canard in the wing plane. This interference resulted in the in-plane canard having better trimmed performance at Mach 2.86 for the same center-of-gravity location. The trends shown for the trim drag polars do not account for any differences in subsonic stability level that may exist for the different canard configurations. Pitching effectiveness was not significantly affected by canard height throughout the Mach range.

Langley Research Center,
National Aeronautics and Space Administration,
Hampton, Va., November 22, 1971.

REFERENCES

1. Taylor, Robert T.: Recent Aerodynamic Studies Applicable to High Performance Maneuvering Aircraft. NASA TM X-1272, 1966.

2. Lamb, Milton; and Finch, Virginia M.: Theoretical and Experimental Longitudinal Aerodynamic Characteristics at Mach 1.60 to 4.63 of a Variable-Sweep Fighter Model With Wing Sweeps of 44° and 71°. NASA TM X-2211, 1971.

3. Trescot, Charles D., Jr.: Stability and Control Characteristics at Mach Numbers From 0.60 to 2.86 of a Lightweight Variable-Sweep-Wing Fighter Model. NASA TM X-2007, 1970.

4. Dollyhigh, Samuel M.: Stability and Control Characteristics at Mach Numbers 1.60 to 2.86 of a Variable-Sweep Fighter Configuration With Supercritical Airfoil Sections. NASA TM X-2284, 1971.

5. McKinney, Linwood W.; and Dollyhigh, Samuel M.: Some Trim Drag Considerations for Maneuvering Aircraft. J. Aircraft, vol. 8, no. 8, Aug. 1971, pp. 623-629.

6. Braslow, Albert L.; Hicks, Raymond M.; and Harris, Roy V., Jr.: Use of Grit-Type Boundary-Layer-Transition Trips on Wind-Tunnel Models. NASA TN D-3579, 1966.

TABLE I.- GEOMETRIC CHARACTERISTICS

Wing (both):	
A	2.5
b/2, cm (in.)	50.8 (20.0)
Λ, deg, high-sweep wing	60
Λ, deg, low-sweep wing	44
$\bar{c}$, cm (in.)	23.307 (9.176)
Airfoil section	Circular arc
S_w, sq cm (sq in.)	1032.236 (159.997)
Maximum thickness, percent –	
Root	6
Tip	4
Canards:	
S_c, sq cm (sq in.) (exposed) –	
17.5 percent canard	180.645 (28.0)
24.0 percent canard	247.741 (38.4)
30.0 percent canard	309.677 (48.0)
Semispan, cm (in.) –	
17.5 percent canard	20.320 (8.0)
24.0 percent canard	23.876 (9.4)
30.0 percent canard	26.924 (10.6)
Λ, deg	52
Airfoil section	Circular arc
Maximum thickness, percent –	
Root	6
Tip	4

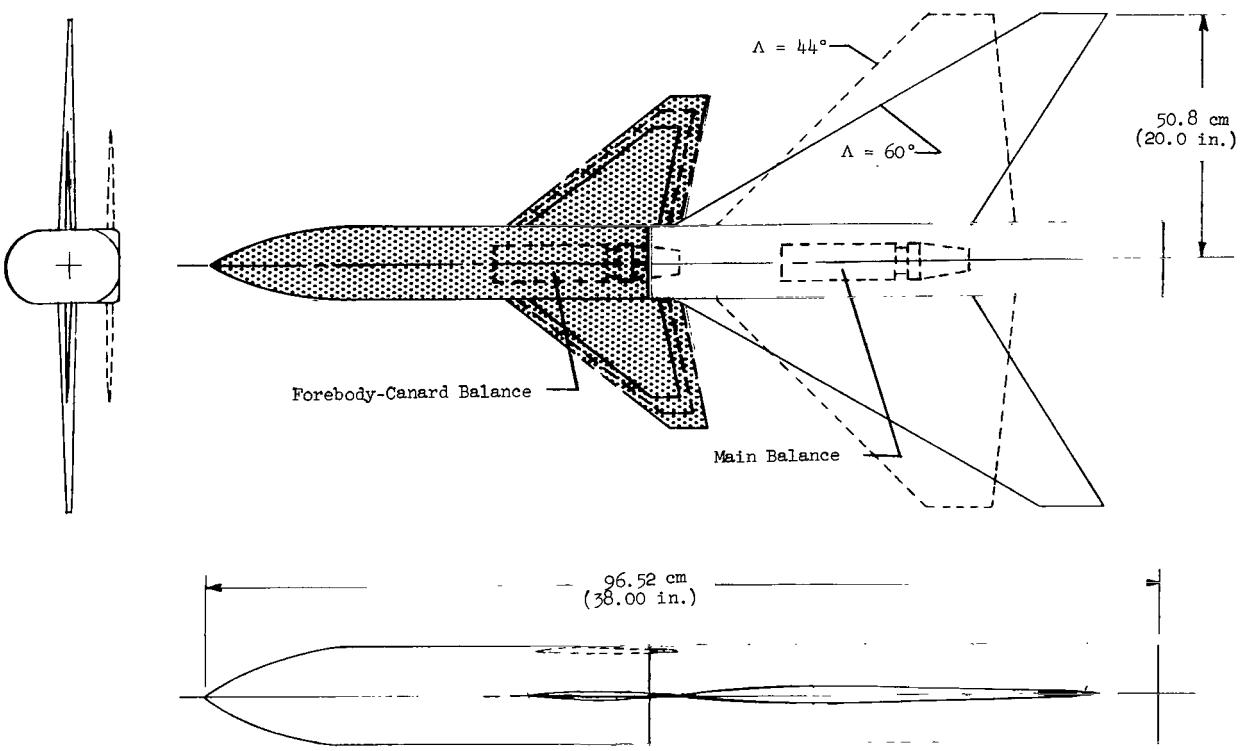

Figure 1.- Three-view drawing of model.

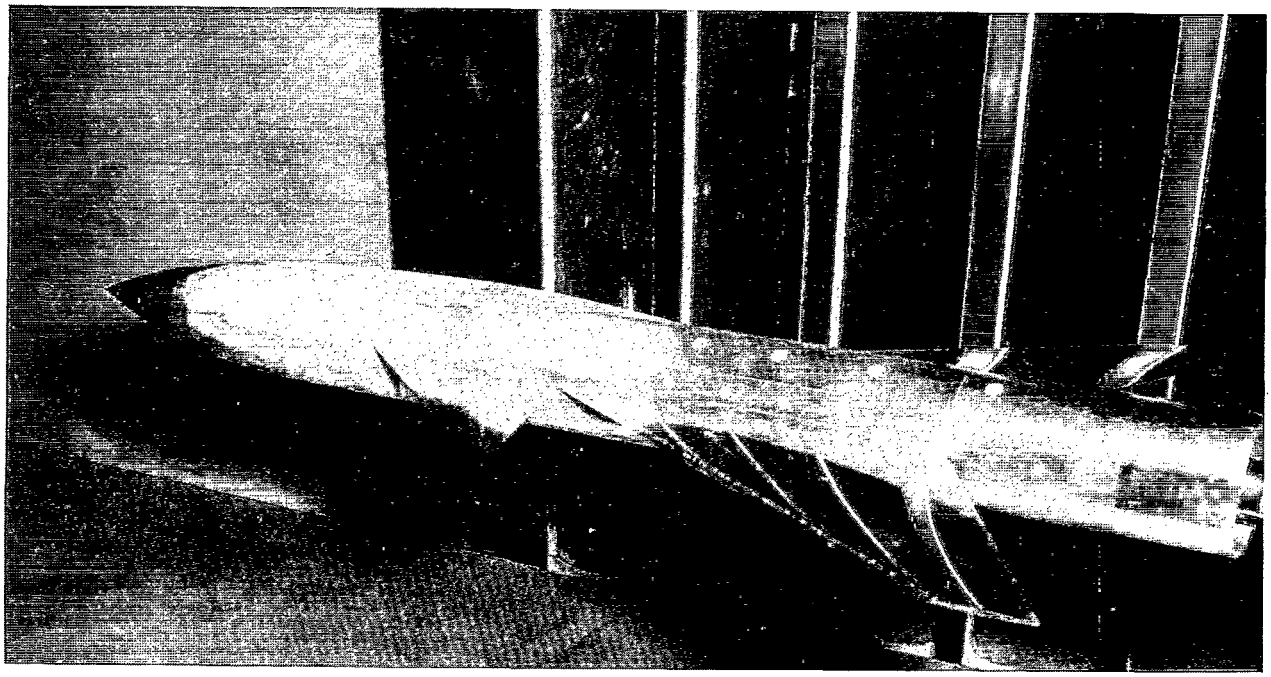

L-71-1404

Figure 2.- Photograph of one of the test configurations.

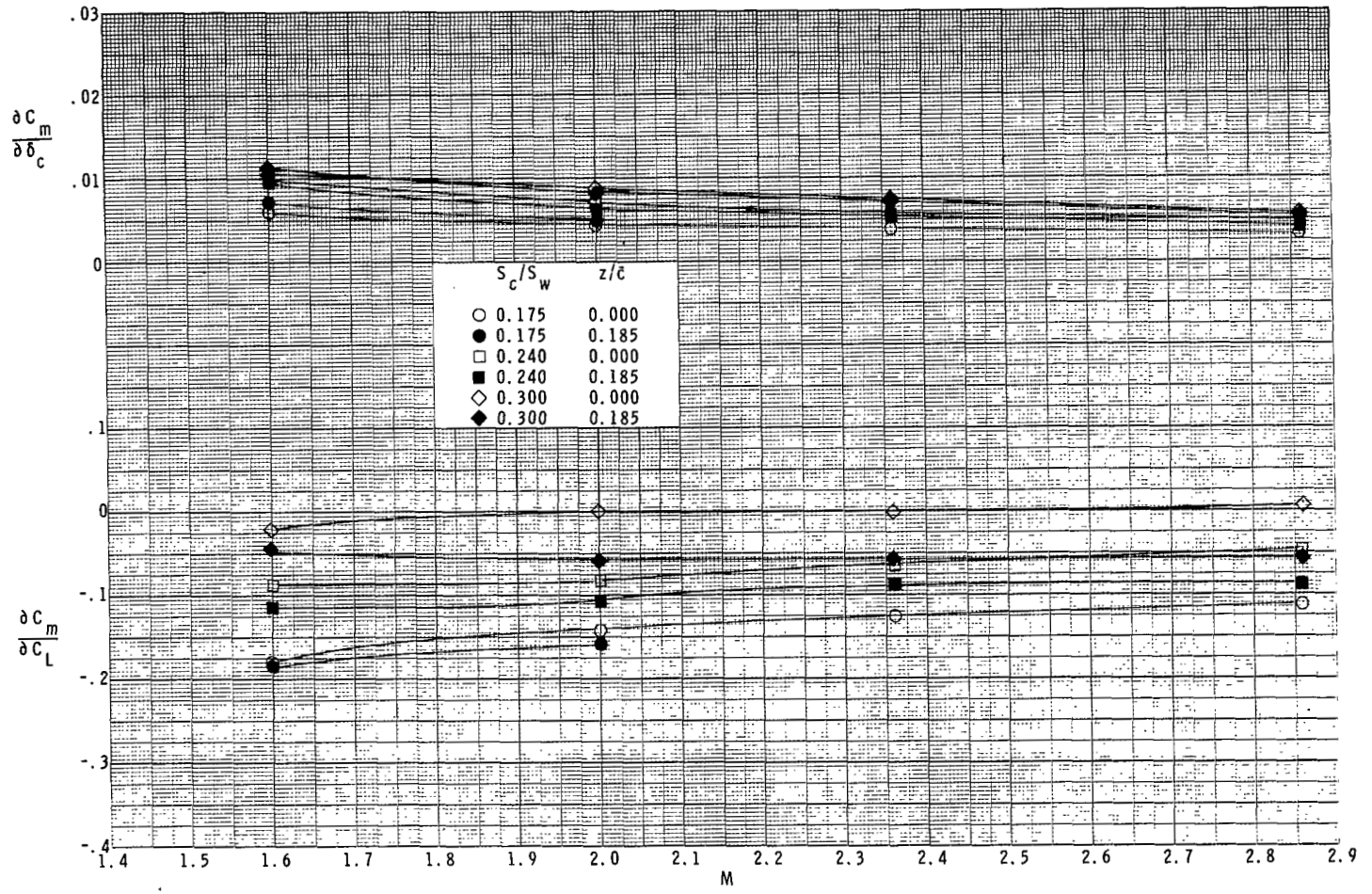

Figure 3.- Summary of pitching effectiveness of canards and longitudinal stability parameter.

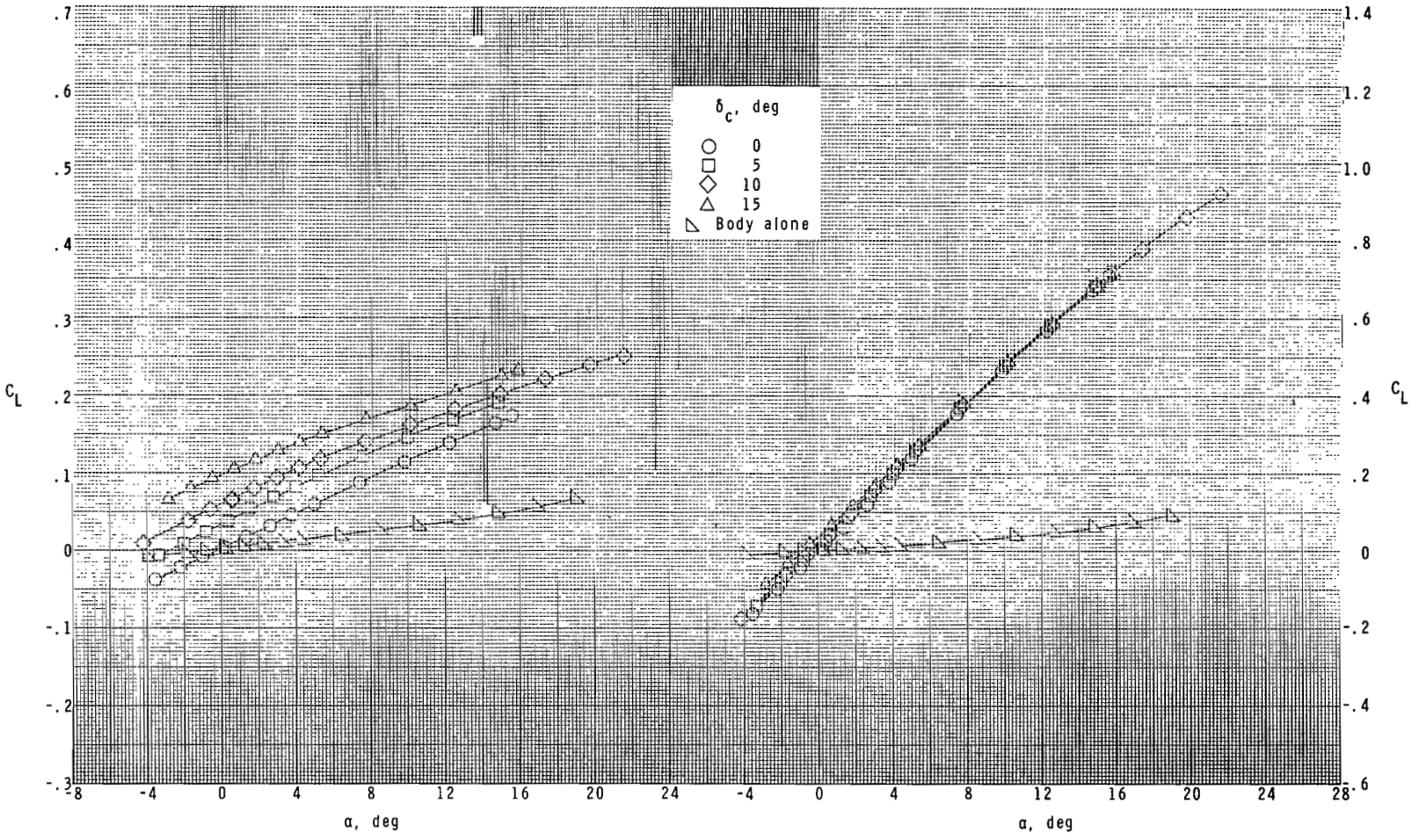

(a) M = 1.60.

Figure 4.- Longitudinal aerodynamic characteristics for $S_c/S_w = 0.175$ and $z/\bar{c} = 0.0$.

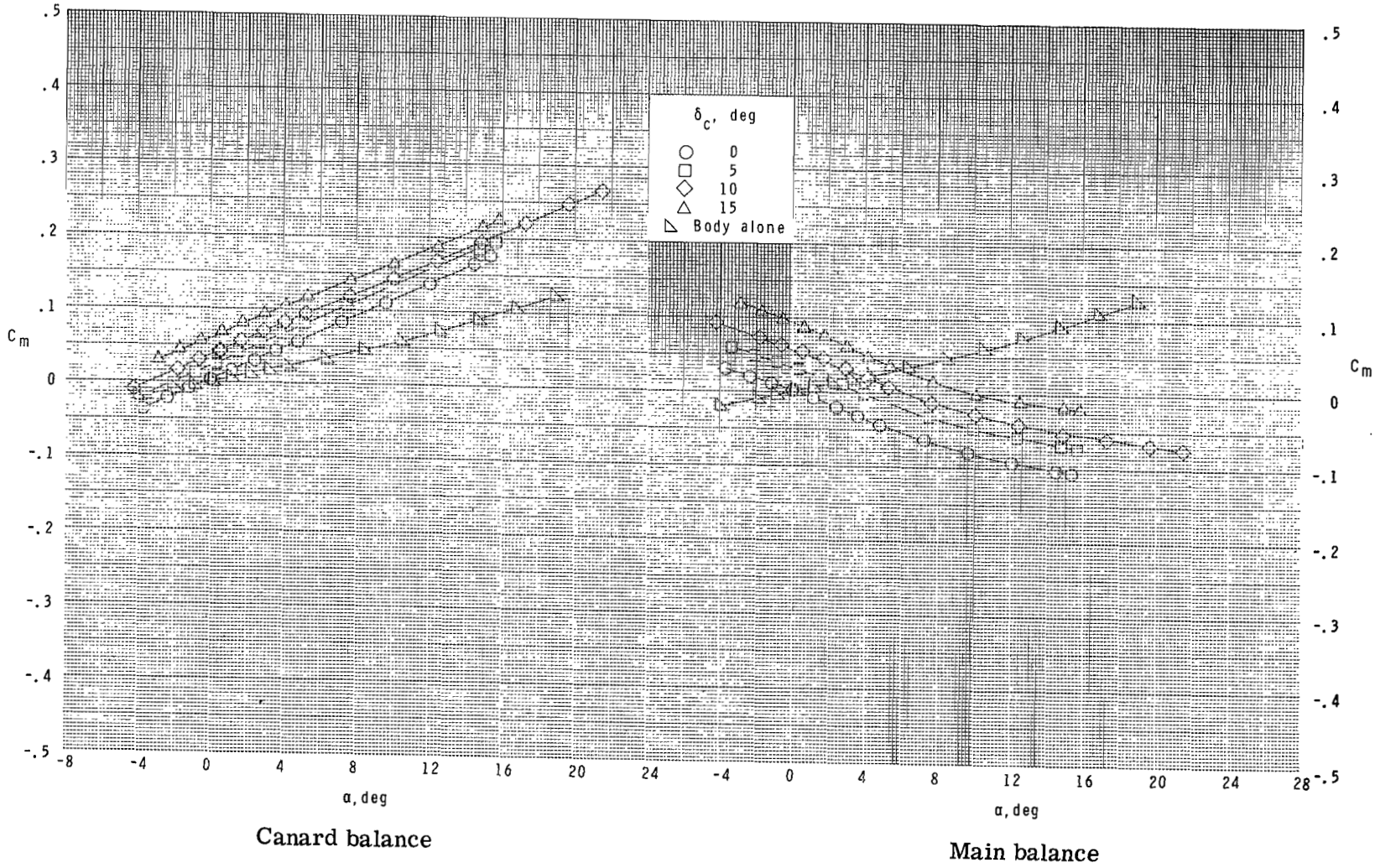

(a) Continued.

Figure 4.- Continued.

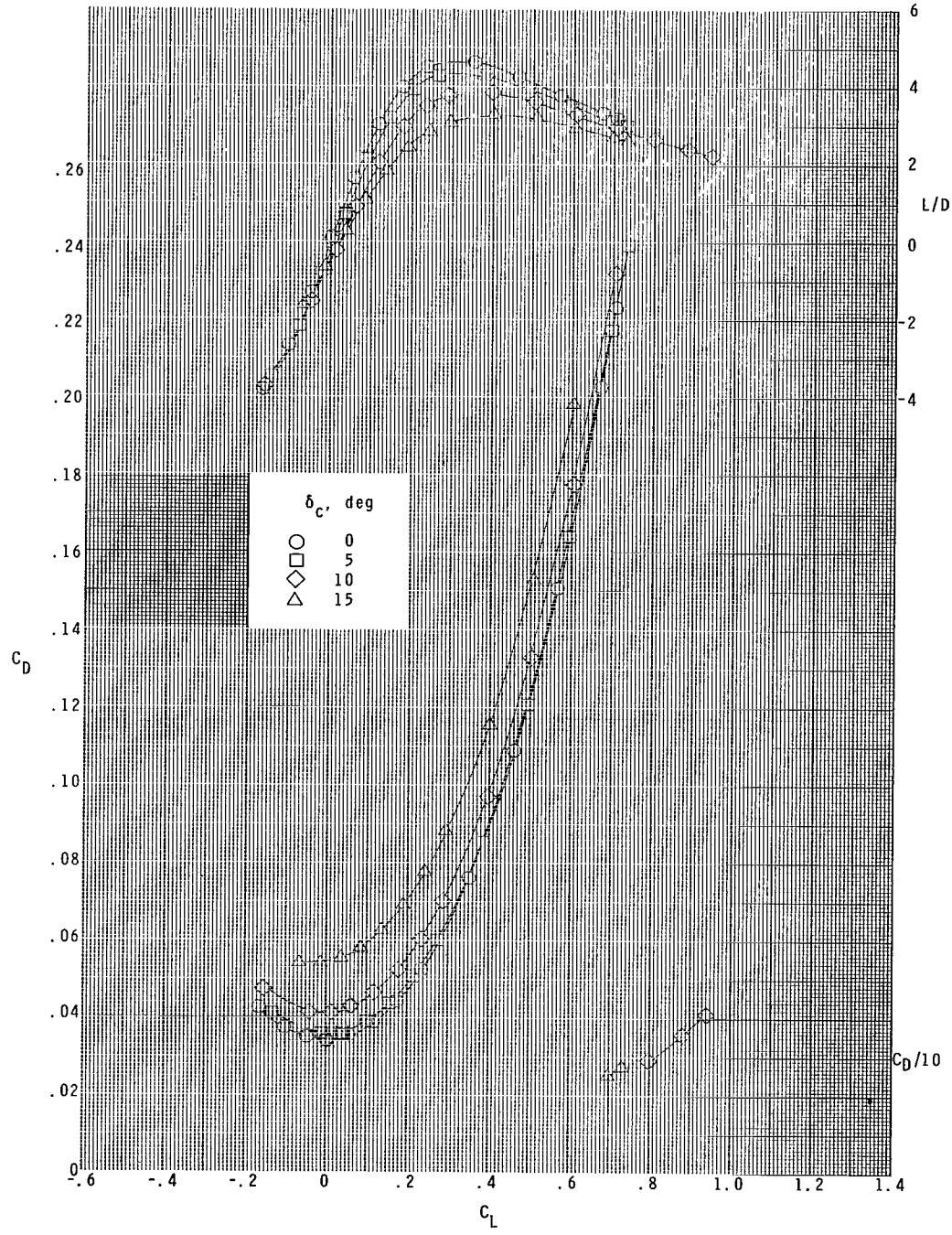

(a) Concluded.

Figure 4.- Continued.

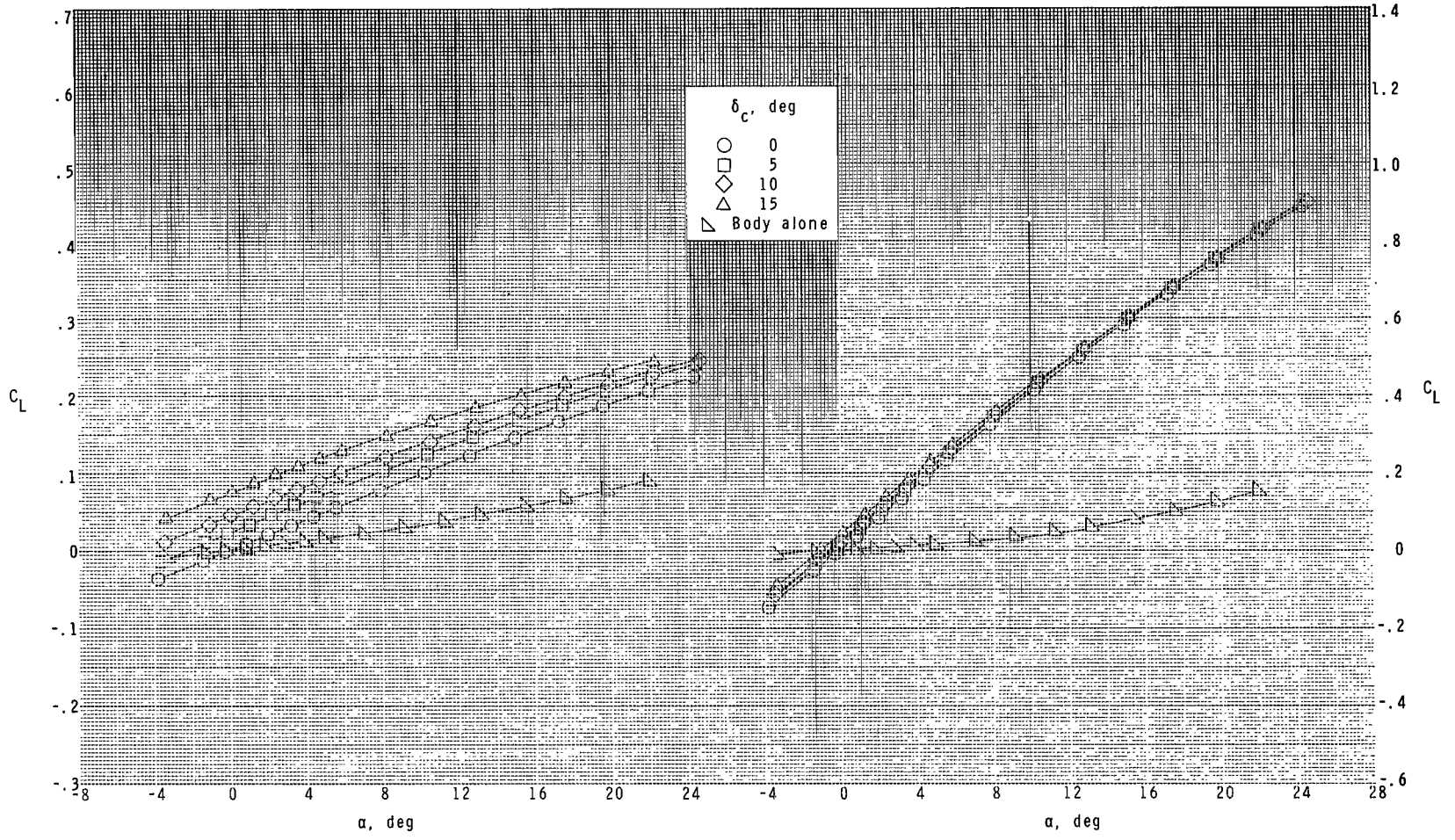

(b) M = 2.00.

Figure 4.- Continued.

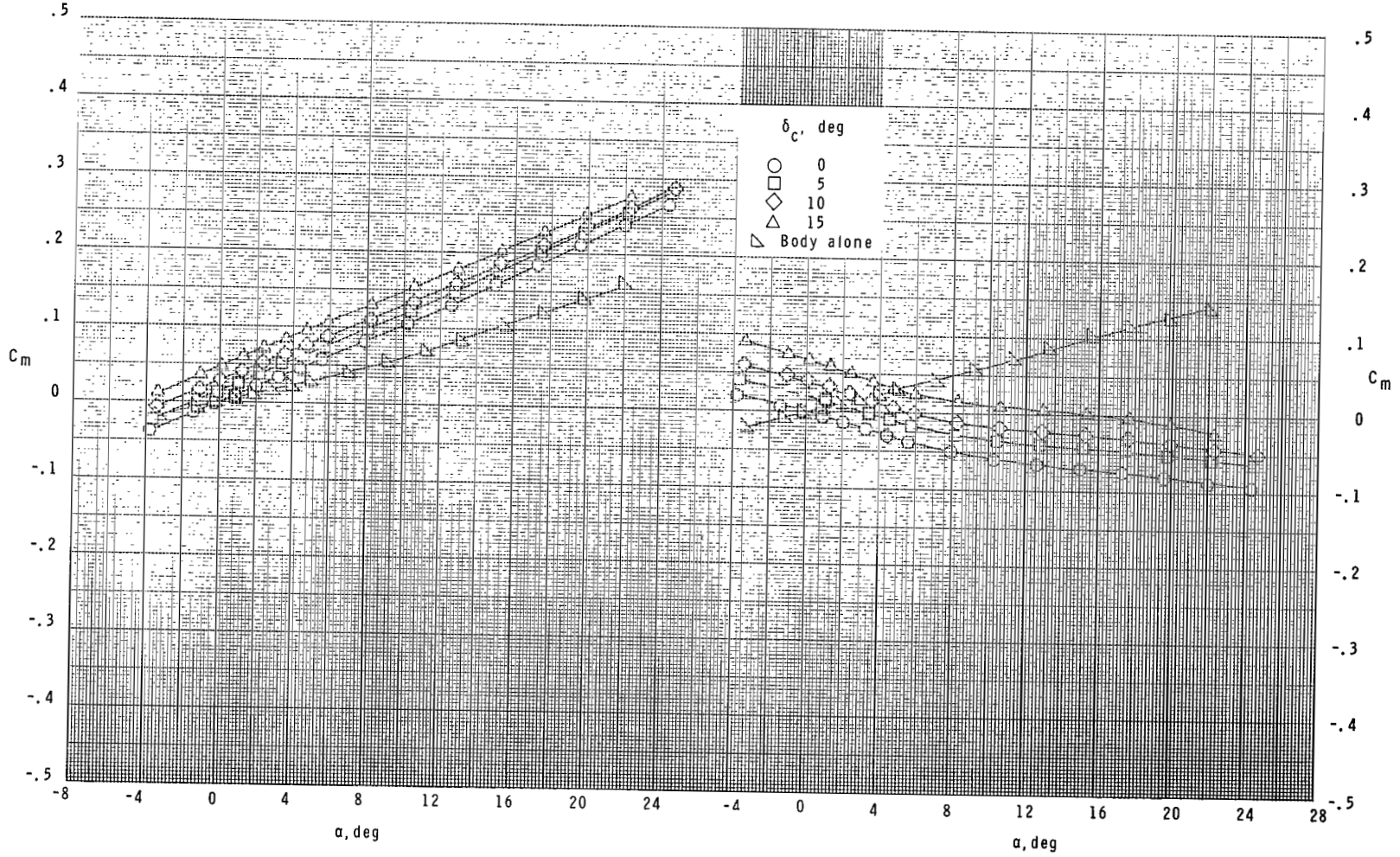

(b) Continued.

Figure 4.- Continued.

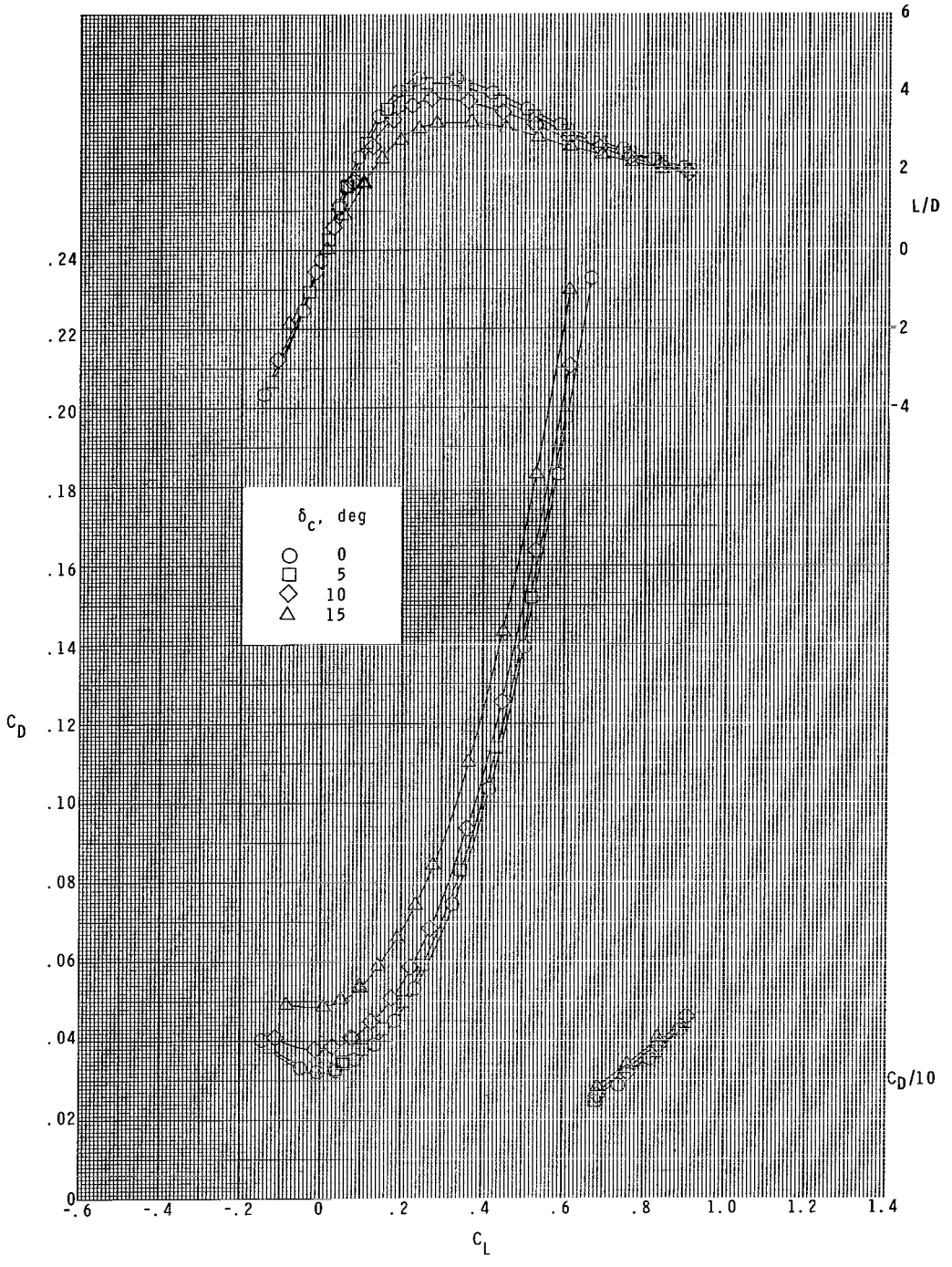

(b) Concluded.

Figure 4.- Continued.

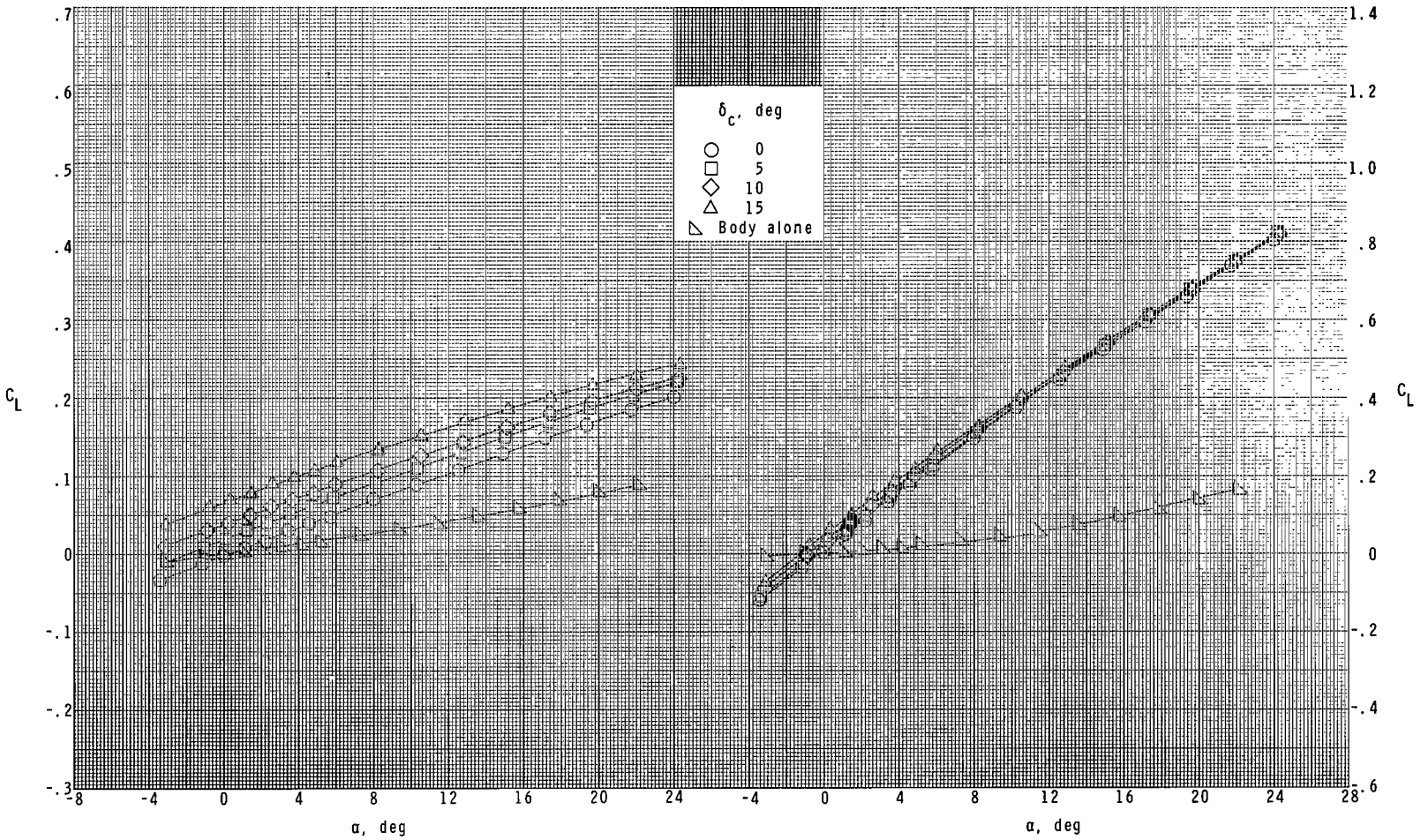

(c) M = 2.36.

Figure 4.- Continued.

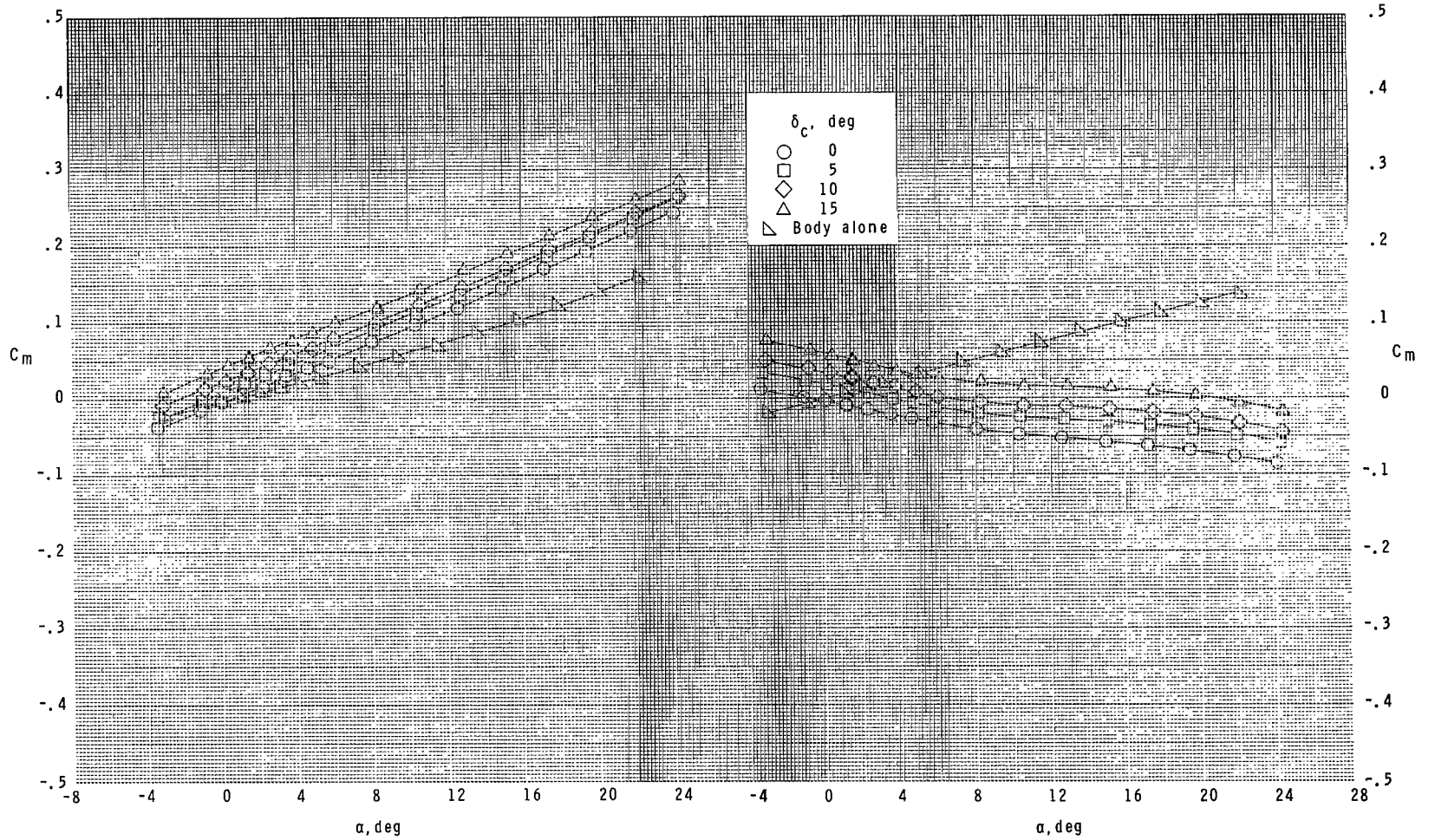

(c) Continued.

Figure 4.- Continued.

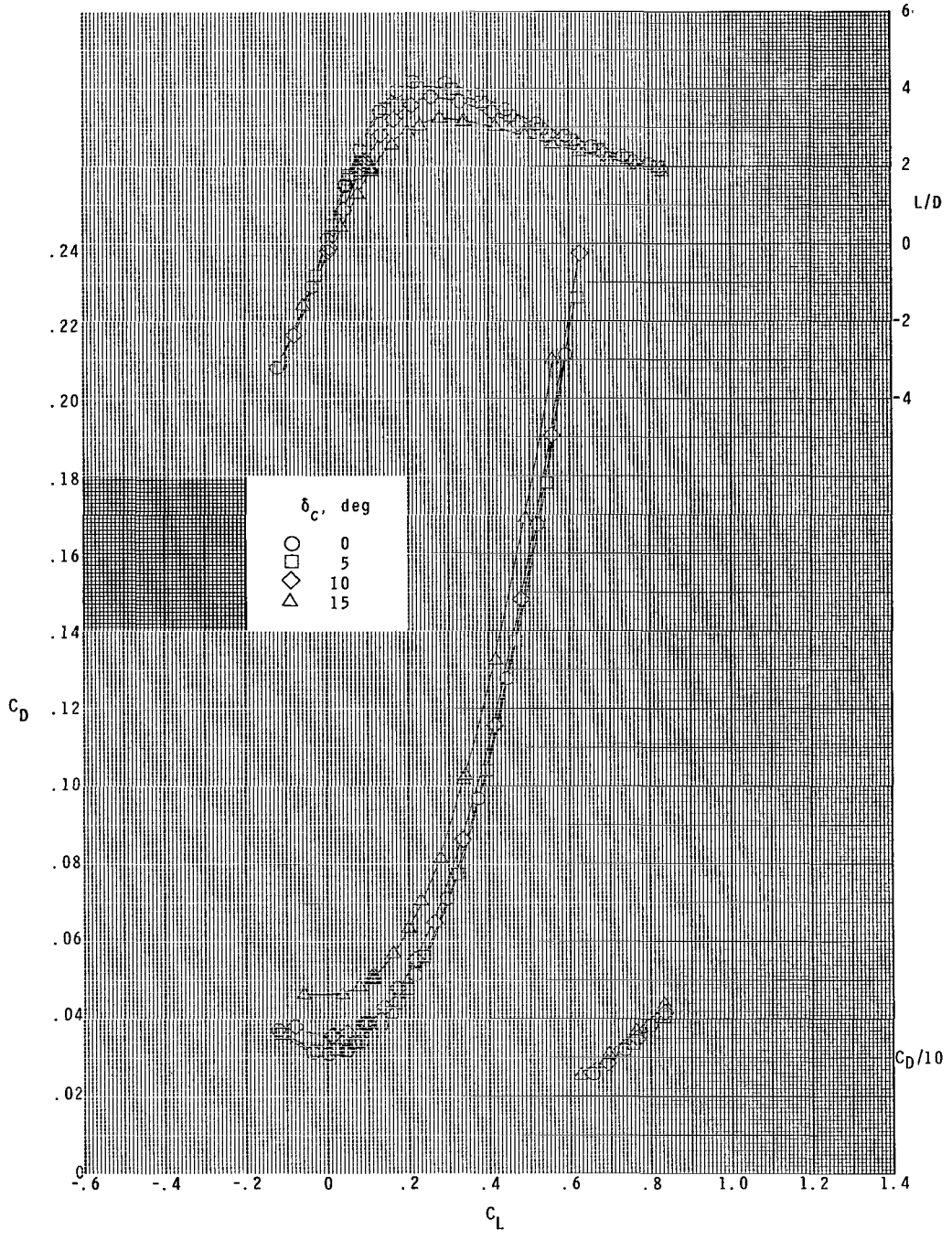

(c) Concluded.

Figure 4.- Continued.

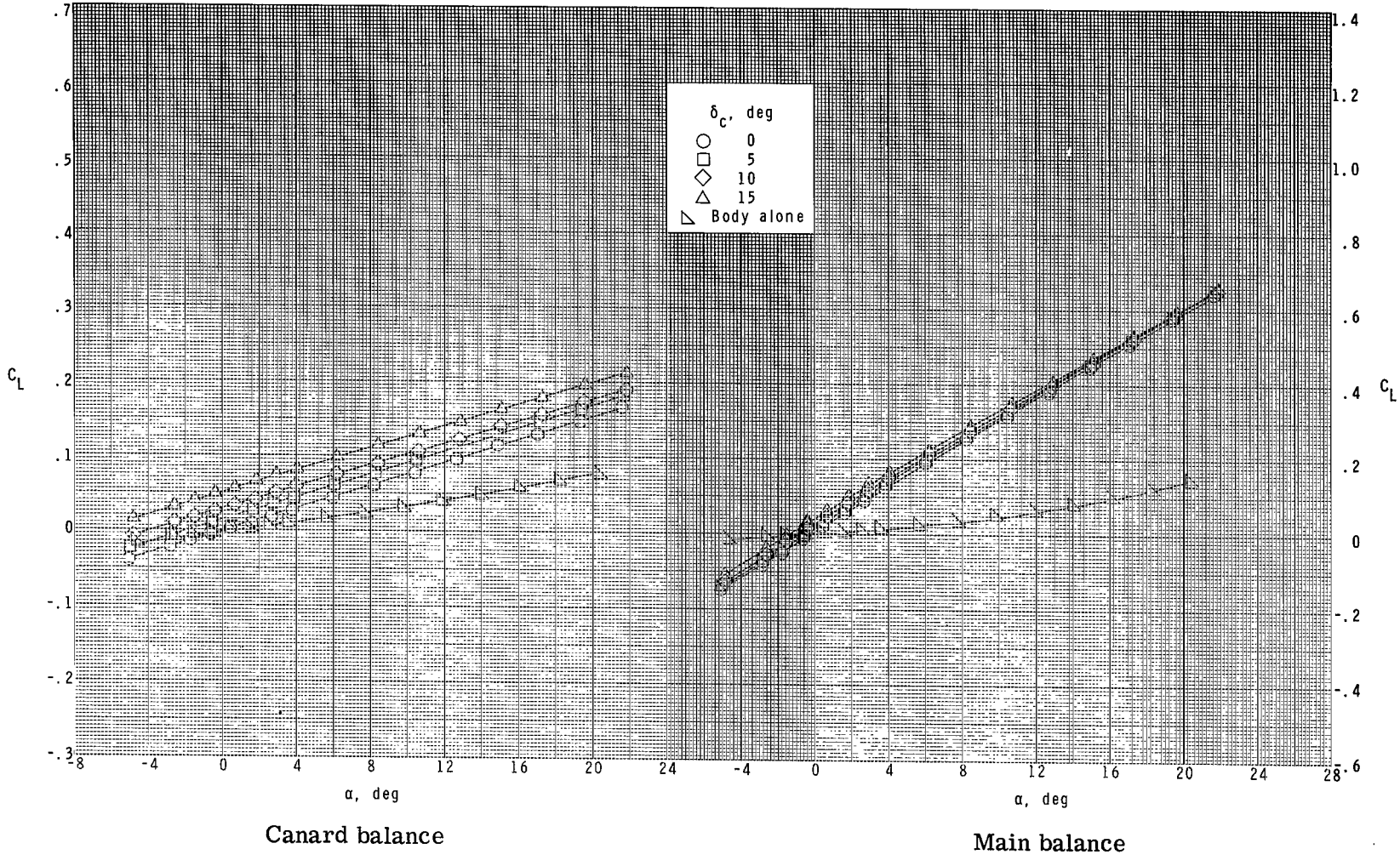

(d) M = 2.86.

Figure 4.- Continued.

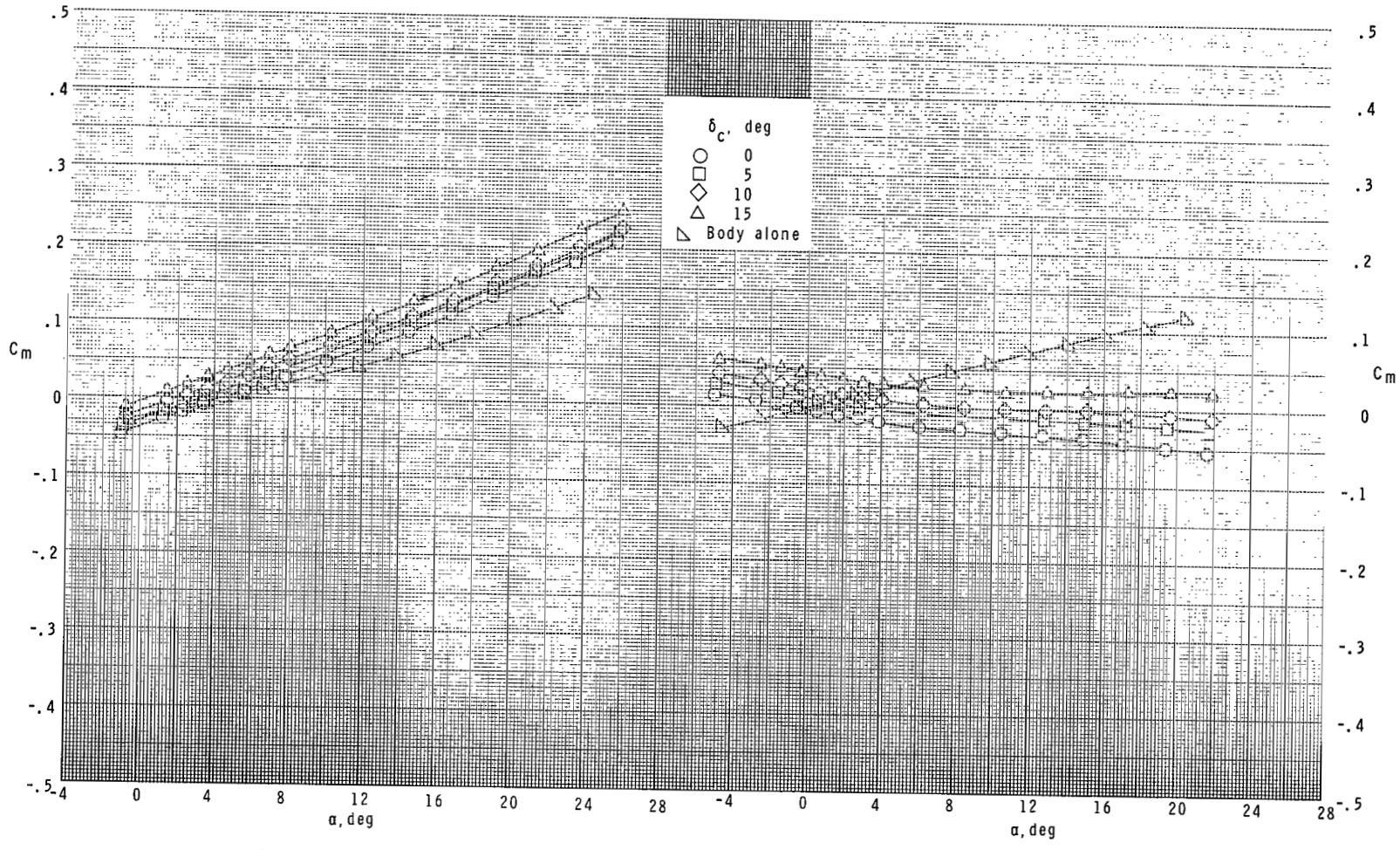

(d) Continued.

Figure 4.- Continued.

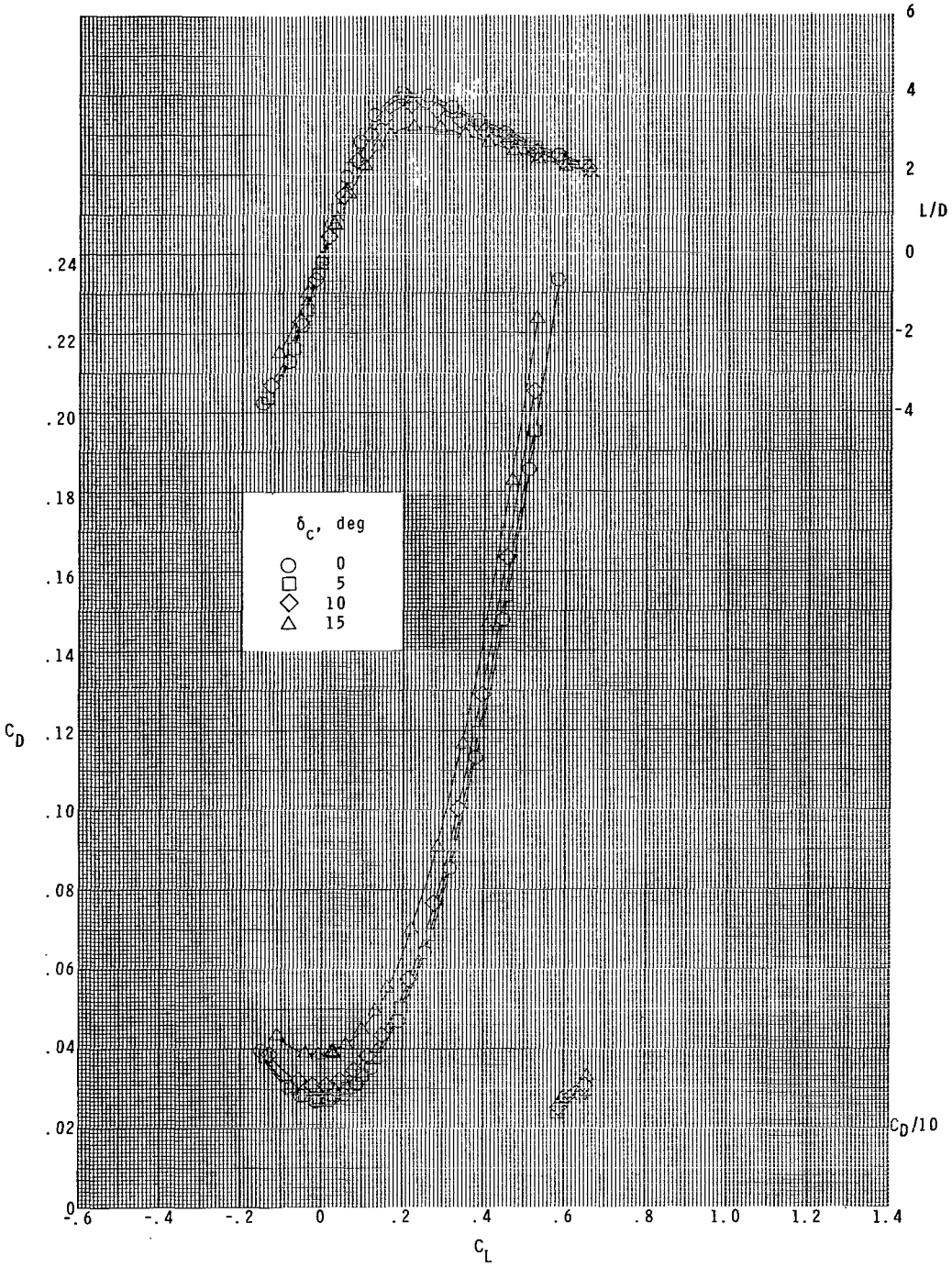

(d) Concluded.

Figure 4.- Concluded.

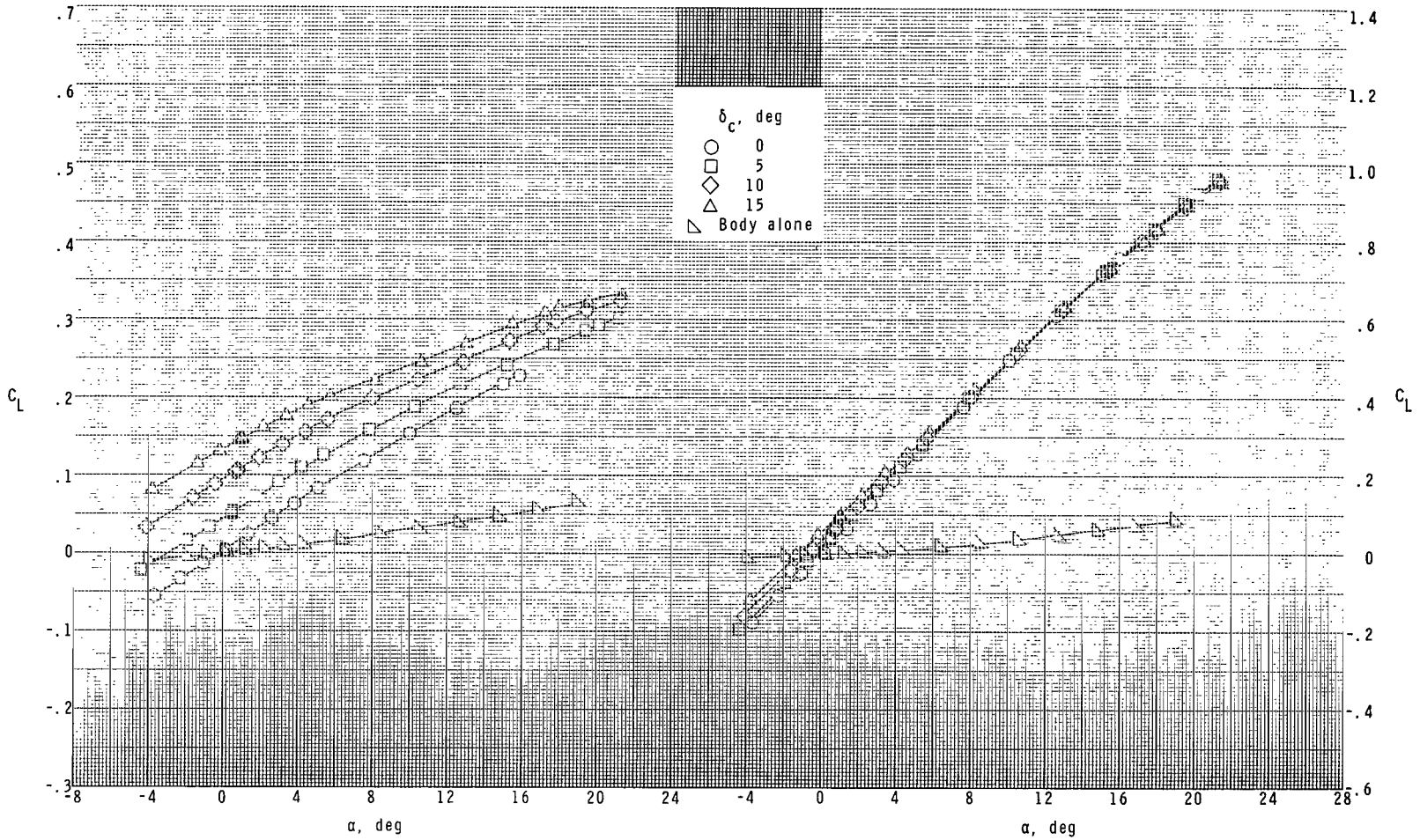

(a) M = 1.60.

Figure 5.- Longitudinal aerodynamic characteristics for $S_c/S_w = 0.240$ and $z/\bar{c} = 0.0$.

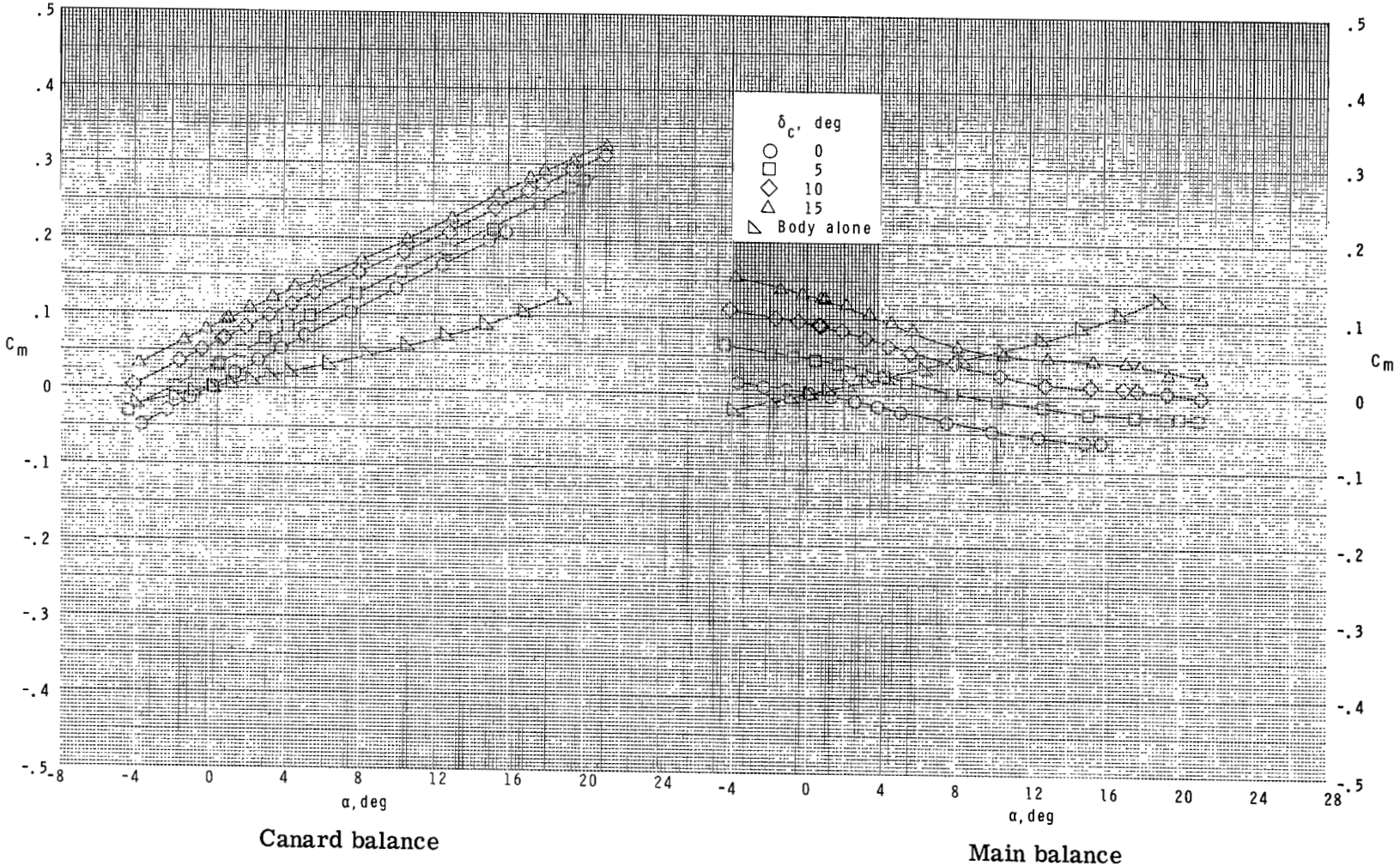

(a) Continued.

Figure 5.- Continued.

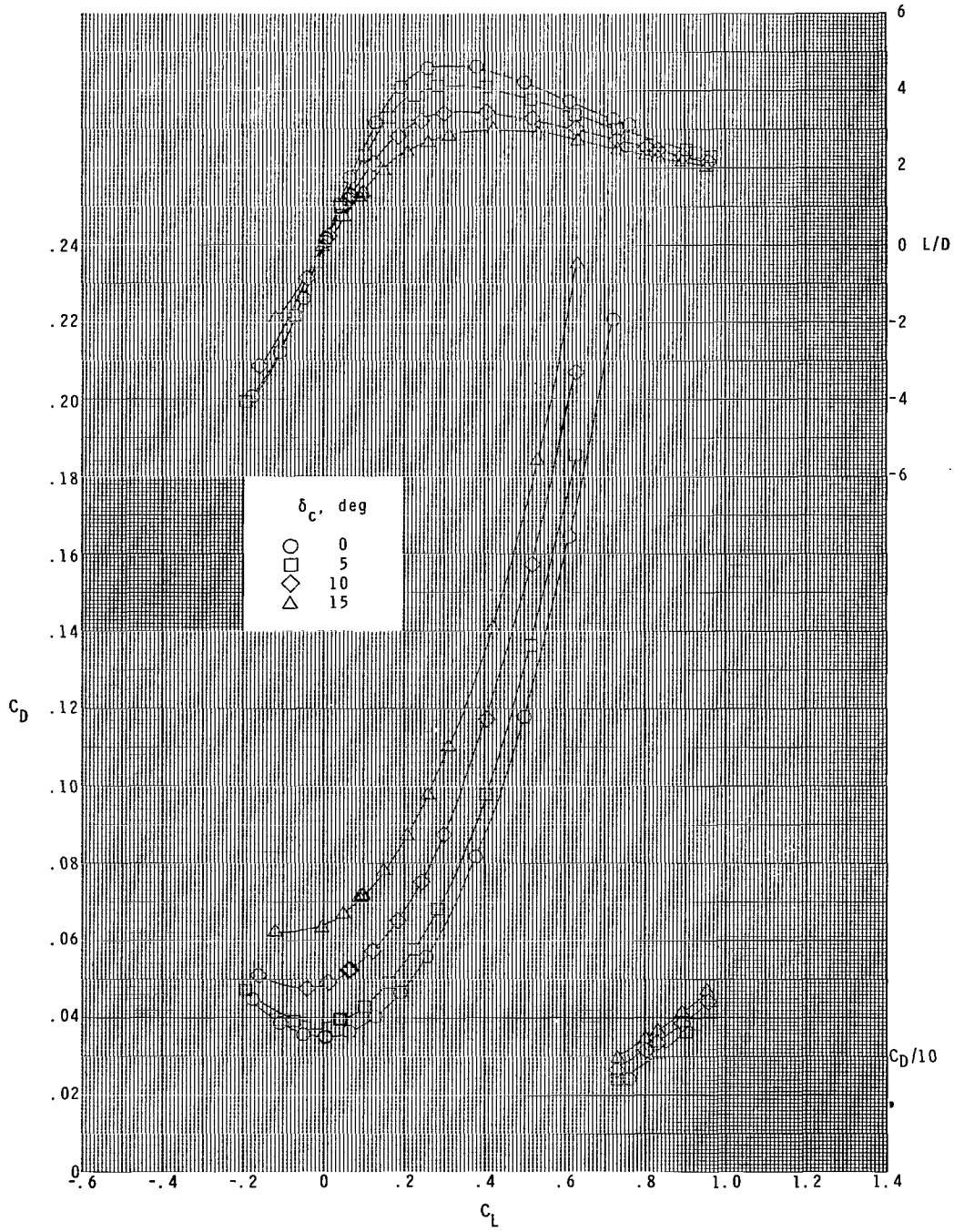

(a) Concluded.

Figure 5.- Continued.

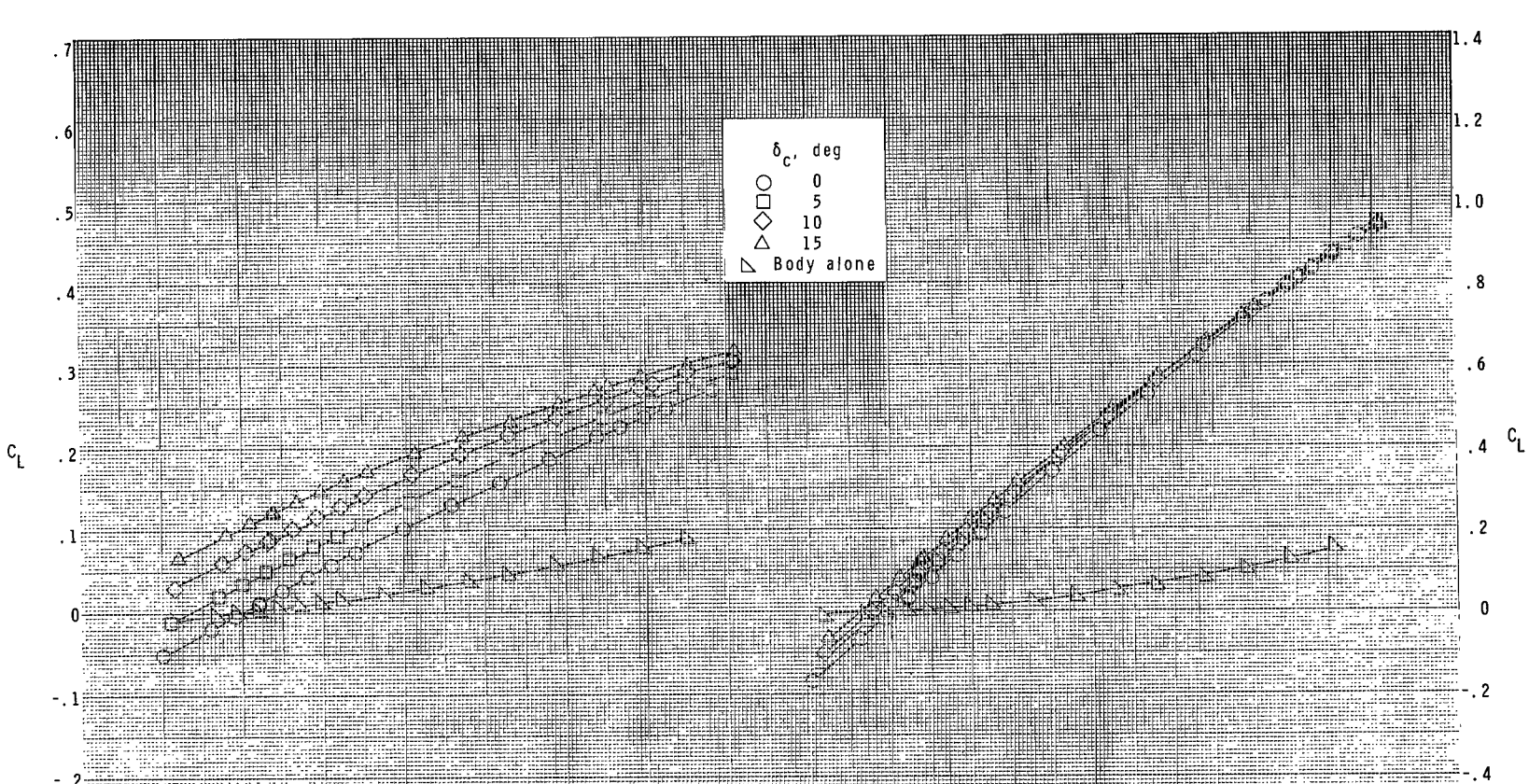

(b) M = 2.00.

Figure 5.- Continued.

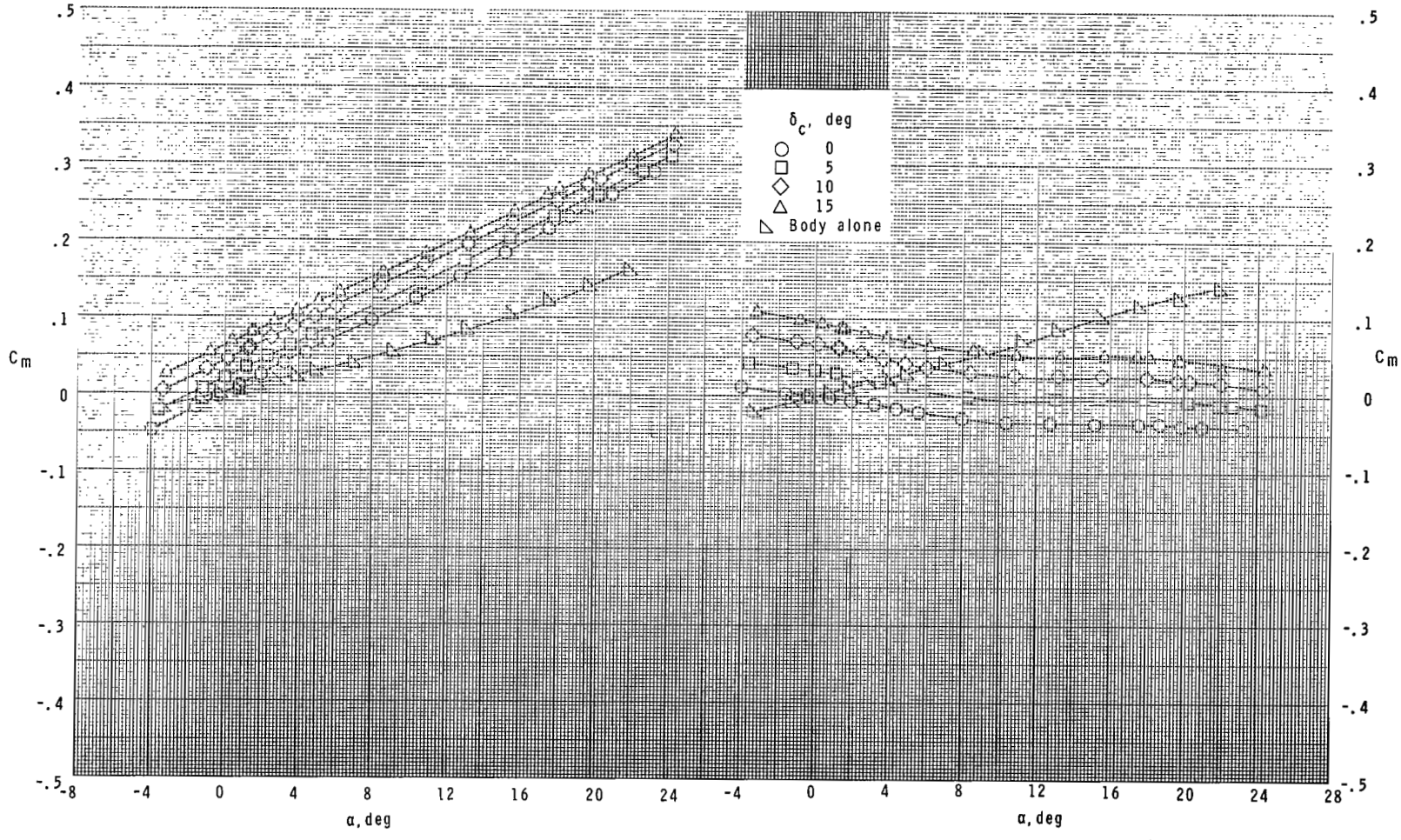

(b) Continued.

Figure 5.- Continued.

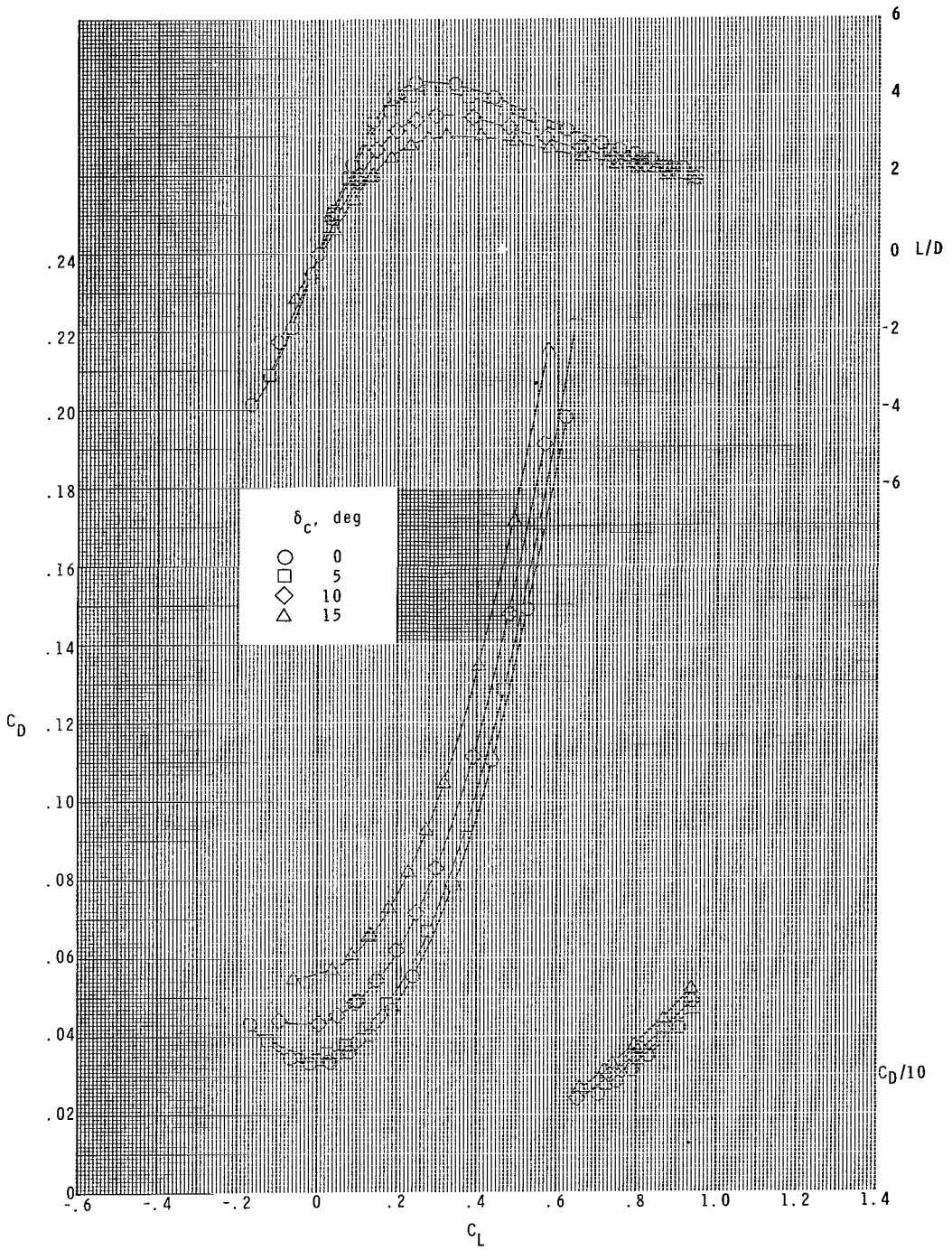

(b) Concluded.

Figure 5.- Continued.

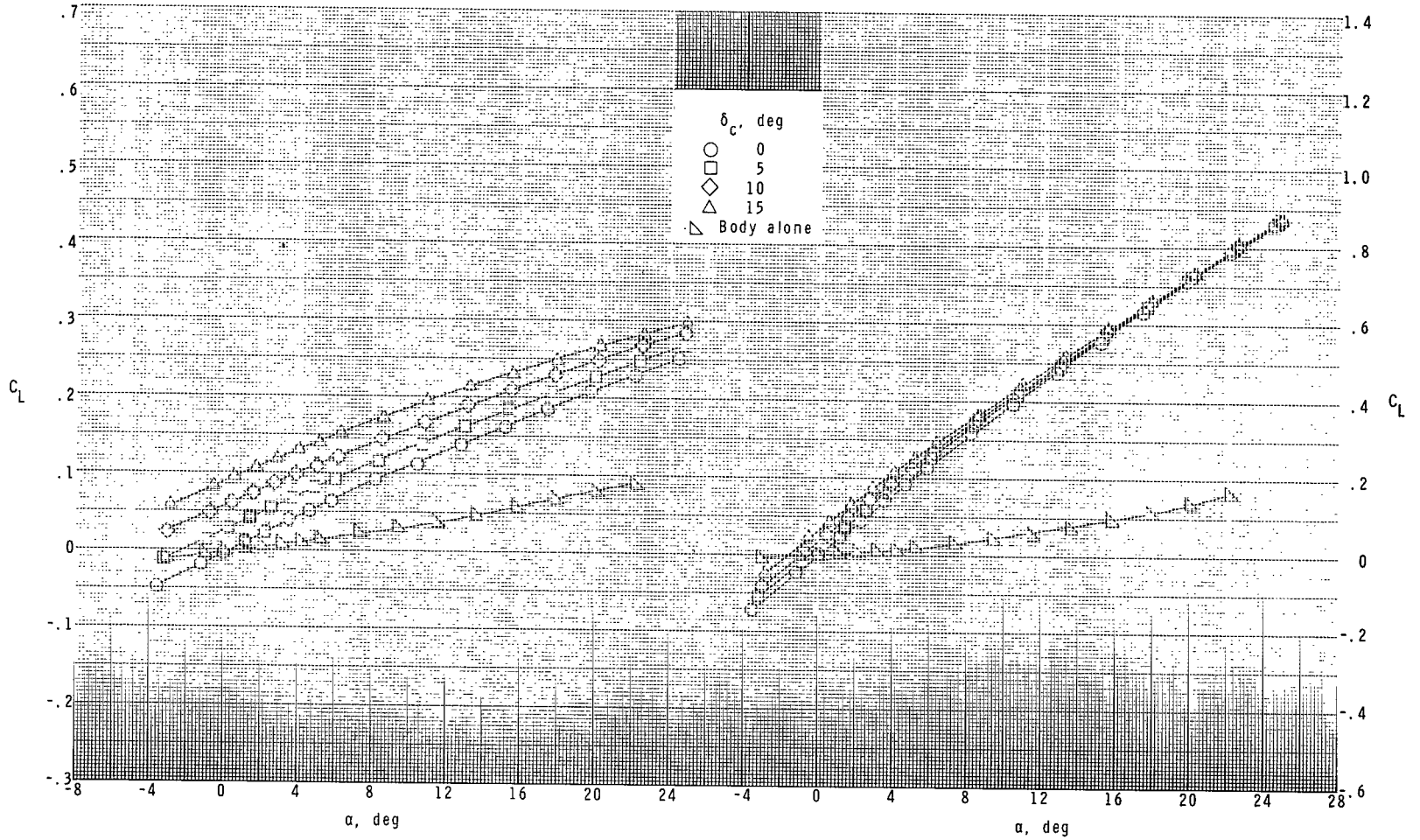

(c) M = 2.36.

Figure 5.- Continued.

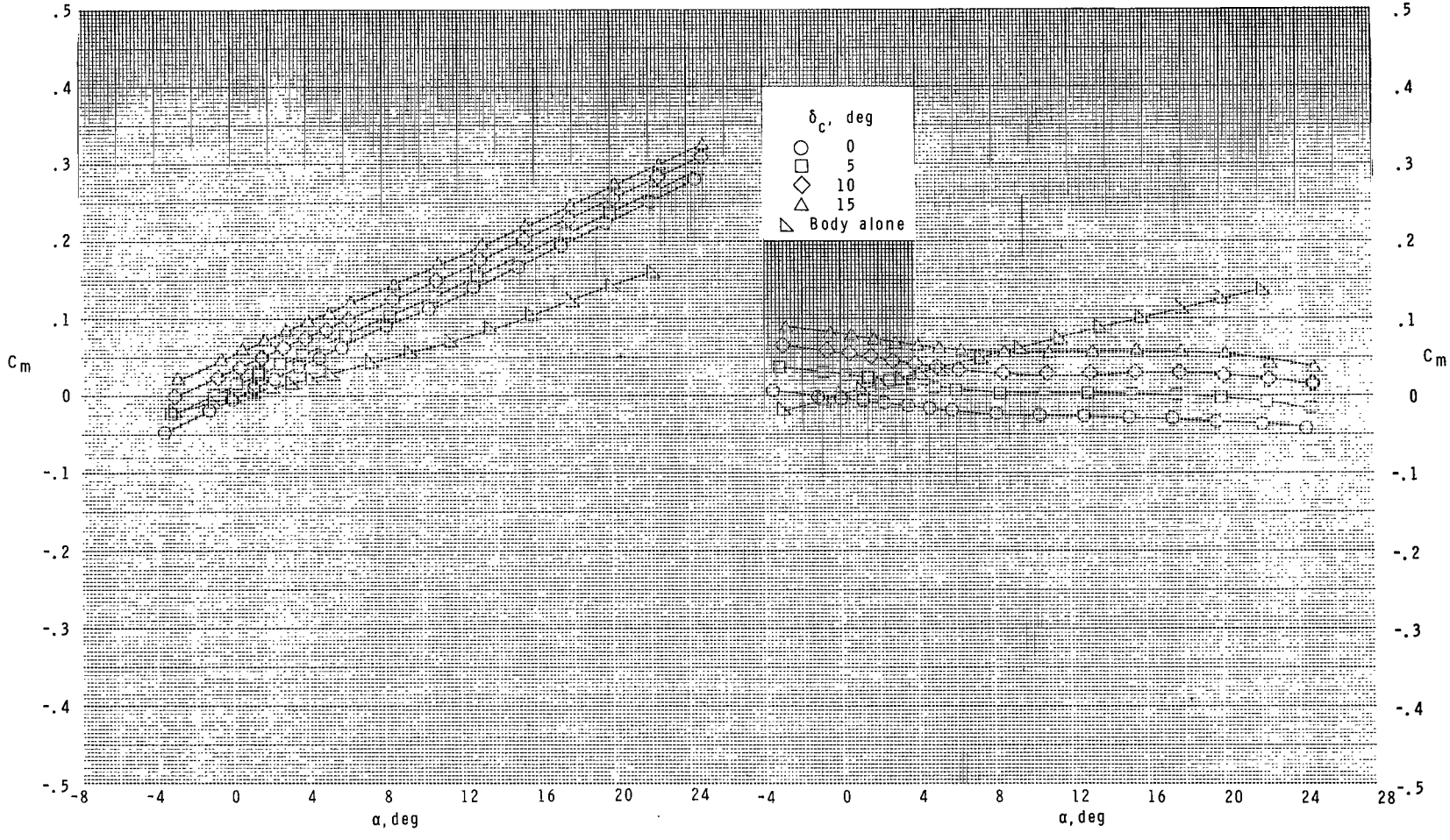

(c) Continued.

Figure 5.- Continued.

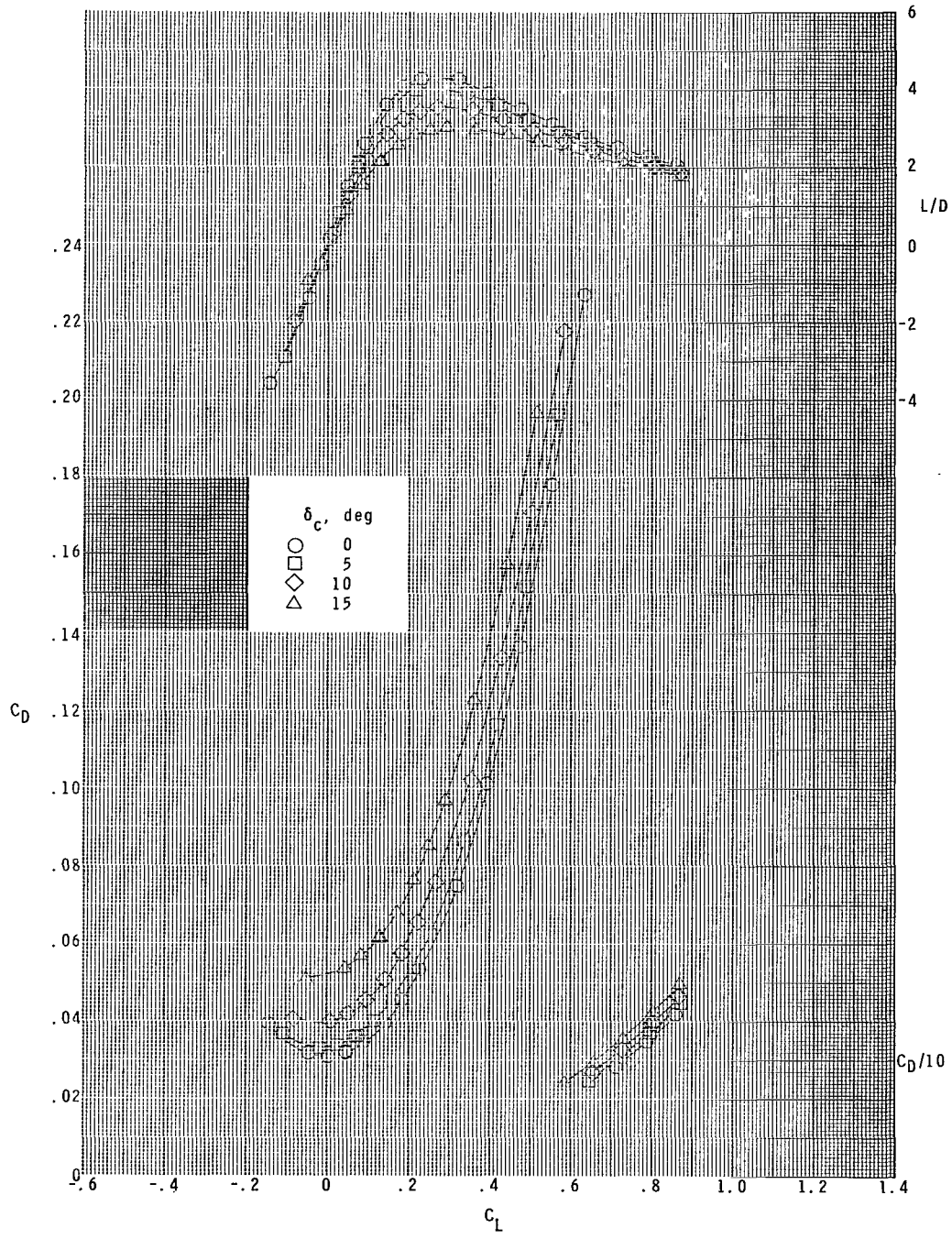

(c) Concluded.

Figure 5.- Continued.

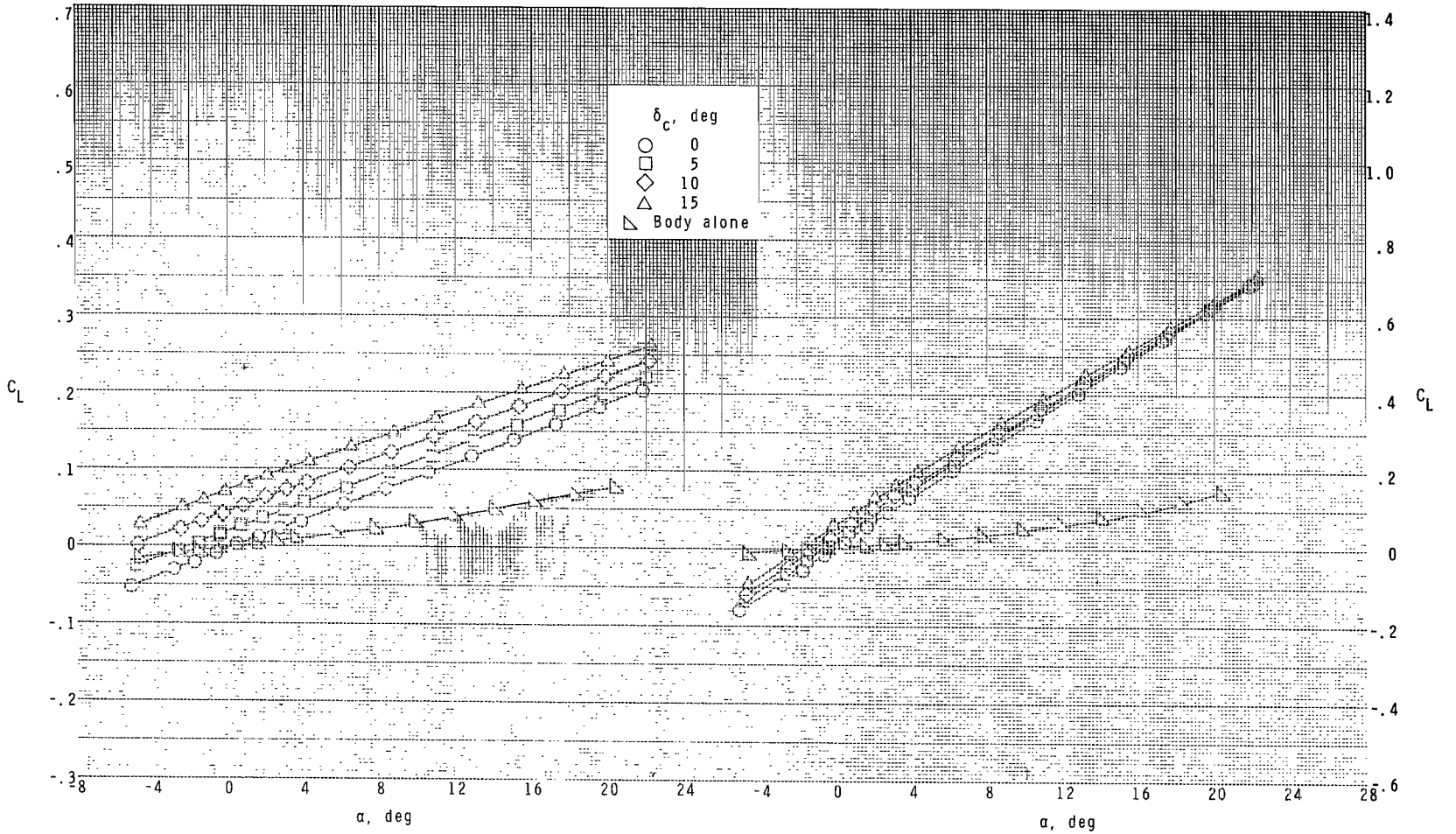

(d) M = 2.86.

Figure 5.- Continued.

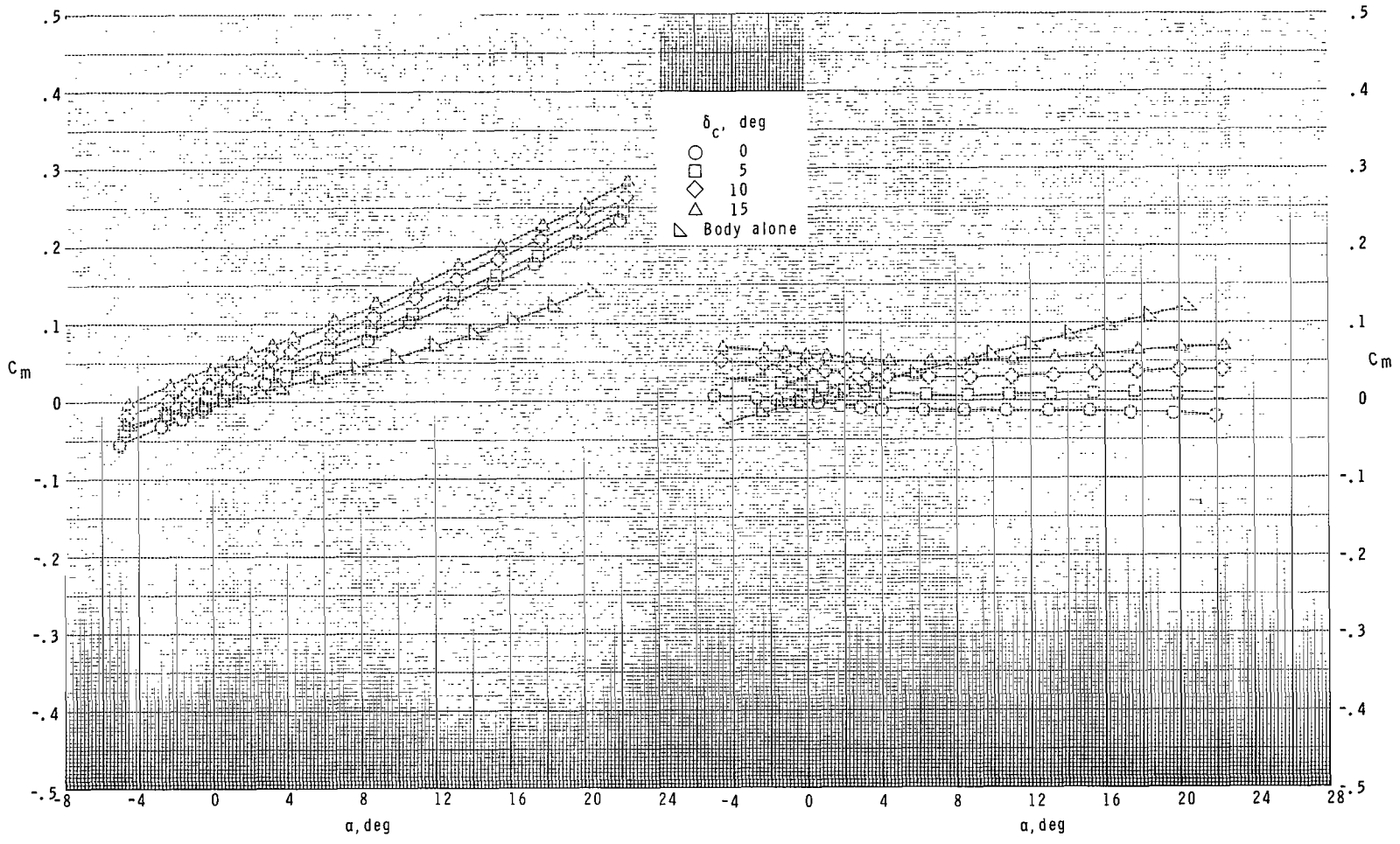

(d) Continued.

Figure 5.- Continued.

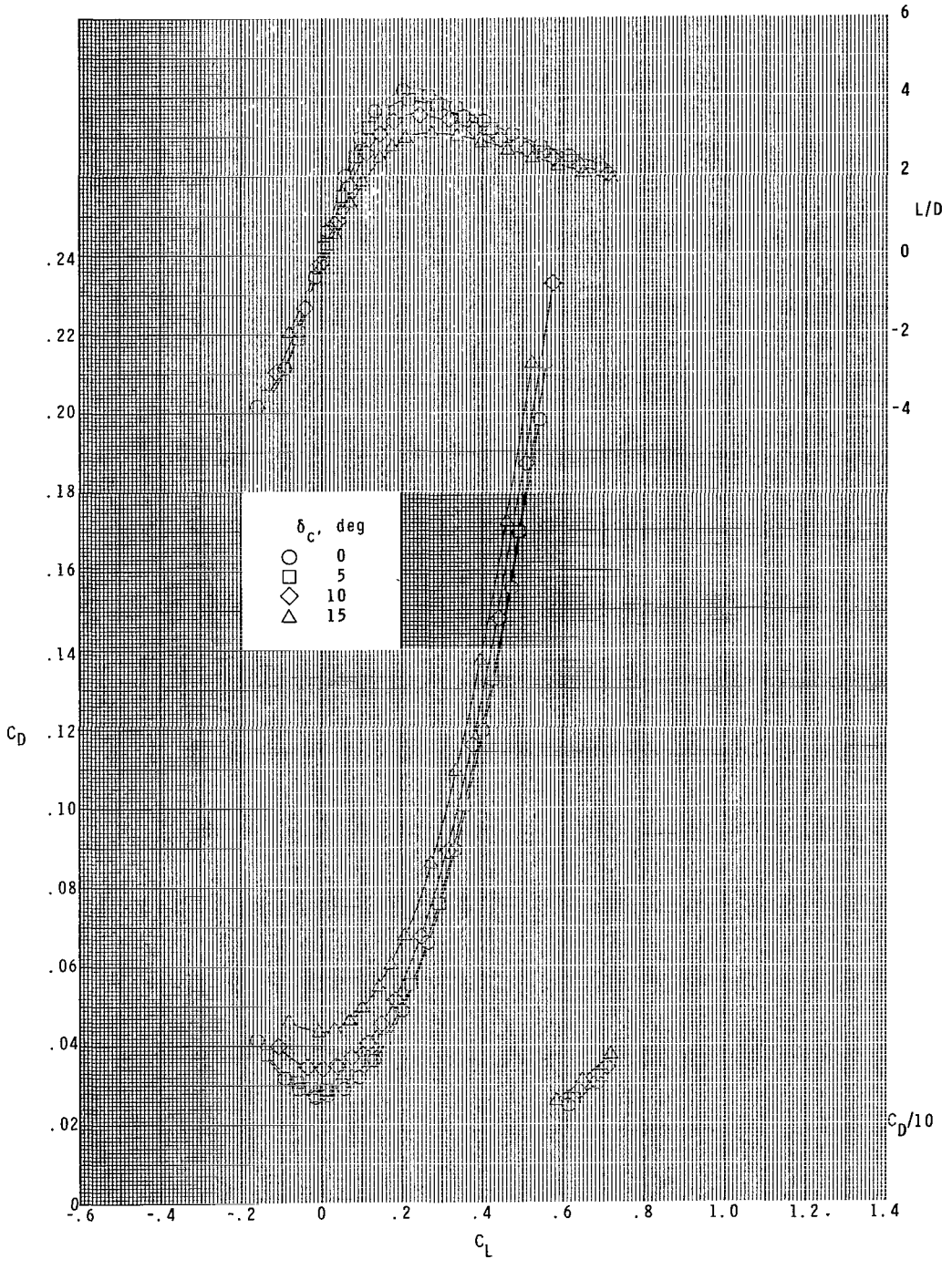

(d) Concluded.

Figure 5.- Concluded.

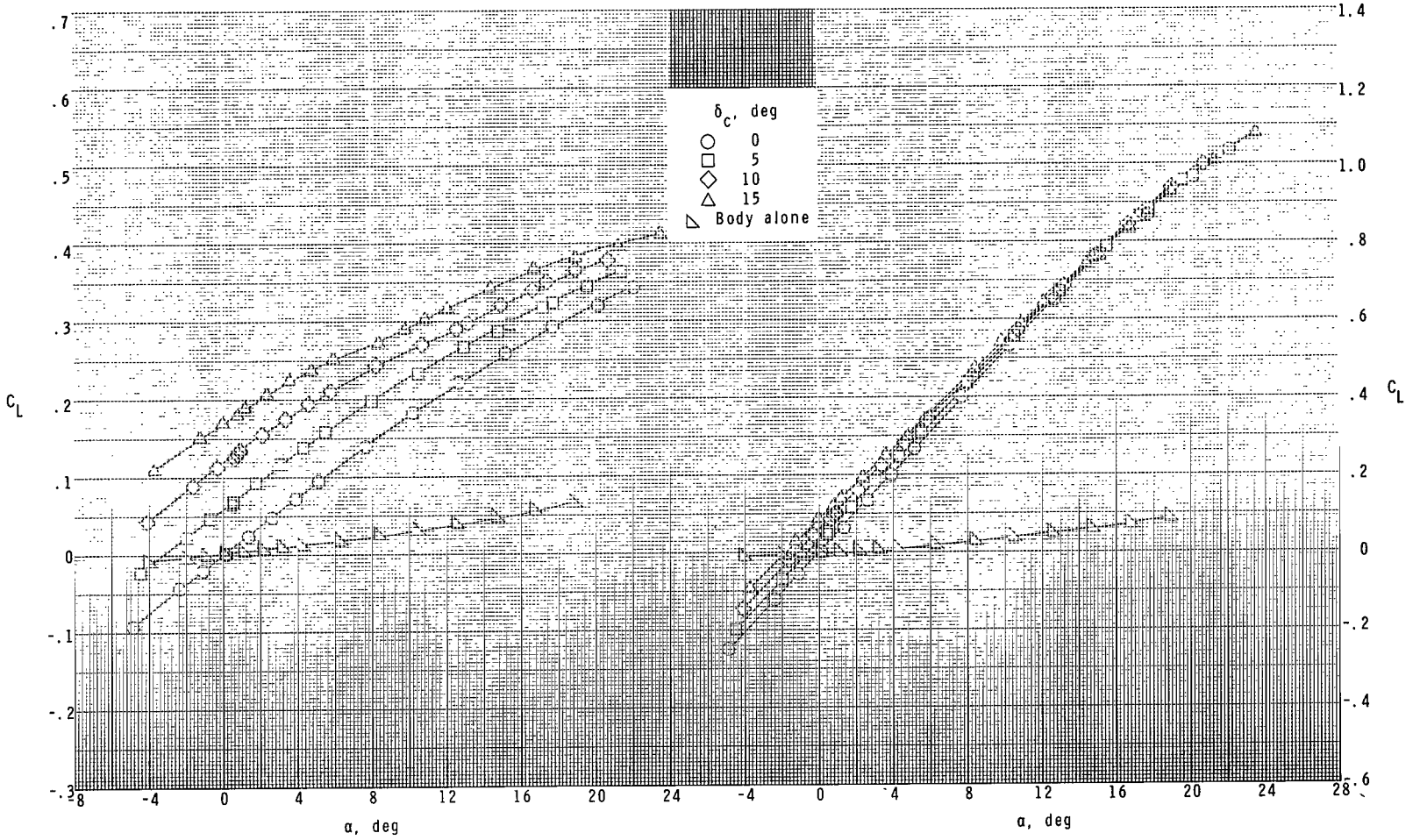

(a) M = 1.60.

Figure 6.- Longitudinal aerodynamic characteristics for $S_c/S_w = 0.300$ and $z/\bar{c} = 0.0$.

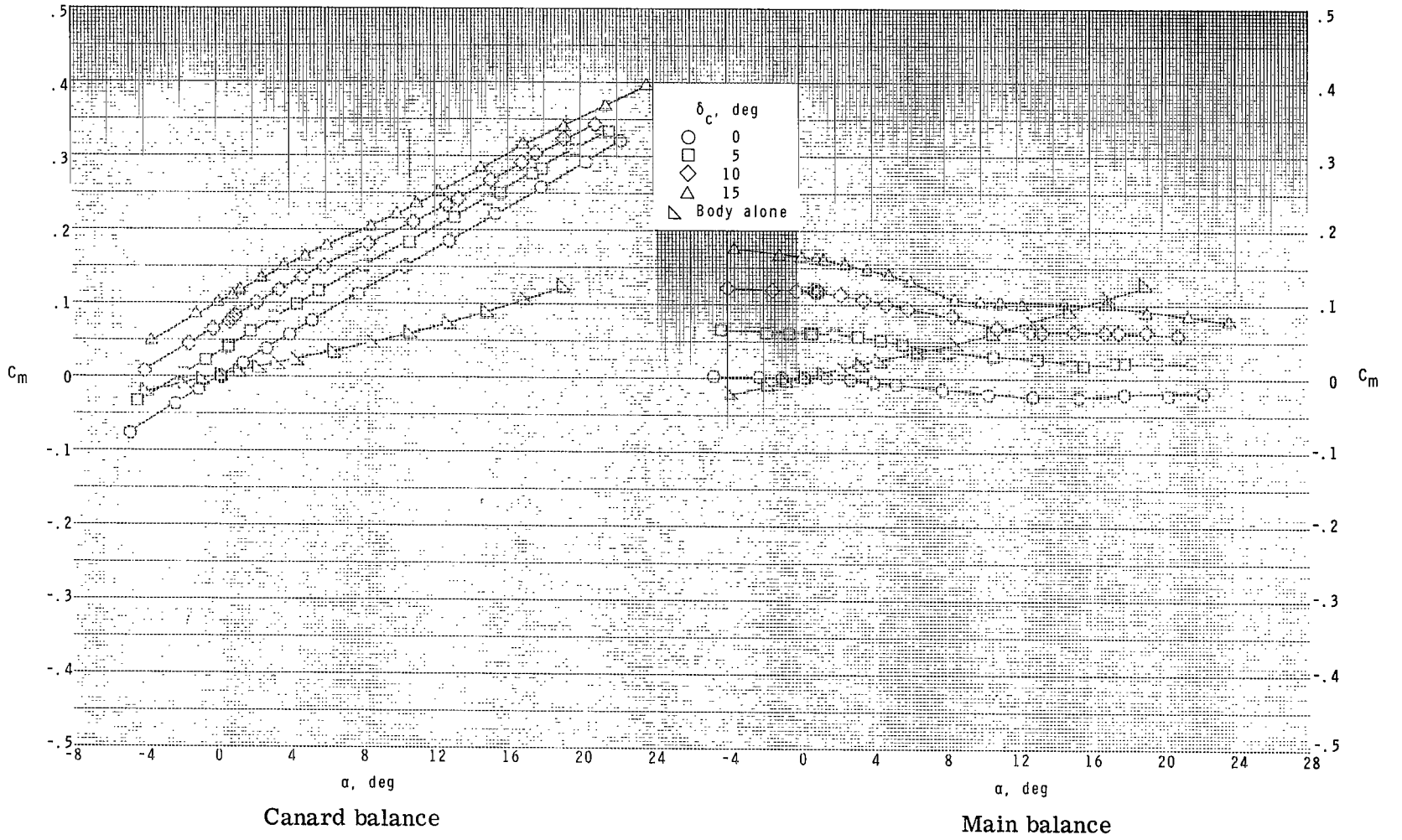

(a) Continued.

Figure 6.- Continued.

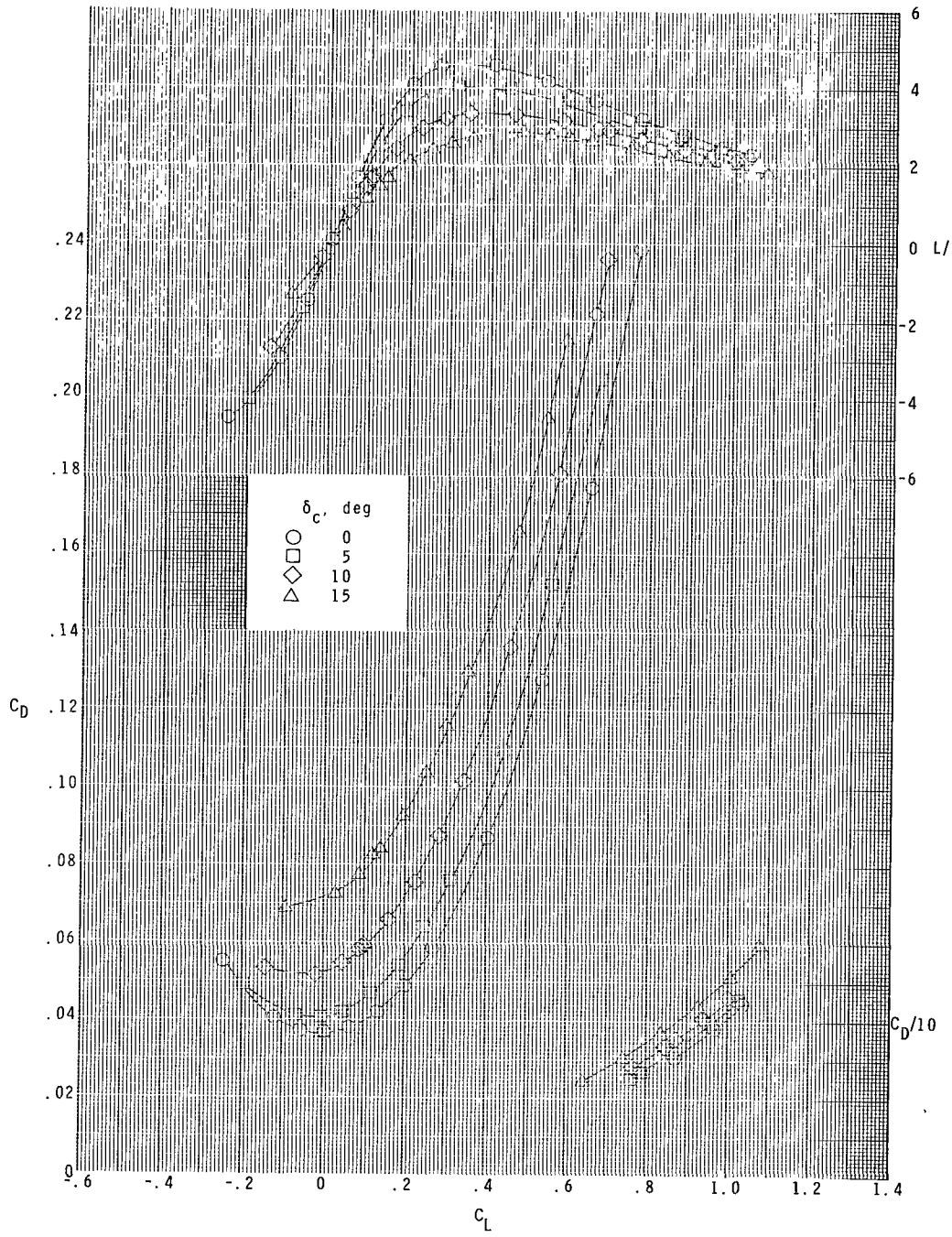

(a) Concluded.

Figure 6.- Continued.

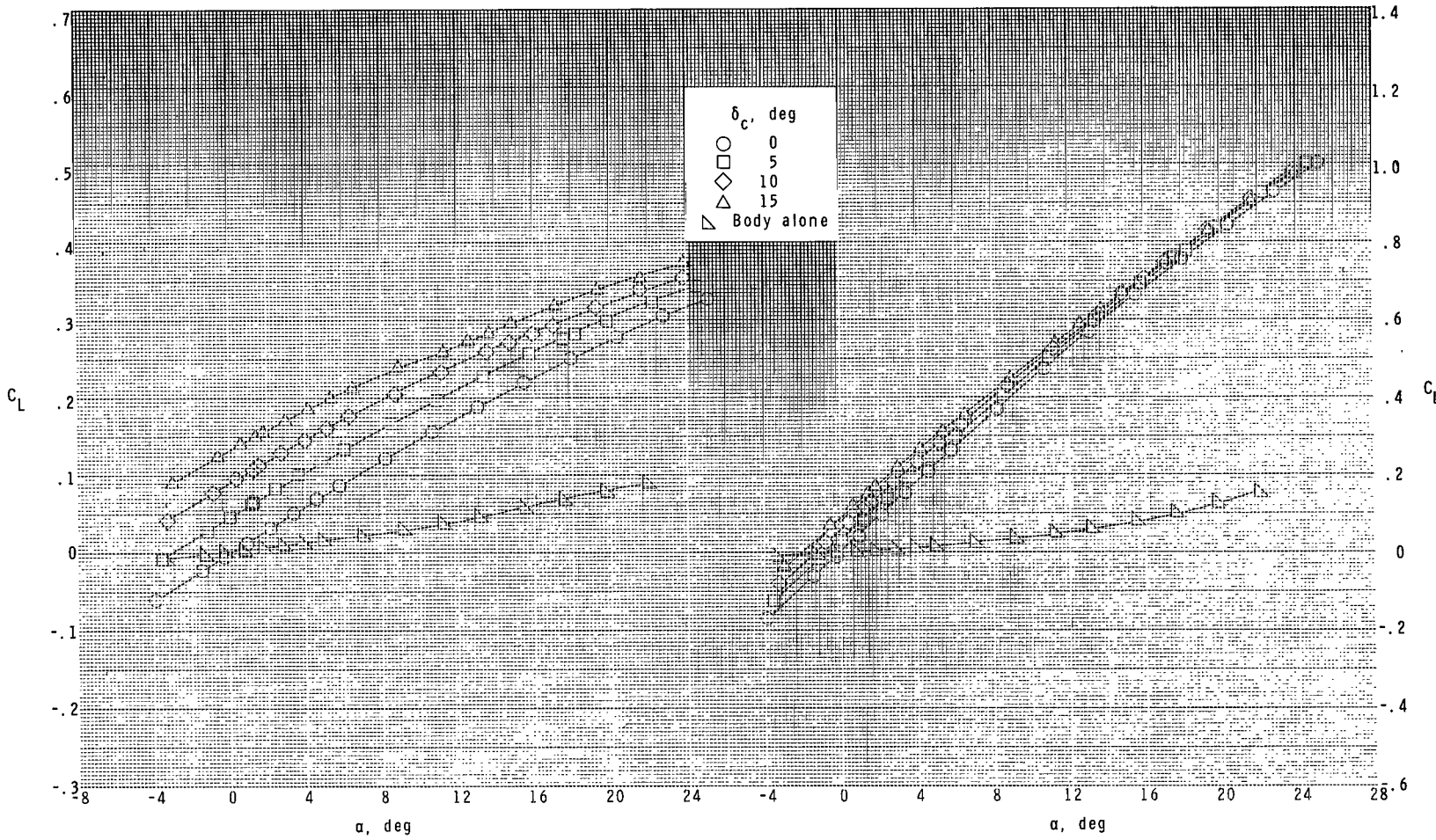

(b) M = 2.00.

Figure 6.- Continued.

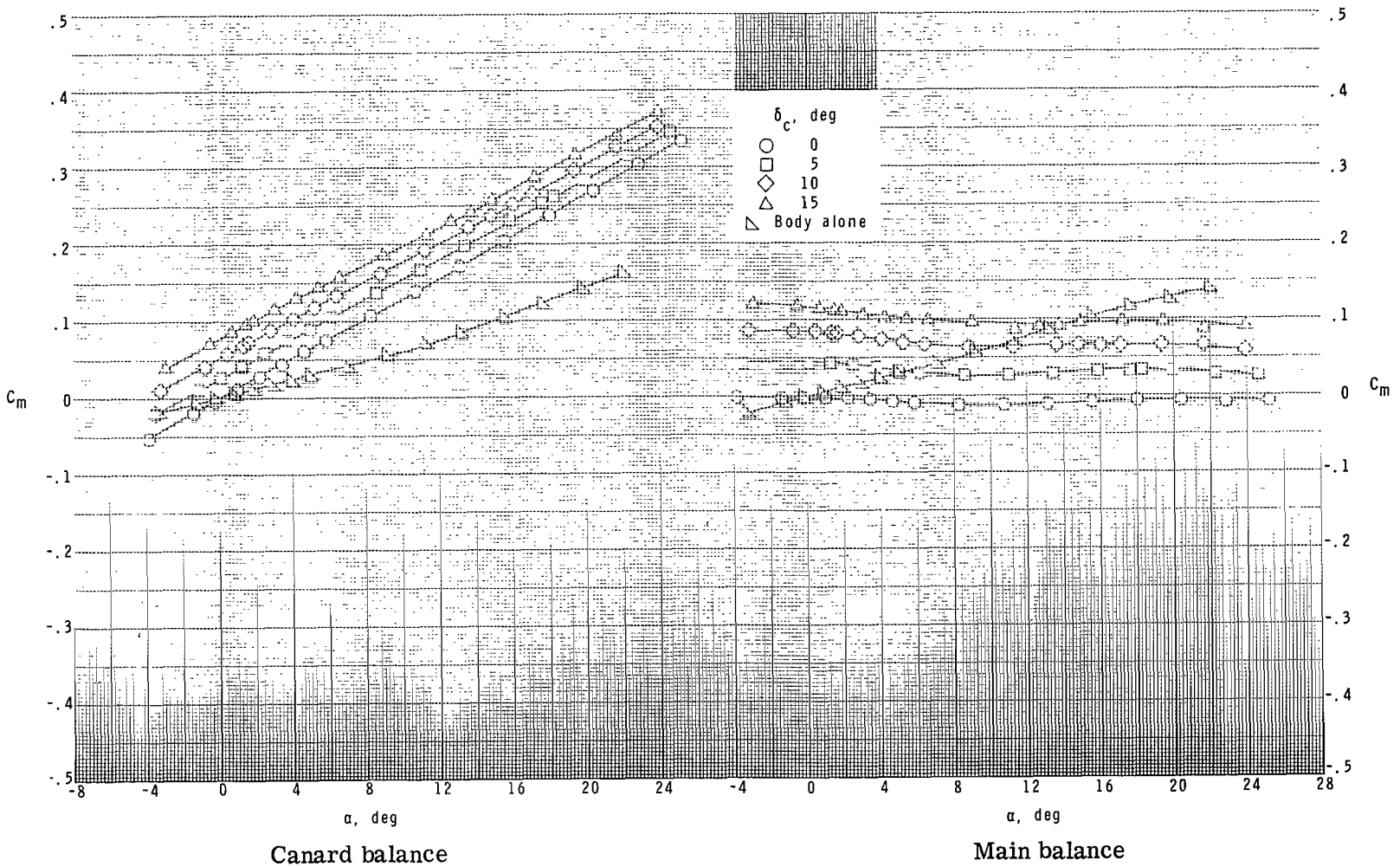

(b) Continued.

Figure 6.- Continued.

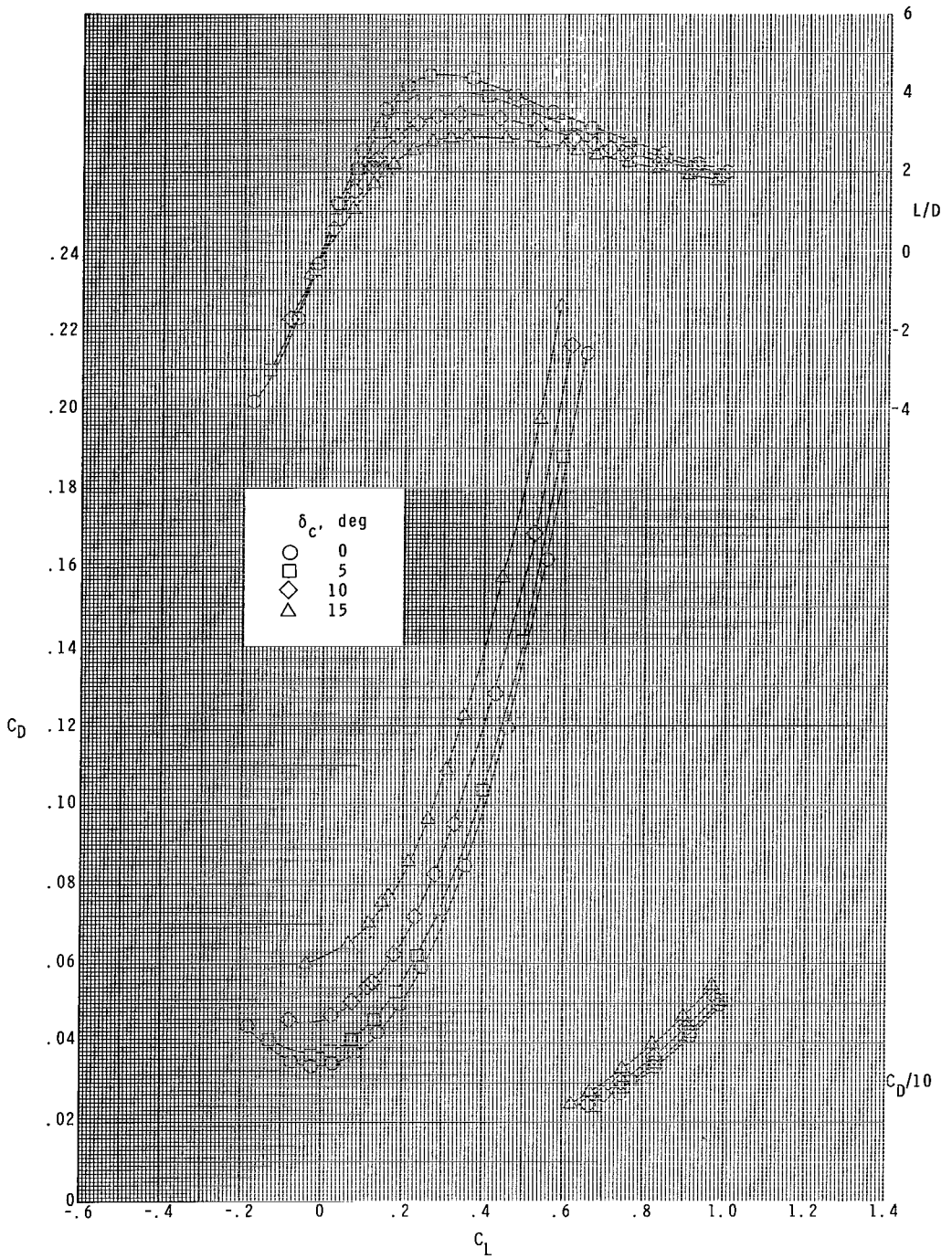

(b) Concluded.

Figure 6.- Continued.

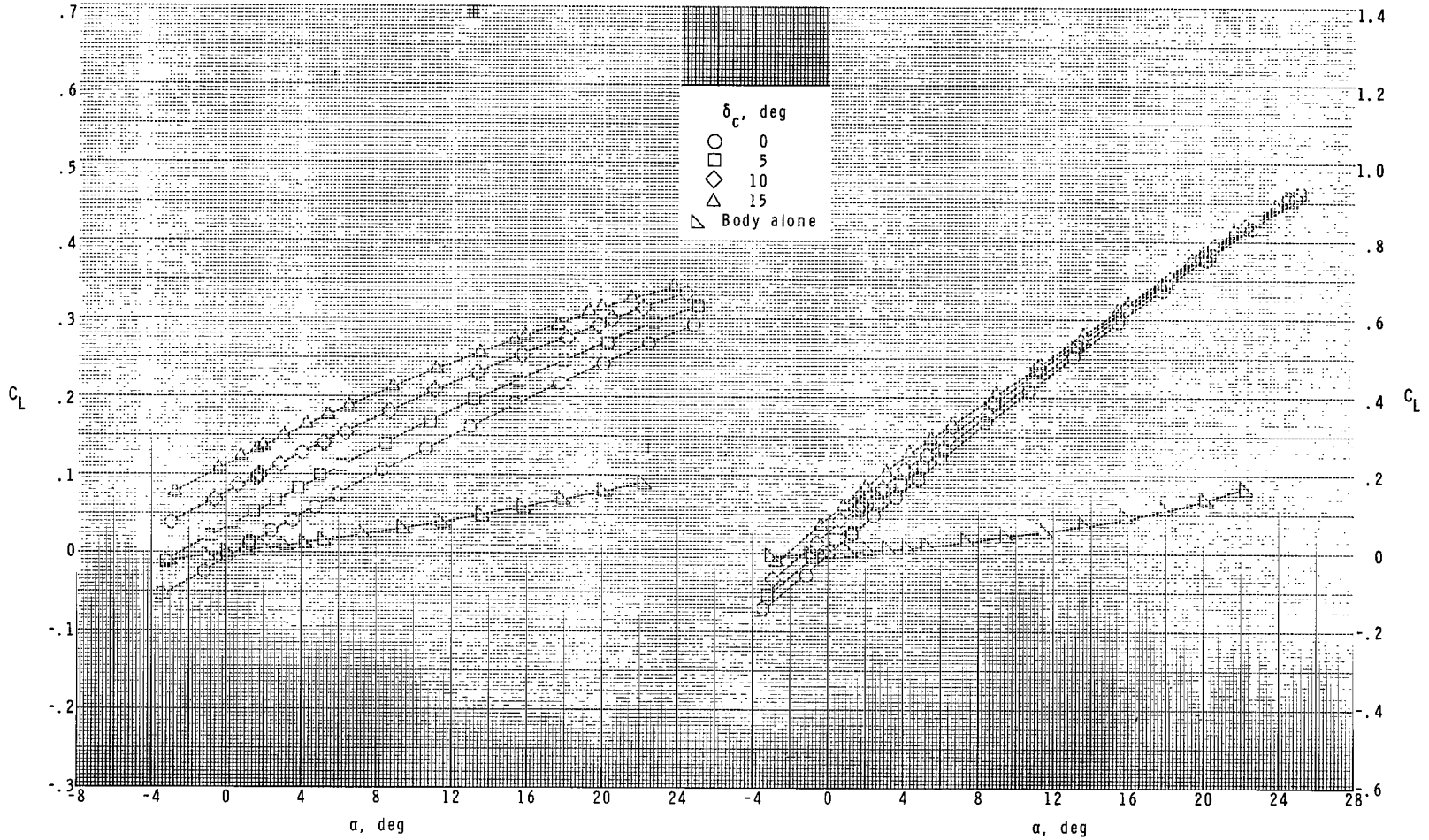

(c) M = 2.36.

Figure 6.- Continued.

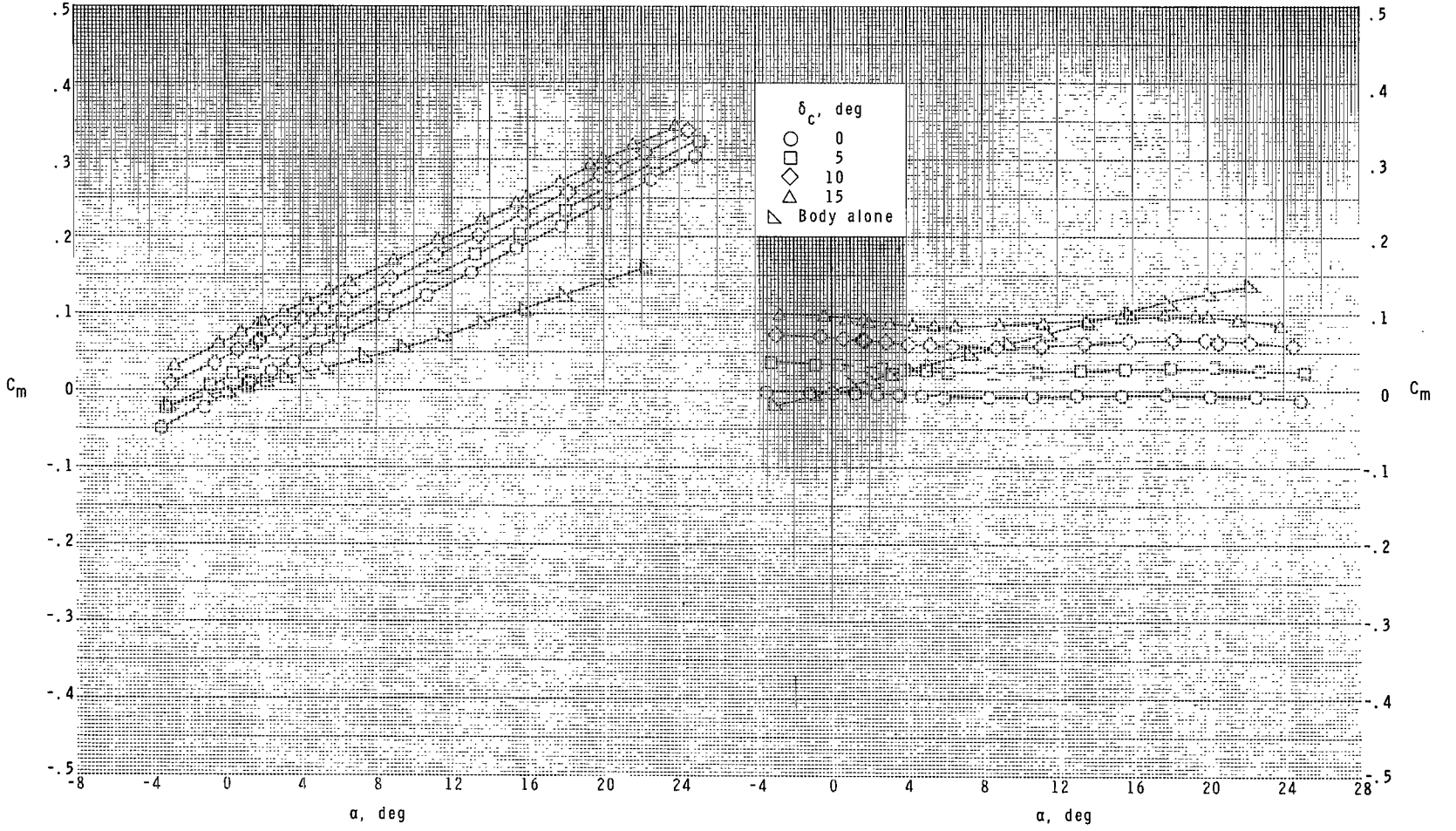

(c) Continued.

Figure 6.- Continued.

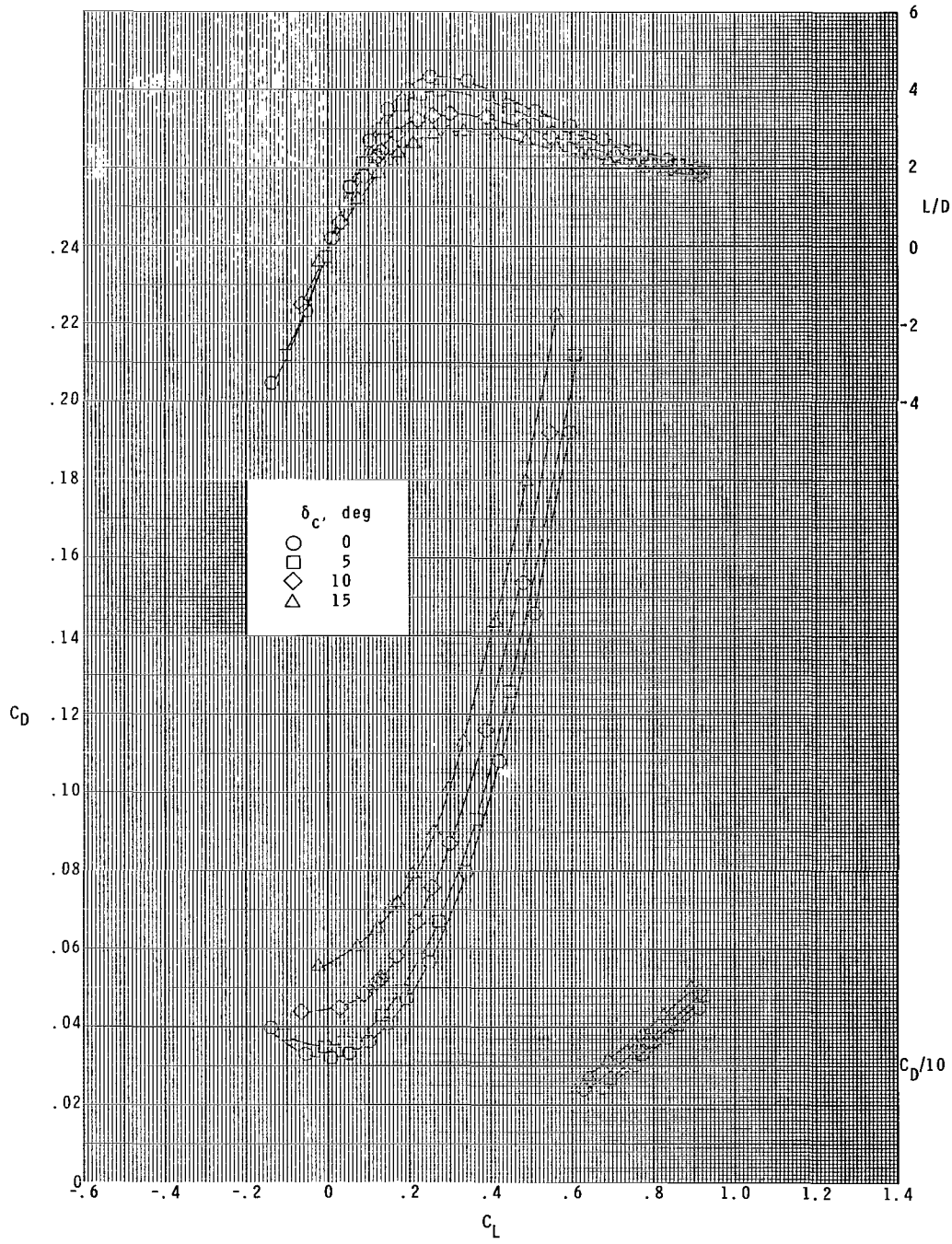

(c) Concluded.

Figure 6.- Continued.

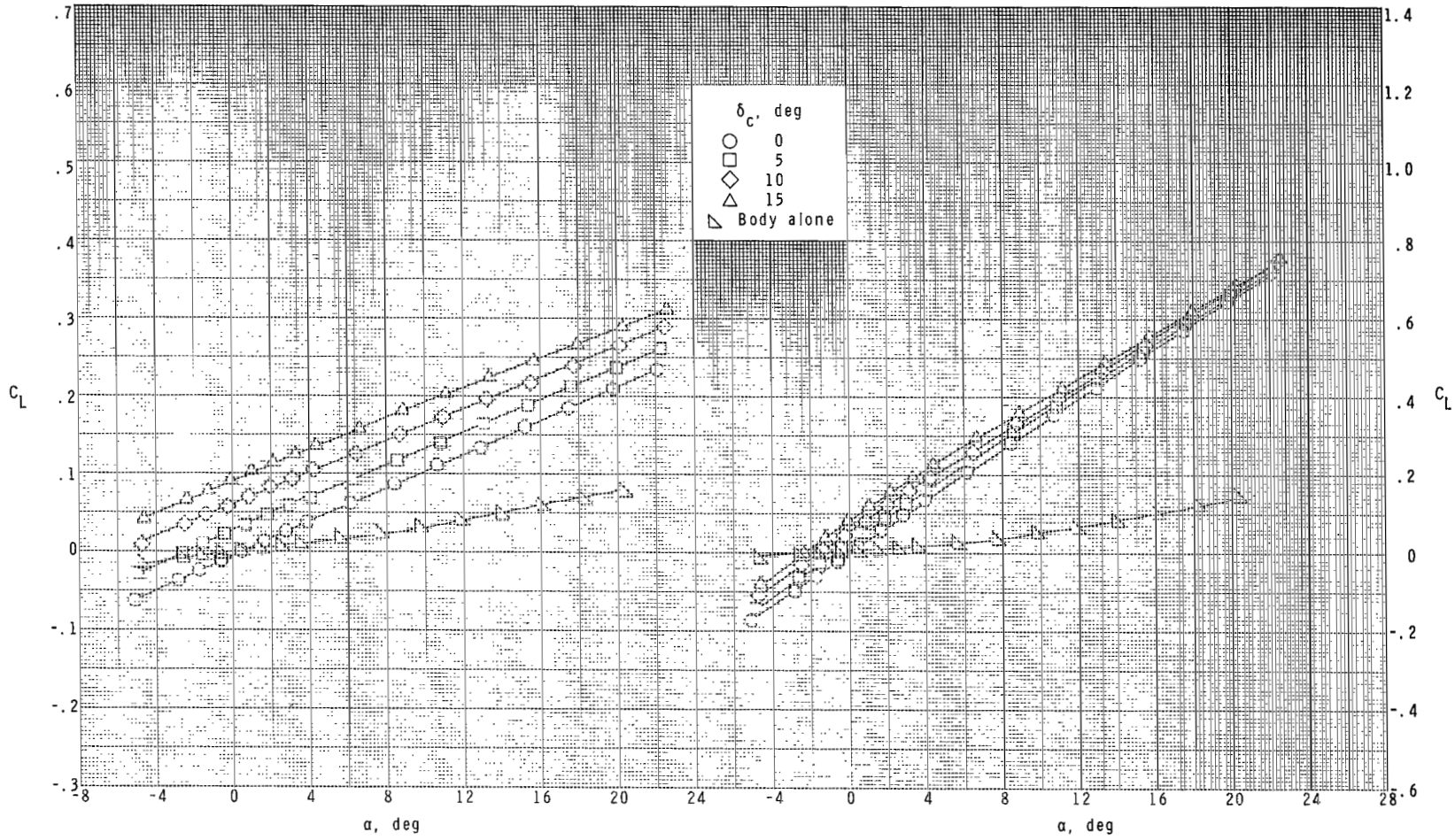

(d) M = 2.86.

Figure 6.- Continued.

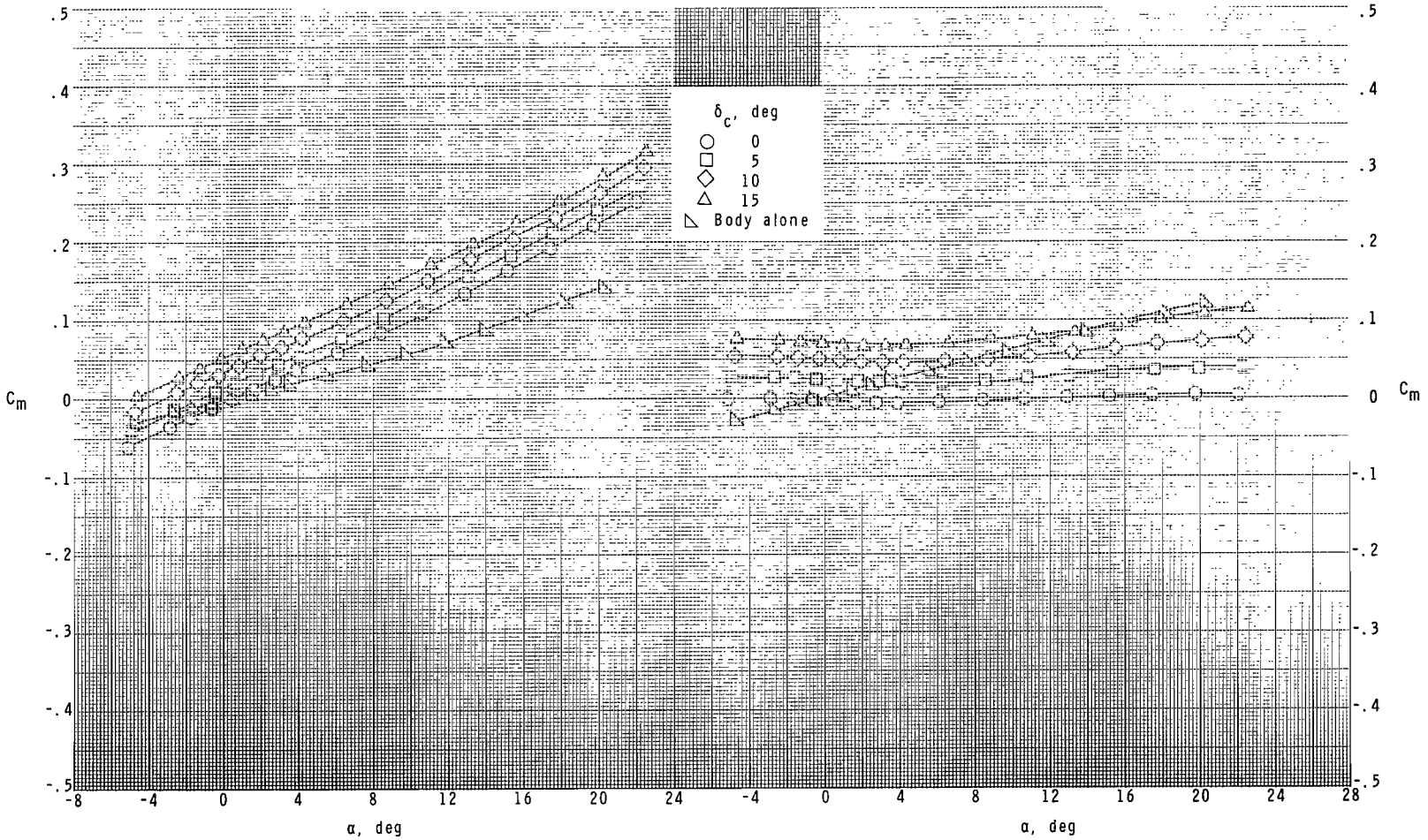

(d) Continued.

Figure 6.- Continued.

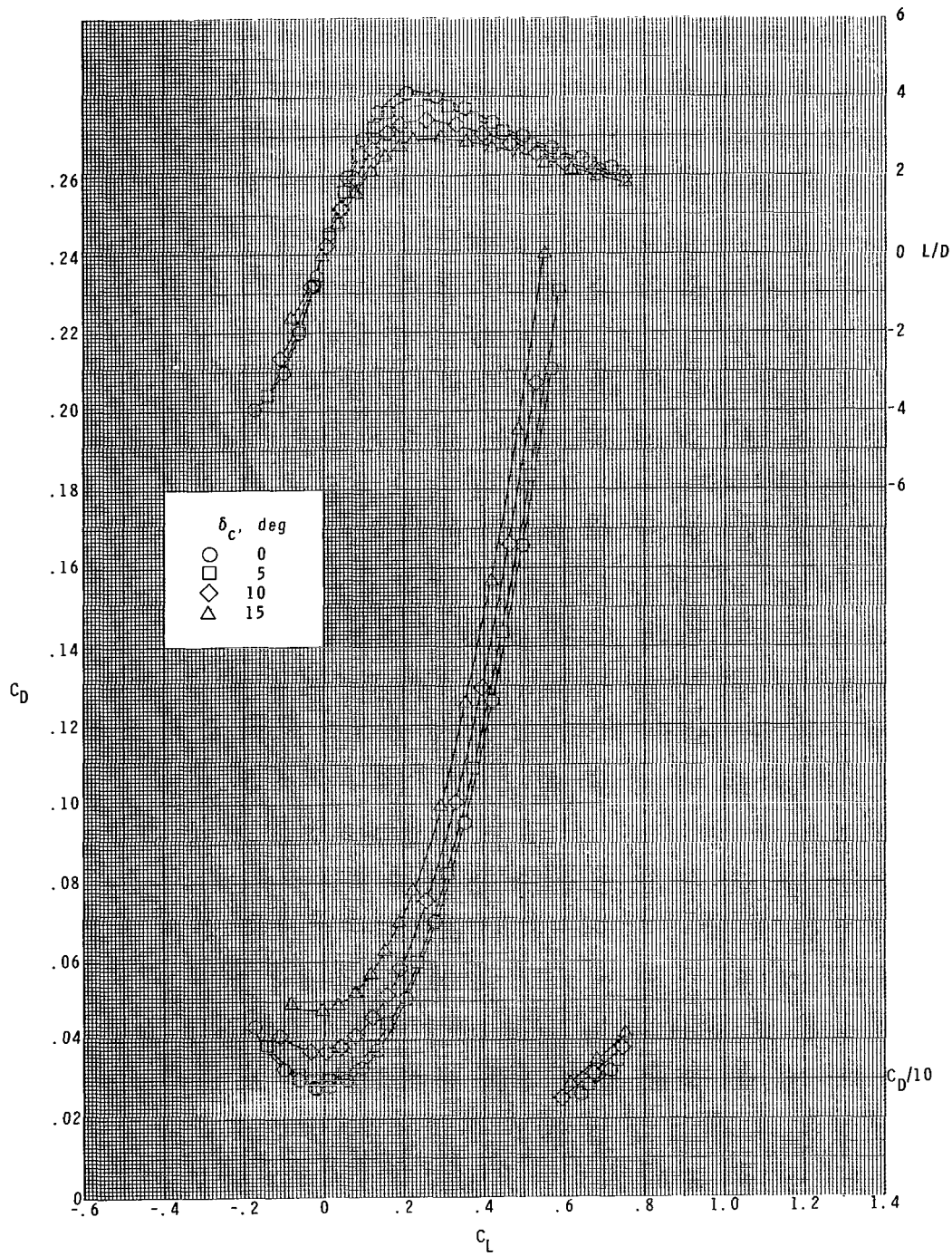

(d) Concluded.

Figure 6.- Concluded.

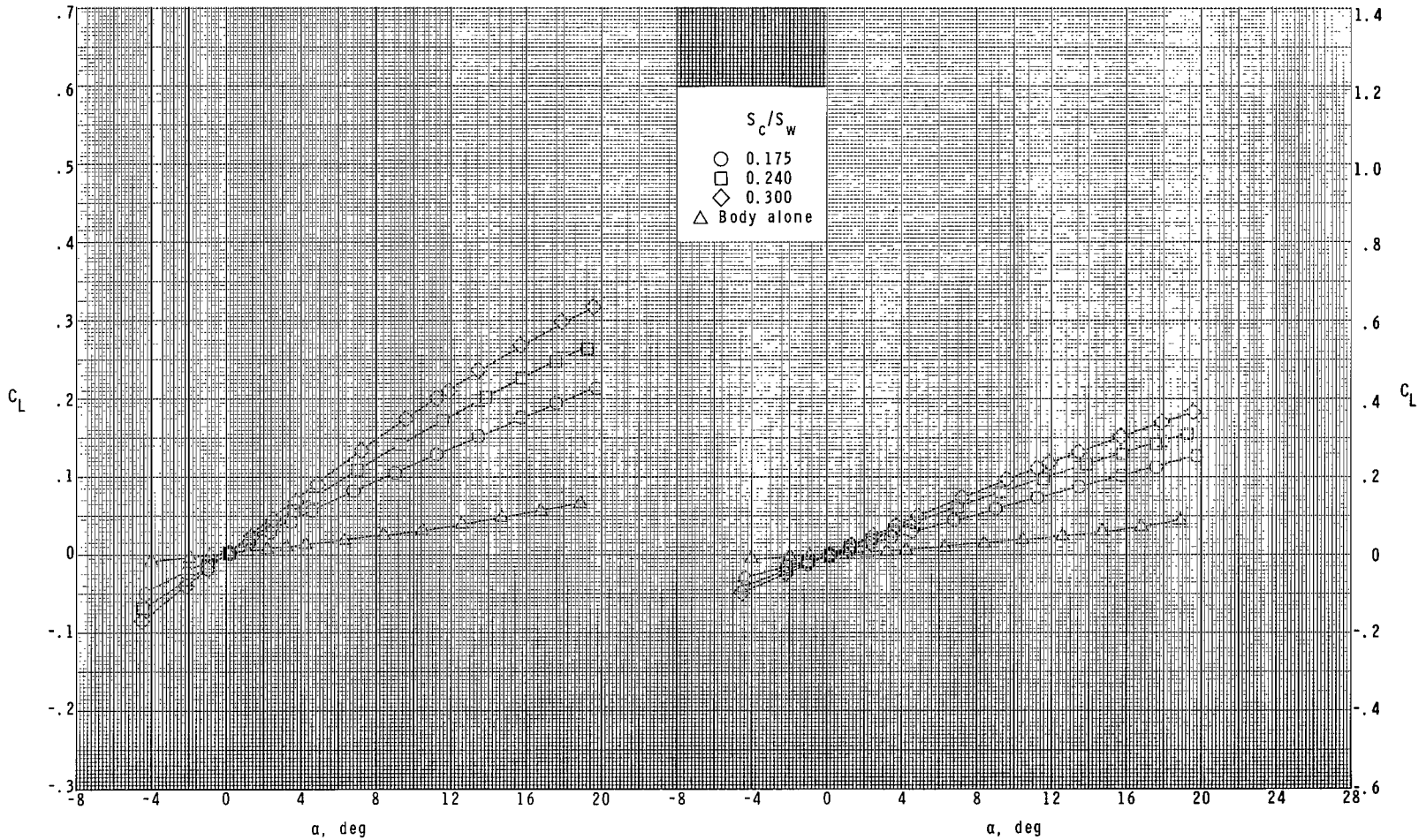

(a) M = 1.60.

Figure 7.- Longitudinal aerodynamic characteristics for all canards $(\delta_c = 0^o)$ with $z/\bar{c} = 0.0$ and wing off.

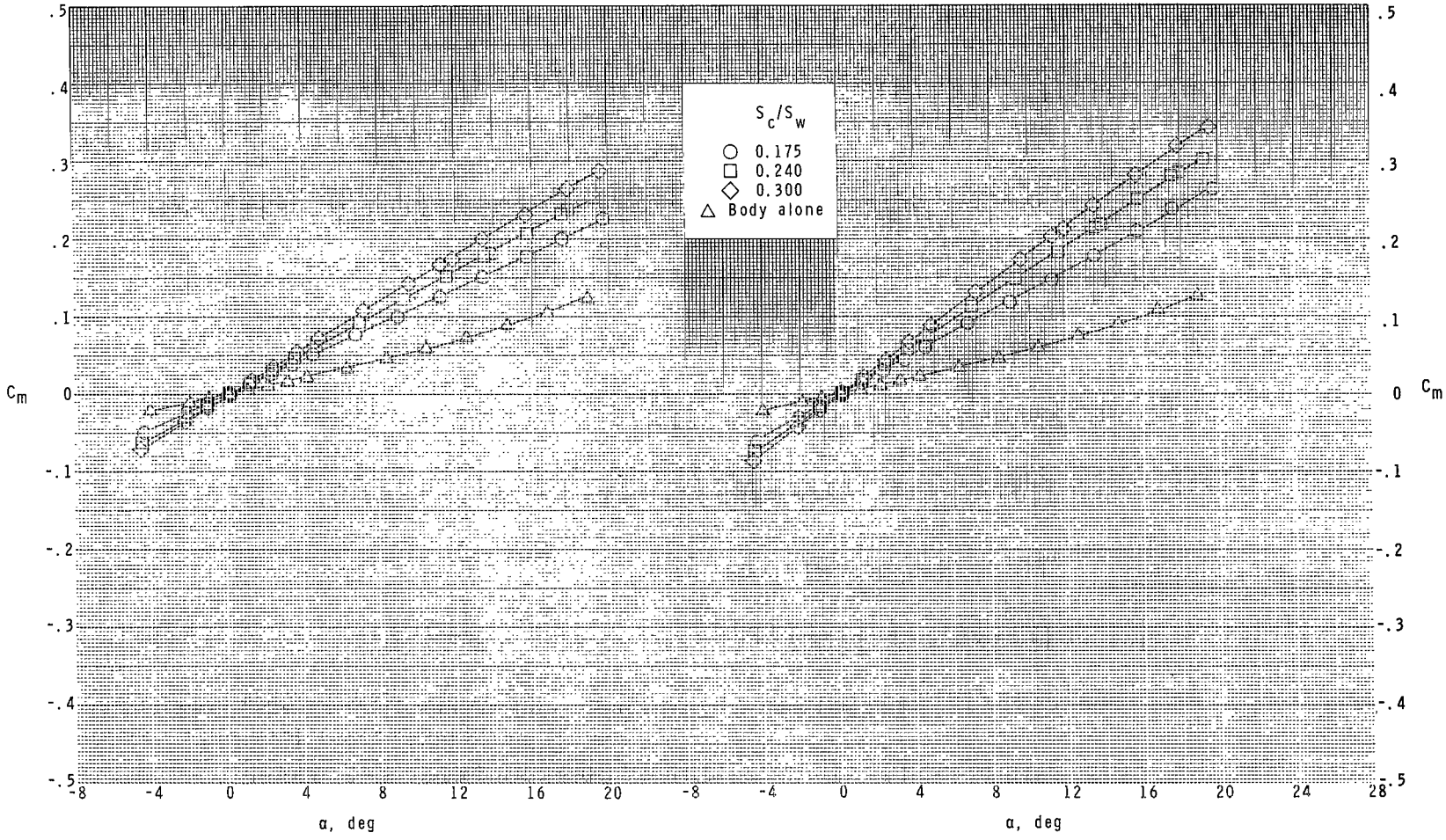

(a) Continued.

Figure 7.- Continued.

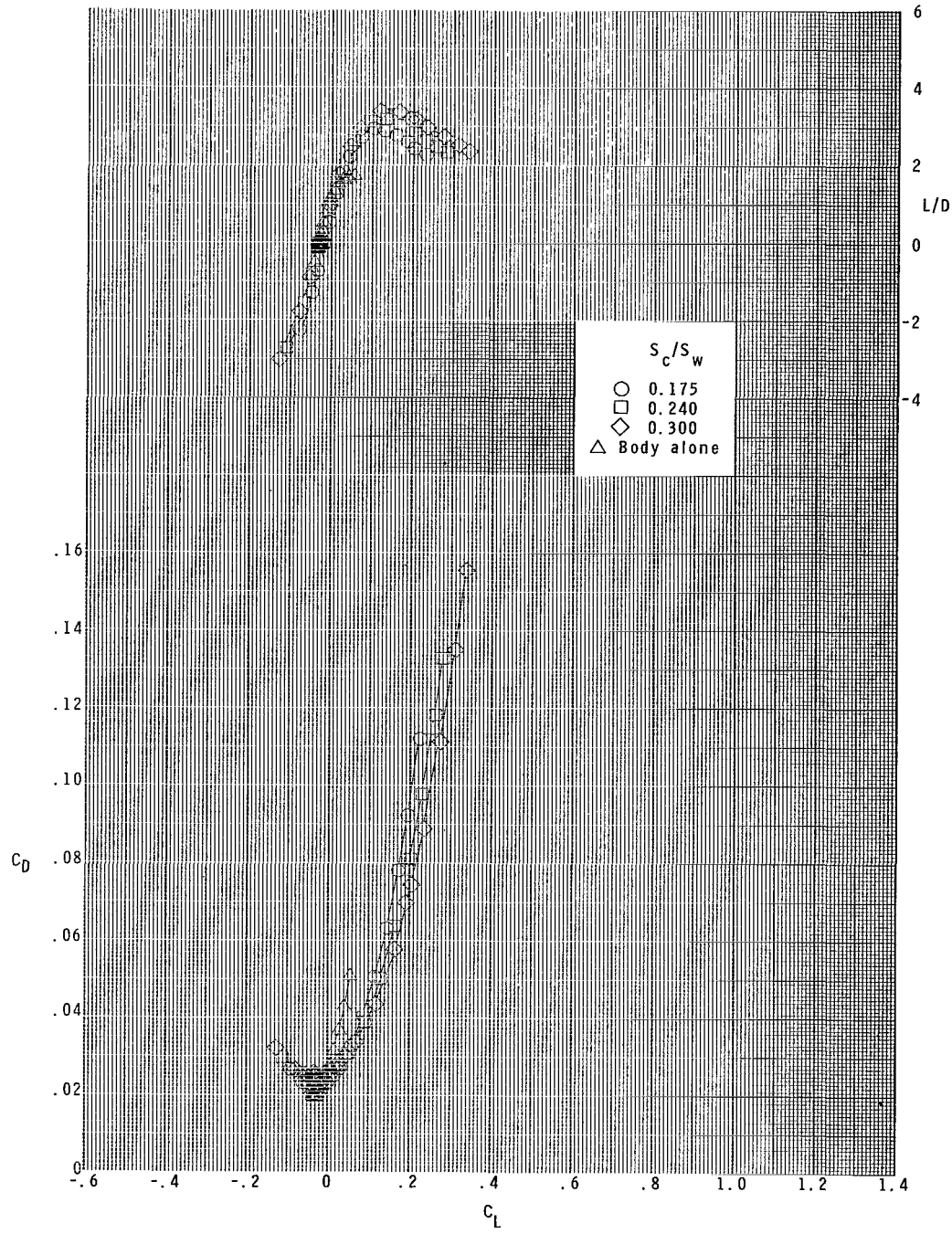

(a) Concluded.

Figure 7.- Continued.

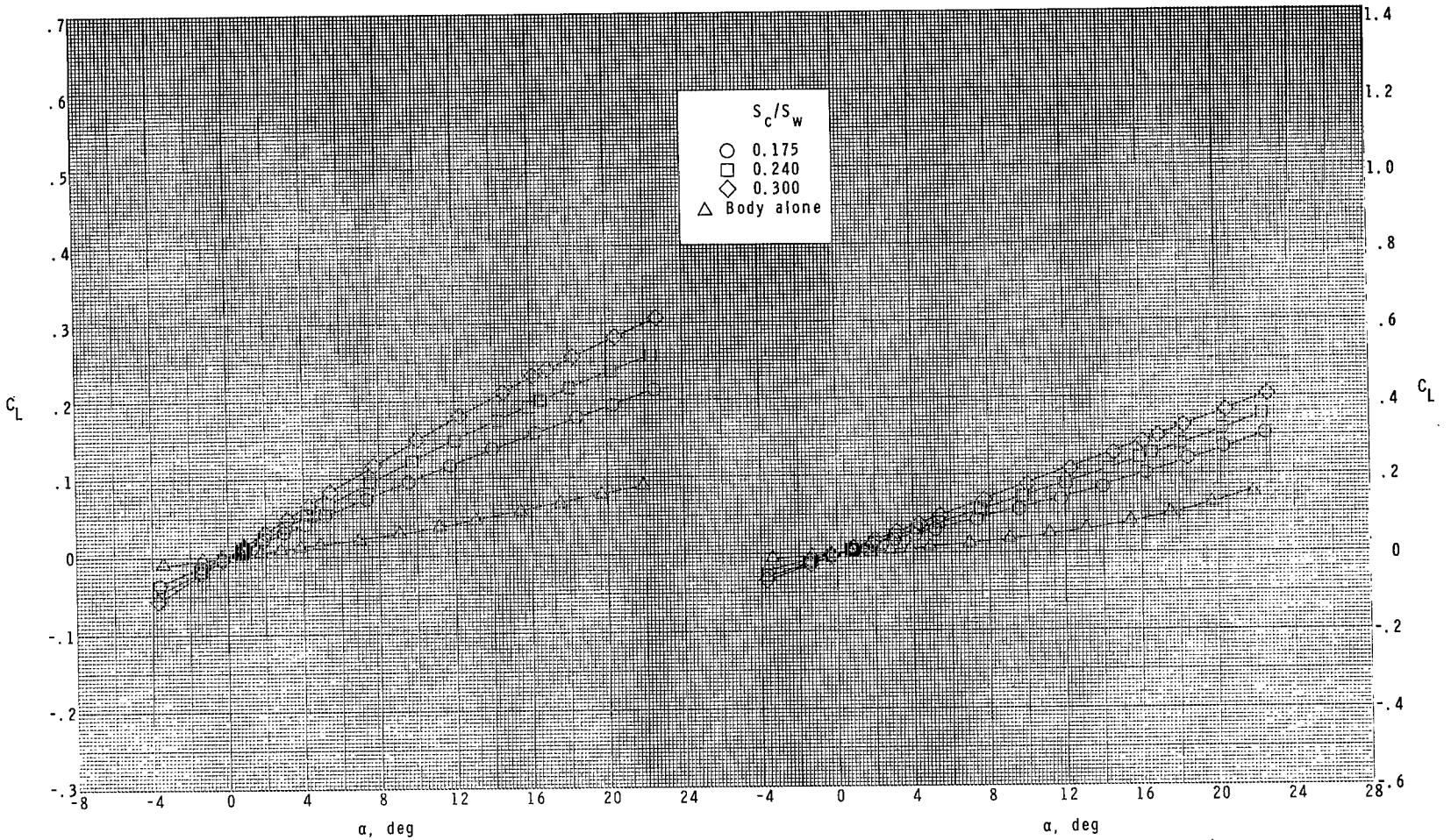

(b) M = 2.00.

Figure 7.- Continued.

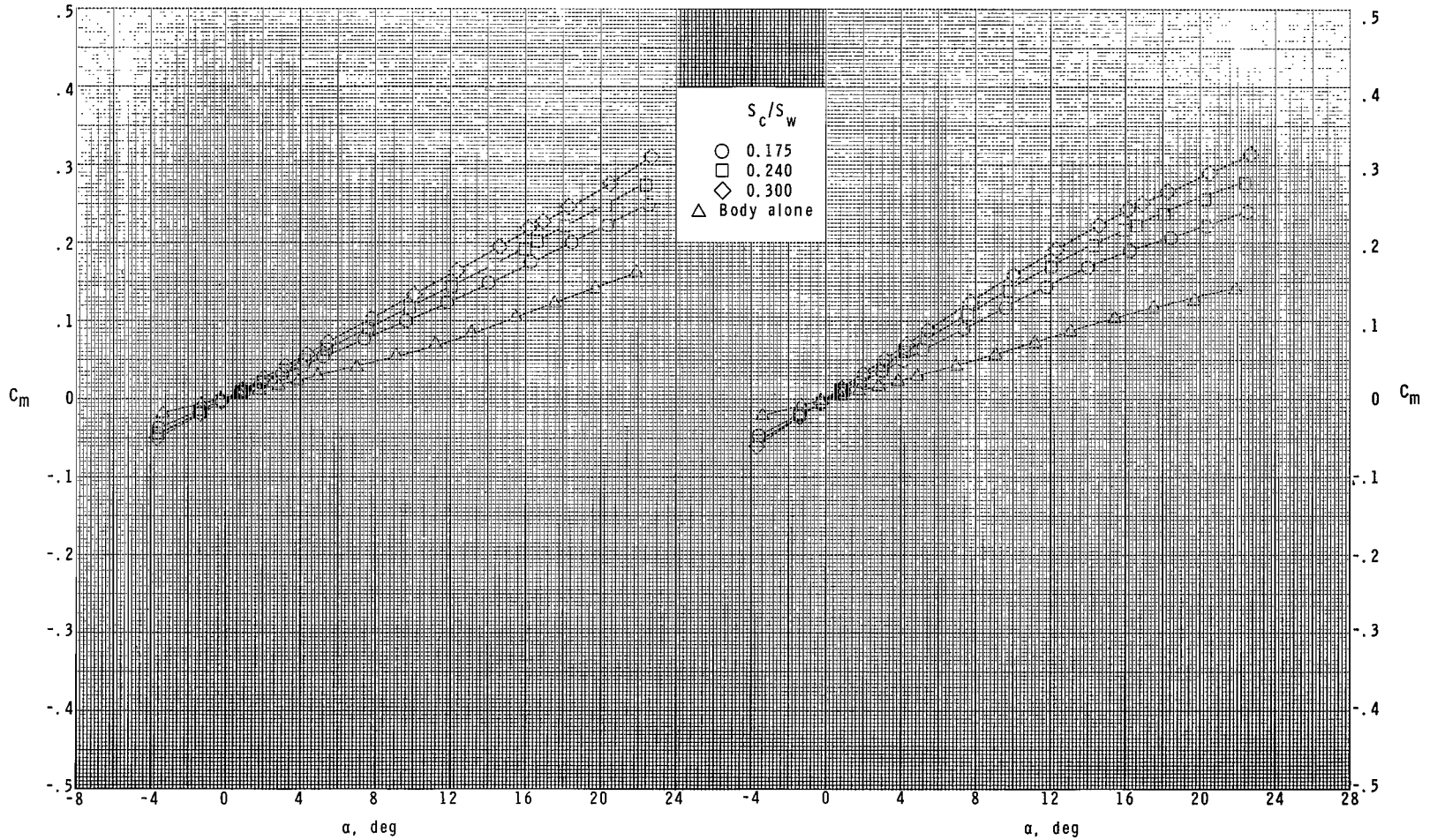

(b) Continued.

Figure 7.- Continued.

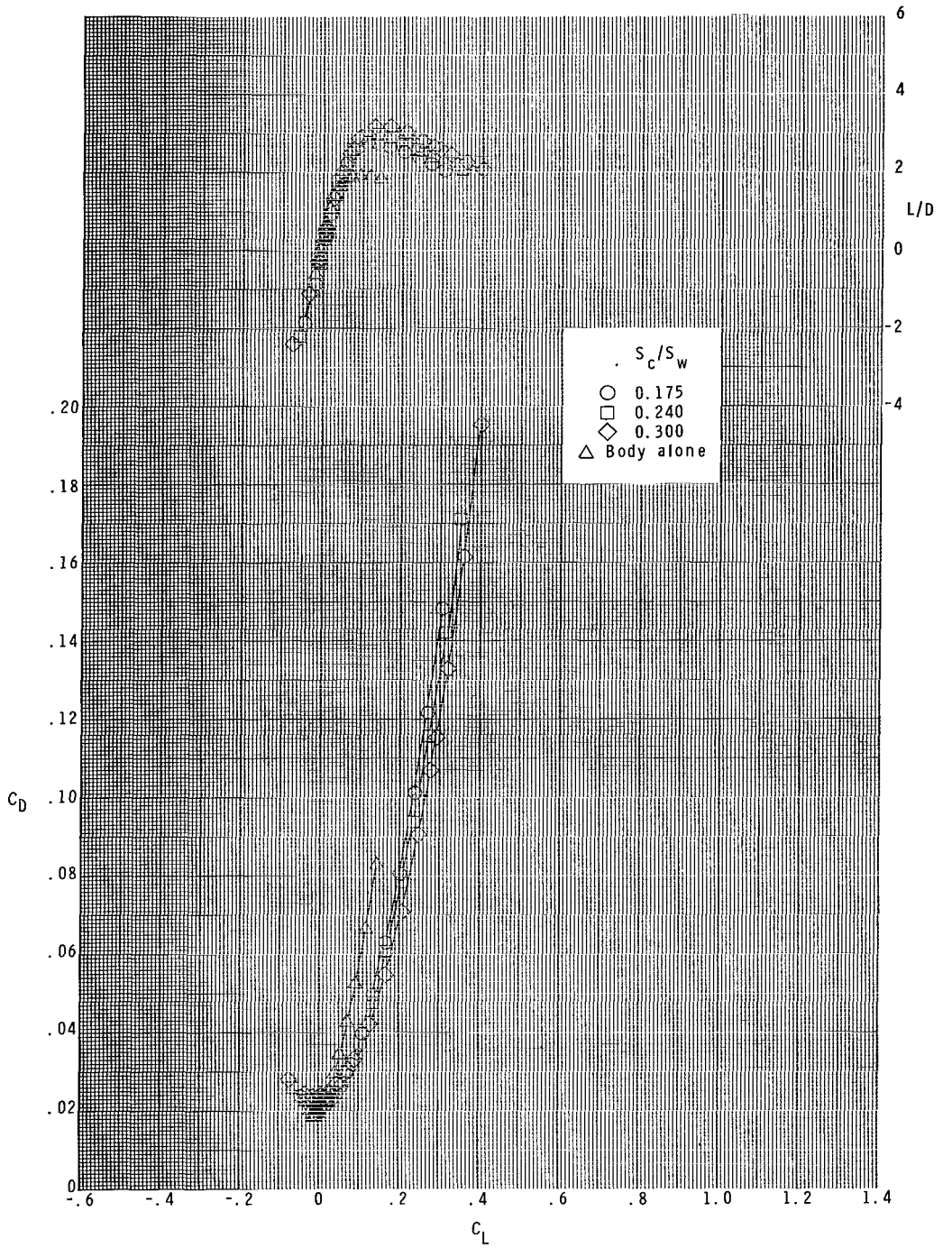

(b) Concluded.

Figure 7.- Continued.

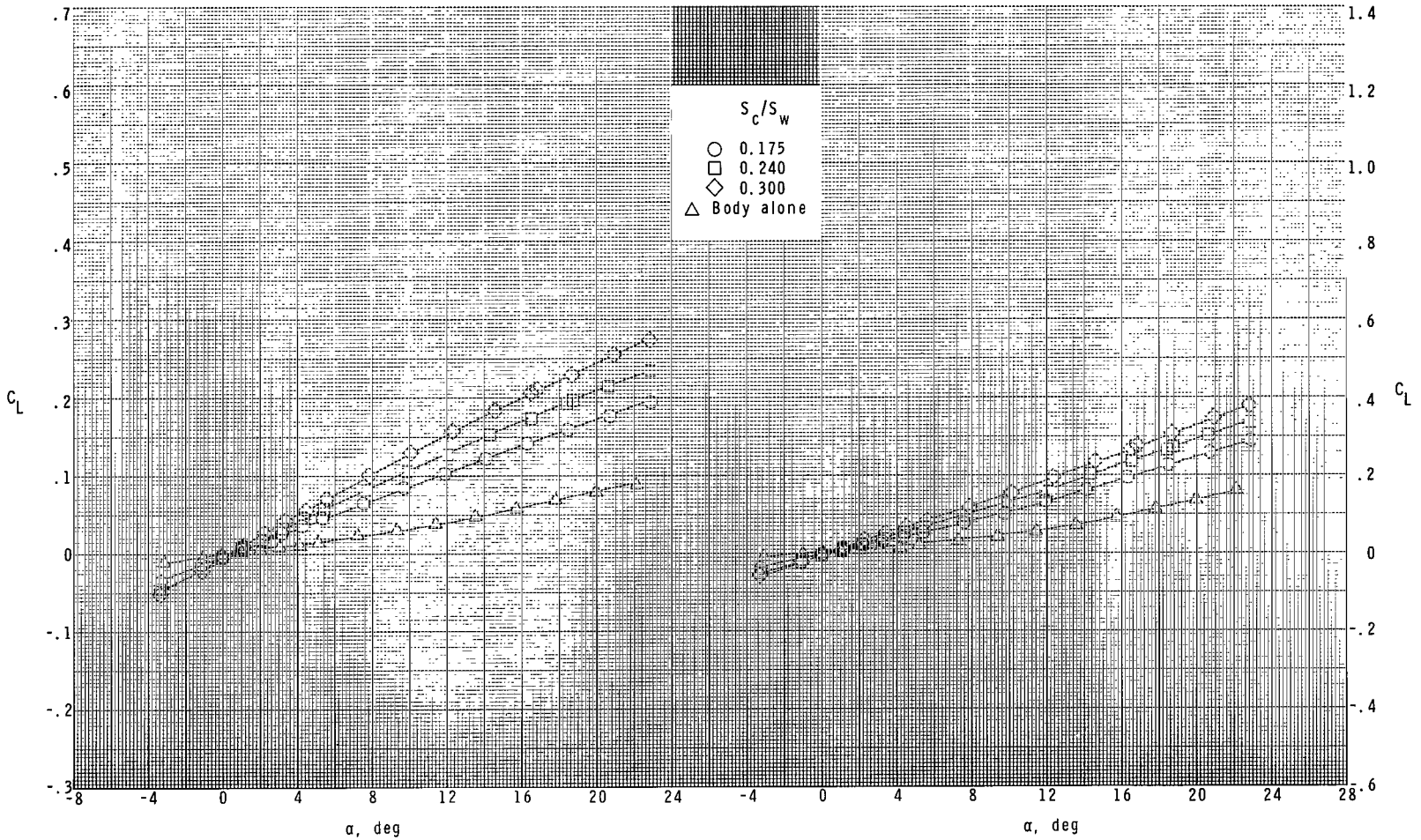

(c) M = 2.36.

Figure 7.- Continued.

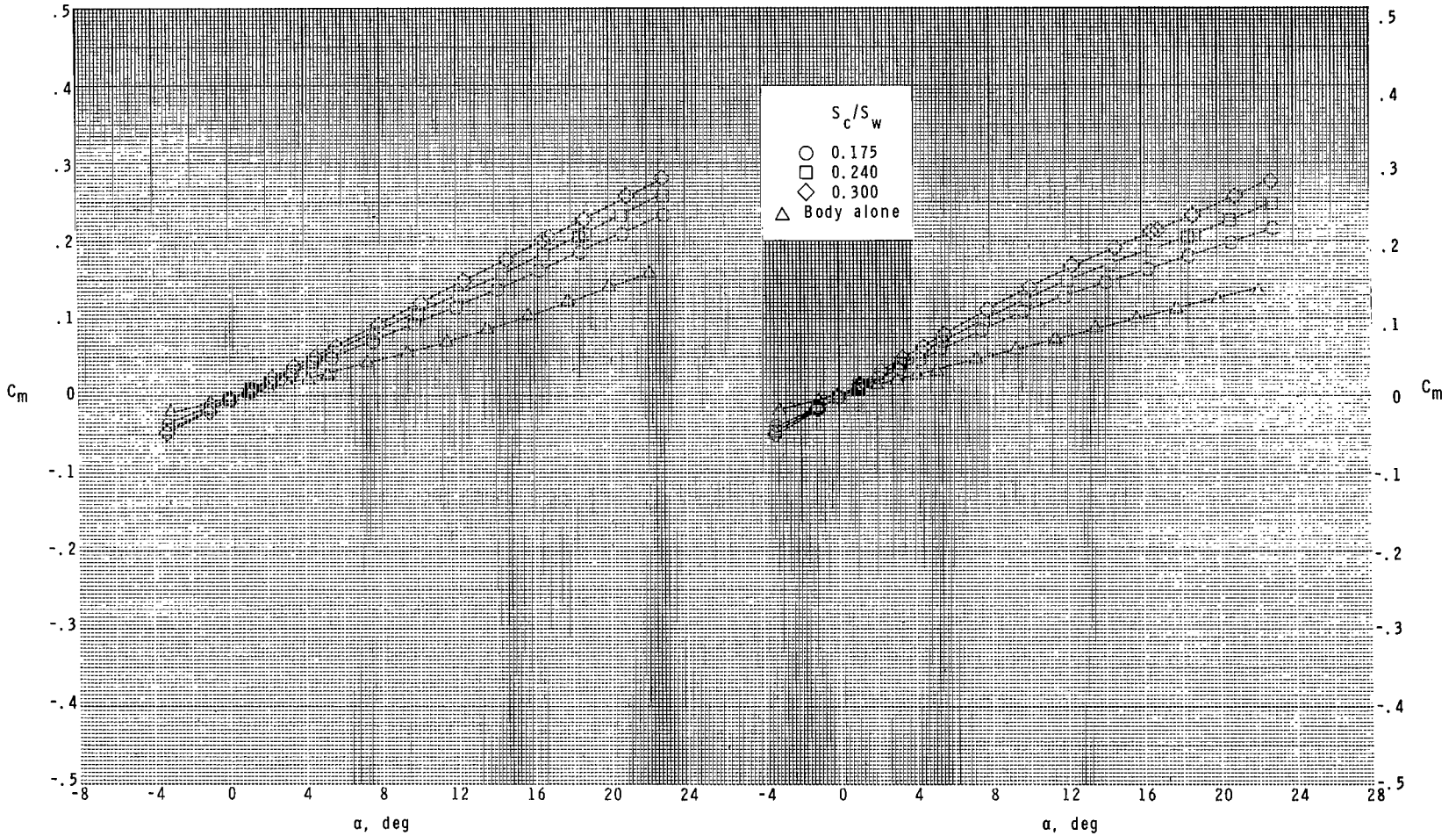

(c) Continued.

Figure 7.- Continued.

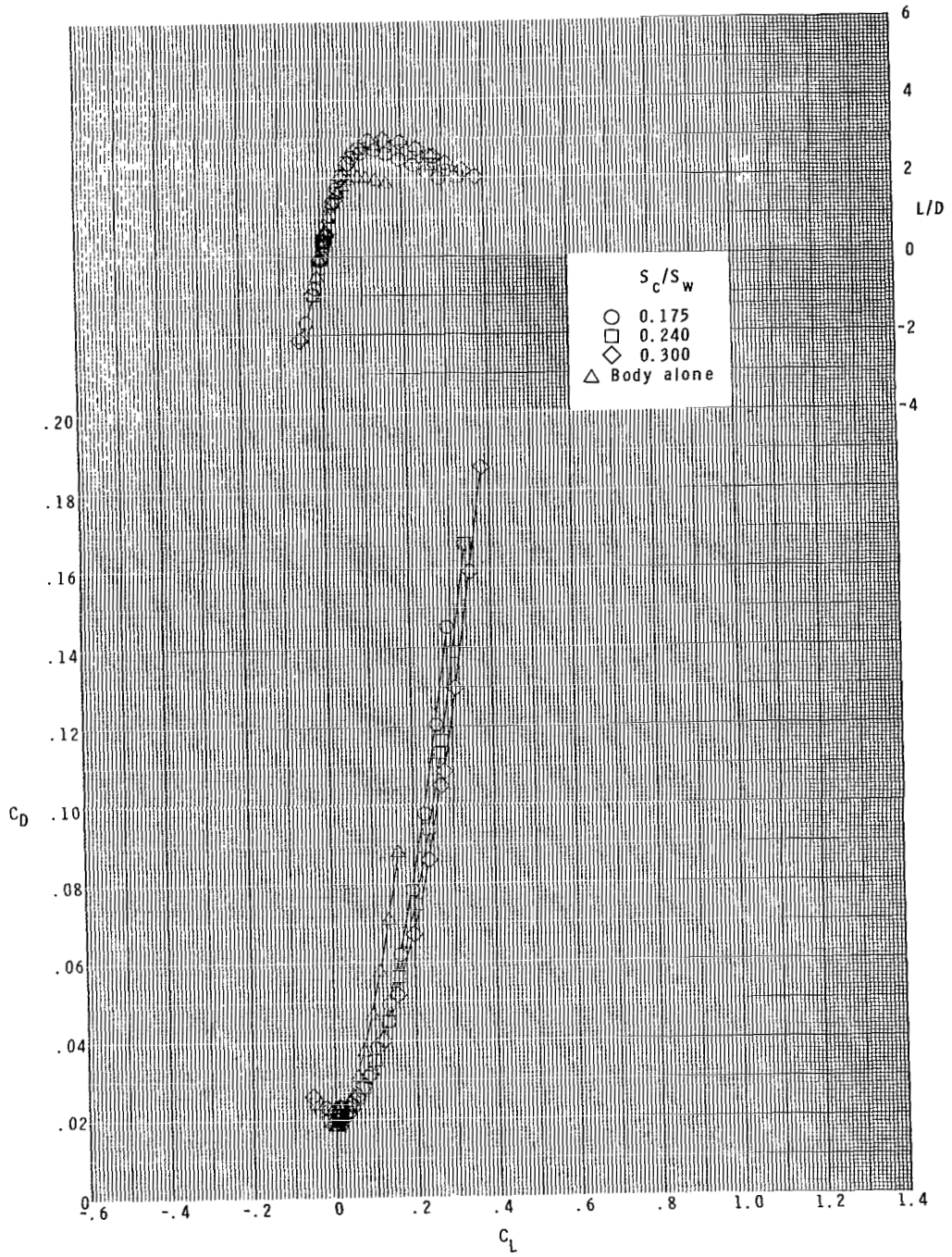

(c) Concluded.

Figure 7.- Continued.

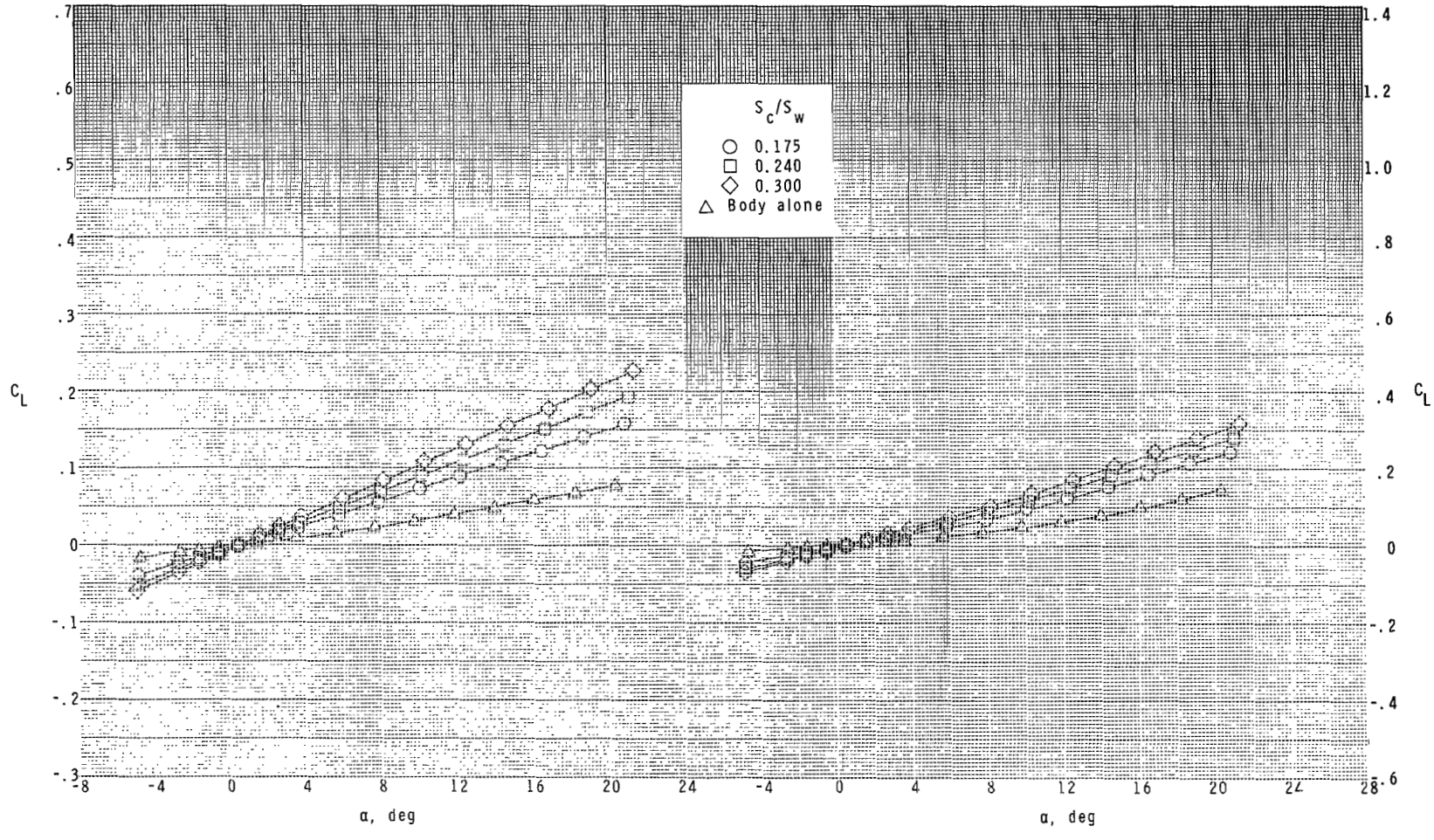

(d) M = 2.86.

Figure 7.- Continued.

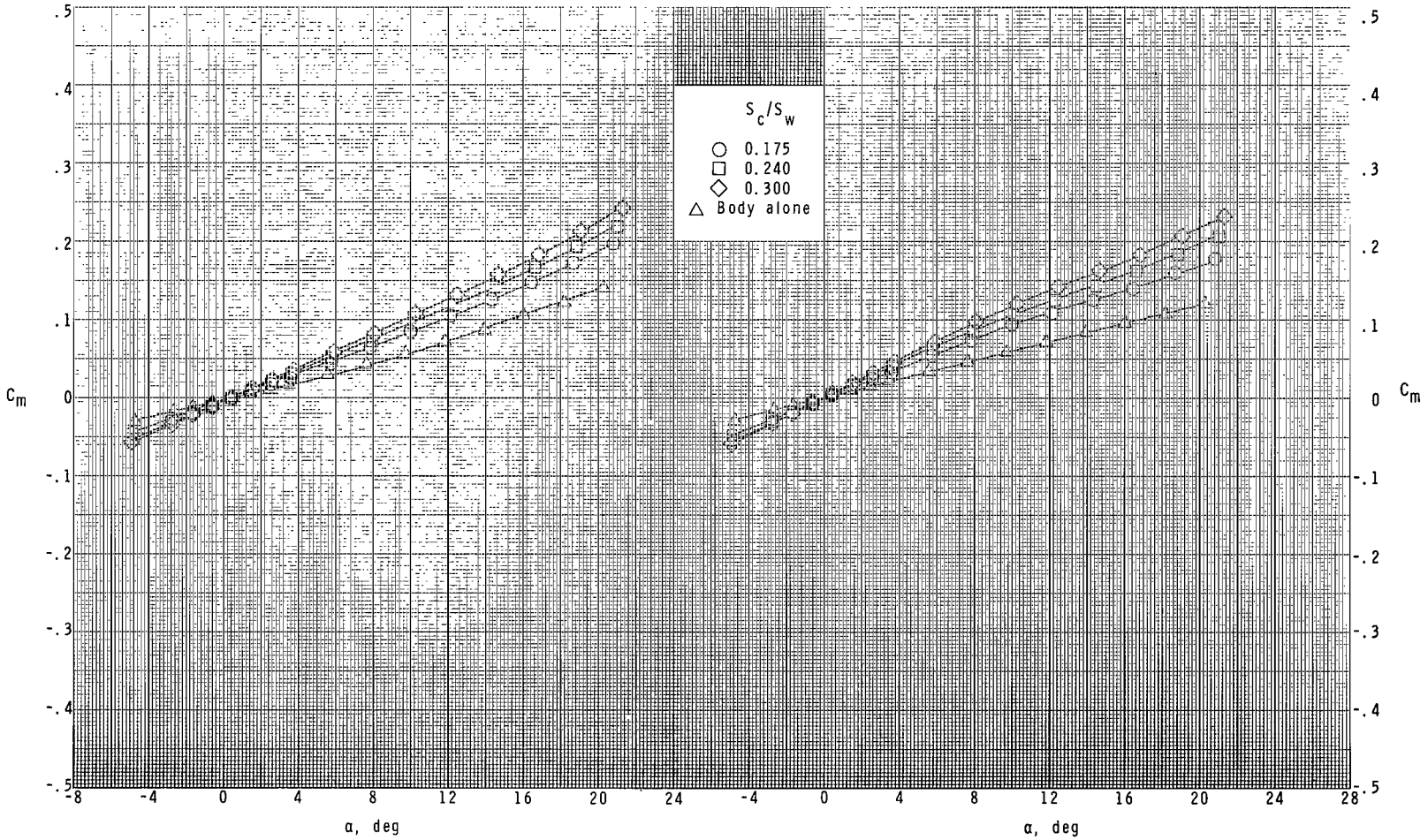

(d) Continued.

Figure 7.- Continued.

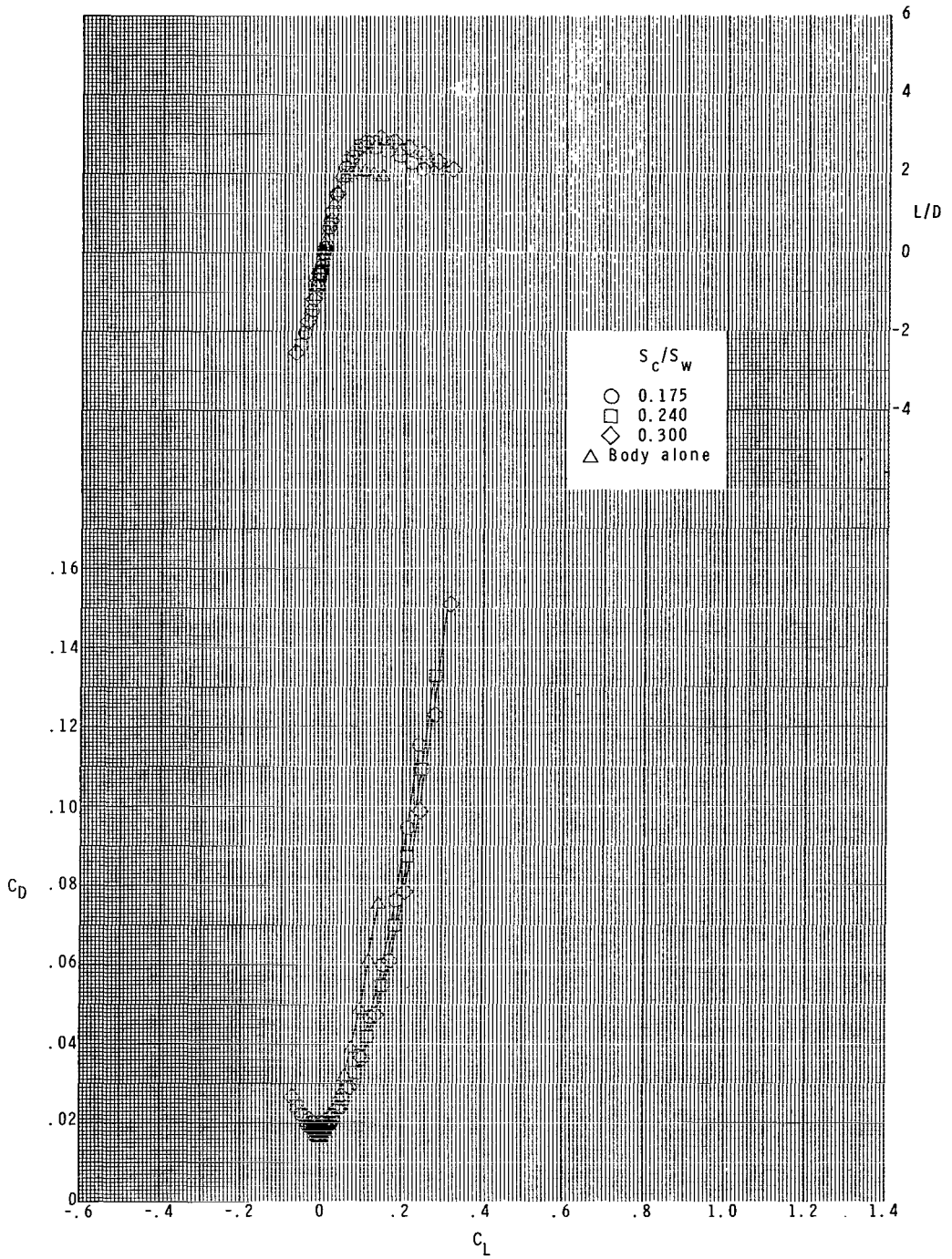

(d) Concluded.

Figure 7.- Concluded.

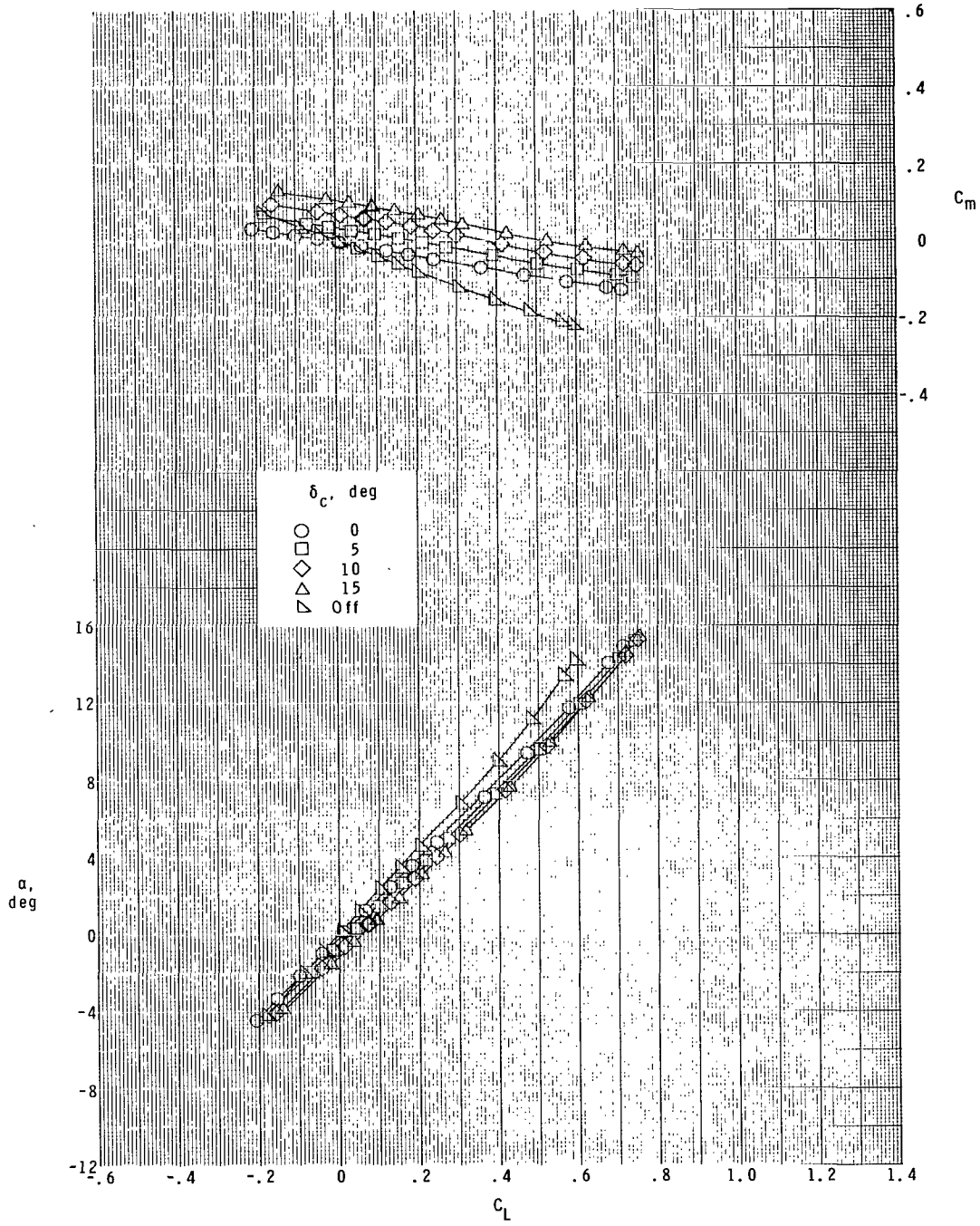

(a) M = 1.60.

Figure 8.- Longitudinal aerodynamic characteristics for $S_c/S_w = 0.175$ and $z/\bar{c} = 0.185$. (Data obtained from main balance.)

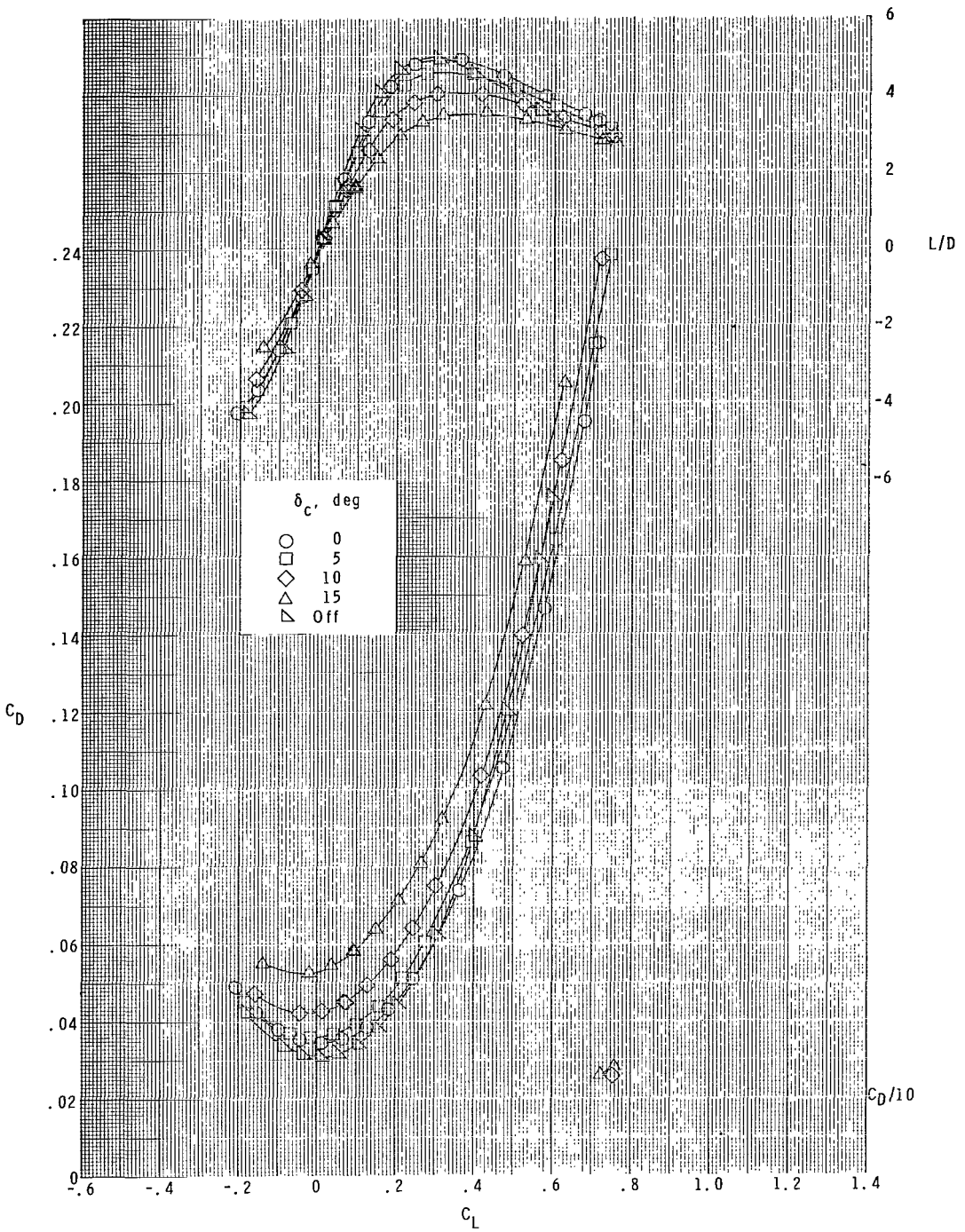

(a) Concluded.

Figure 8.- Continued.

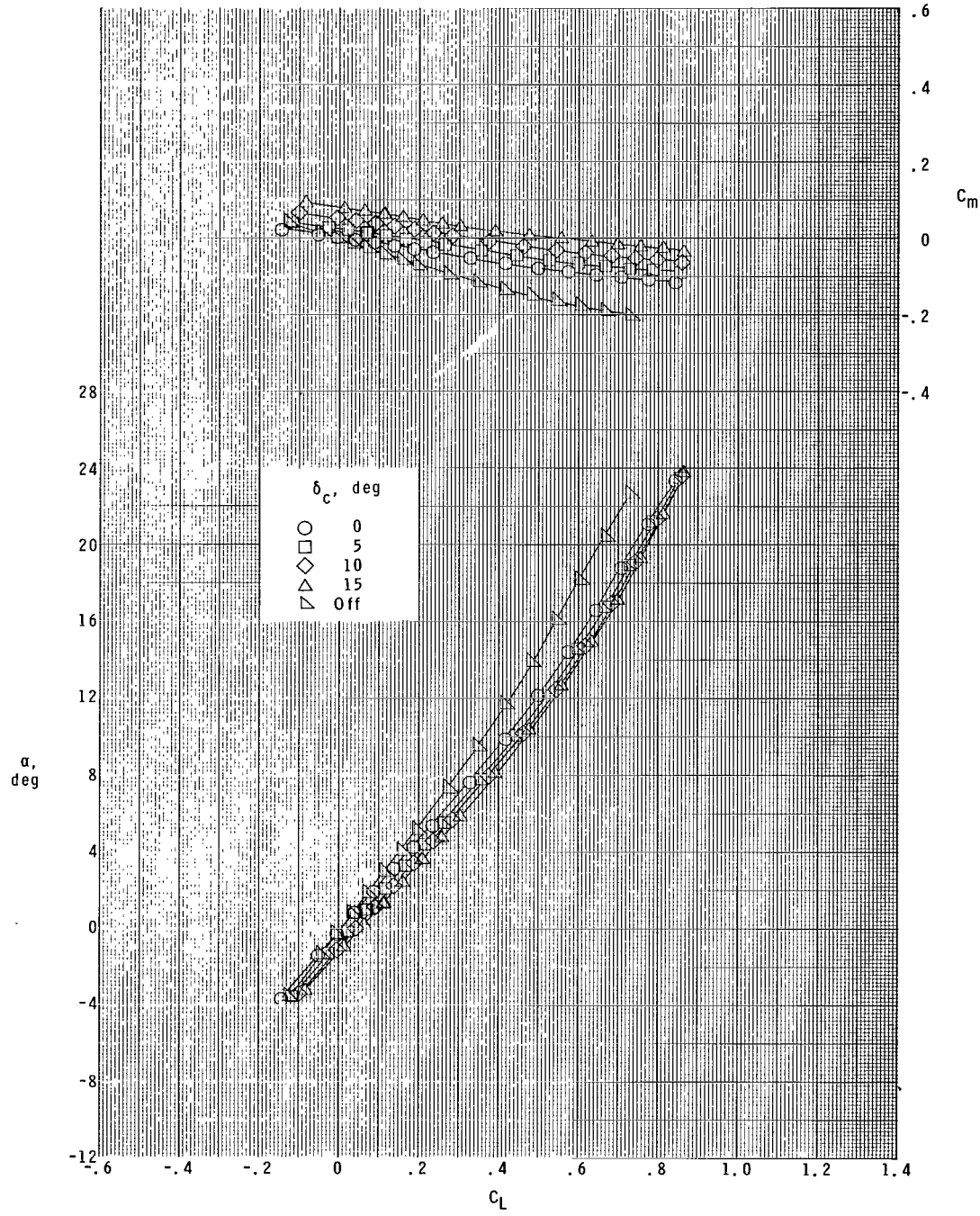

(b) M = 2.00.

Figure 8.- Continued.

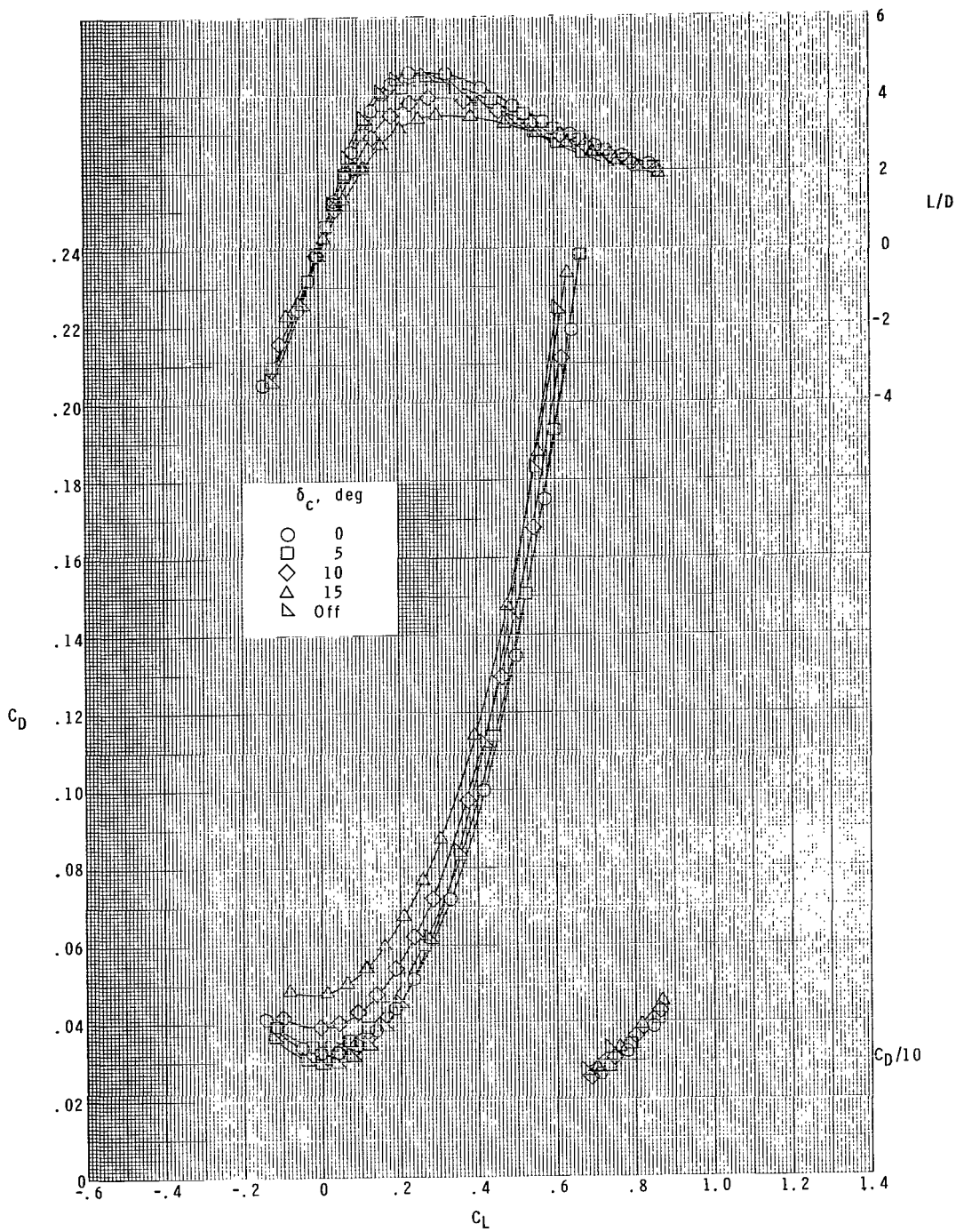

(b) Concluded.

Figure 8.- Concluded.

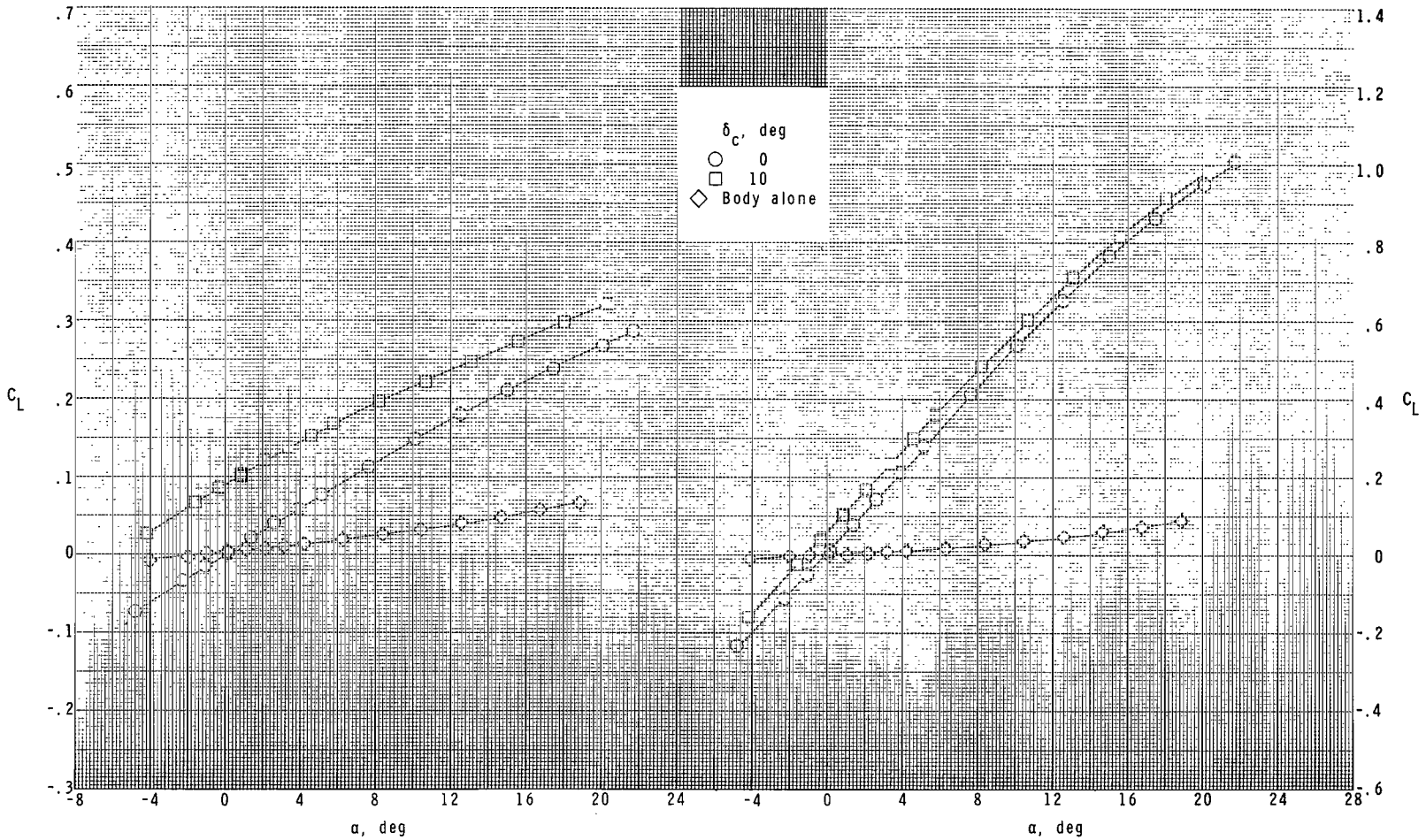

(a) M = 1.60.

Figure 9.- Longitudinal aerodynamic characteristics for $S_c/S_w = 0.240$ and $z/\bar{c} = 0.185$.

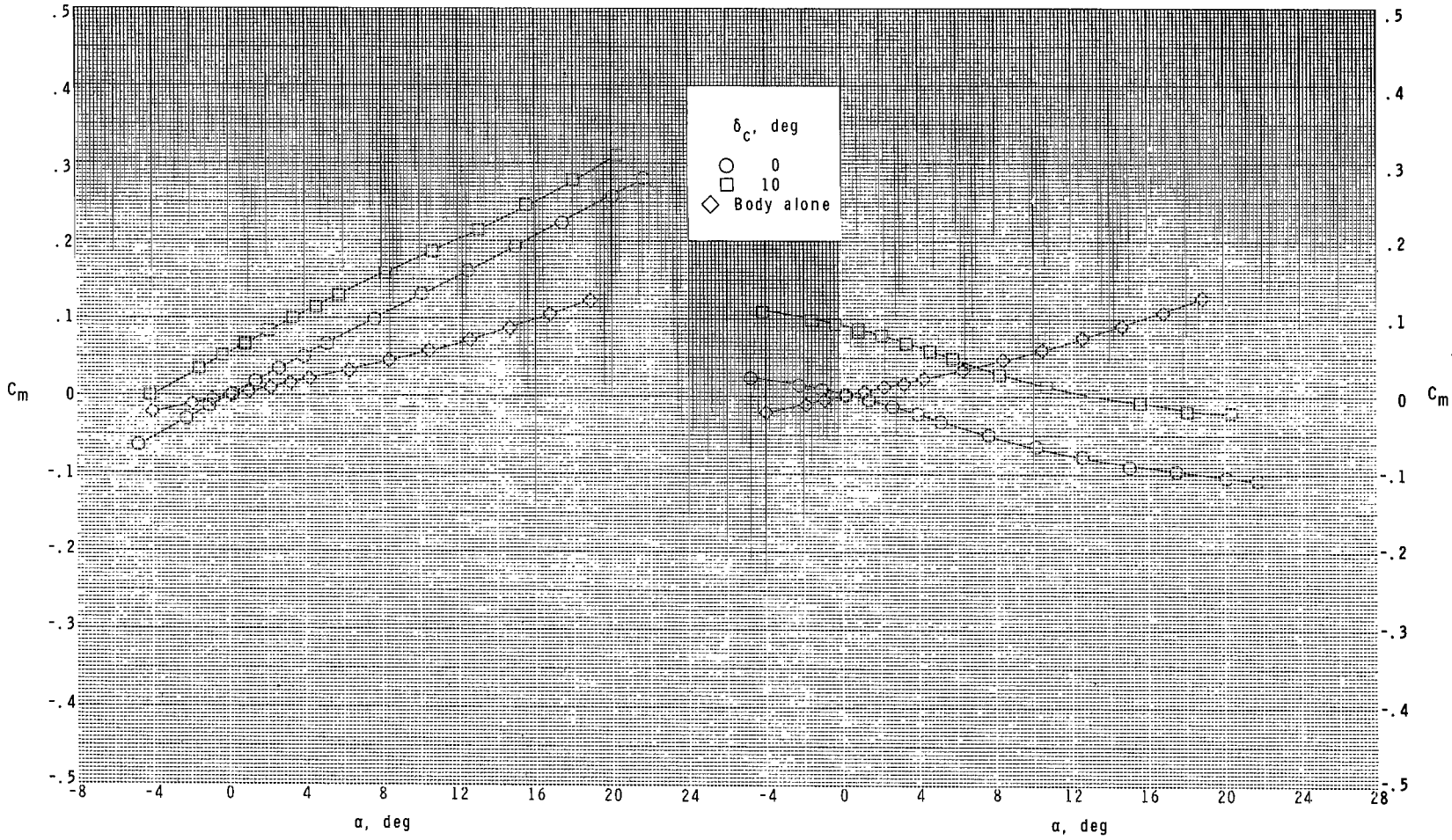

Canard balance

Main balance

(a) Continued.

Figure 9.- Continued.

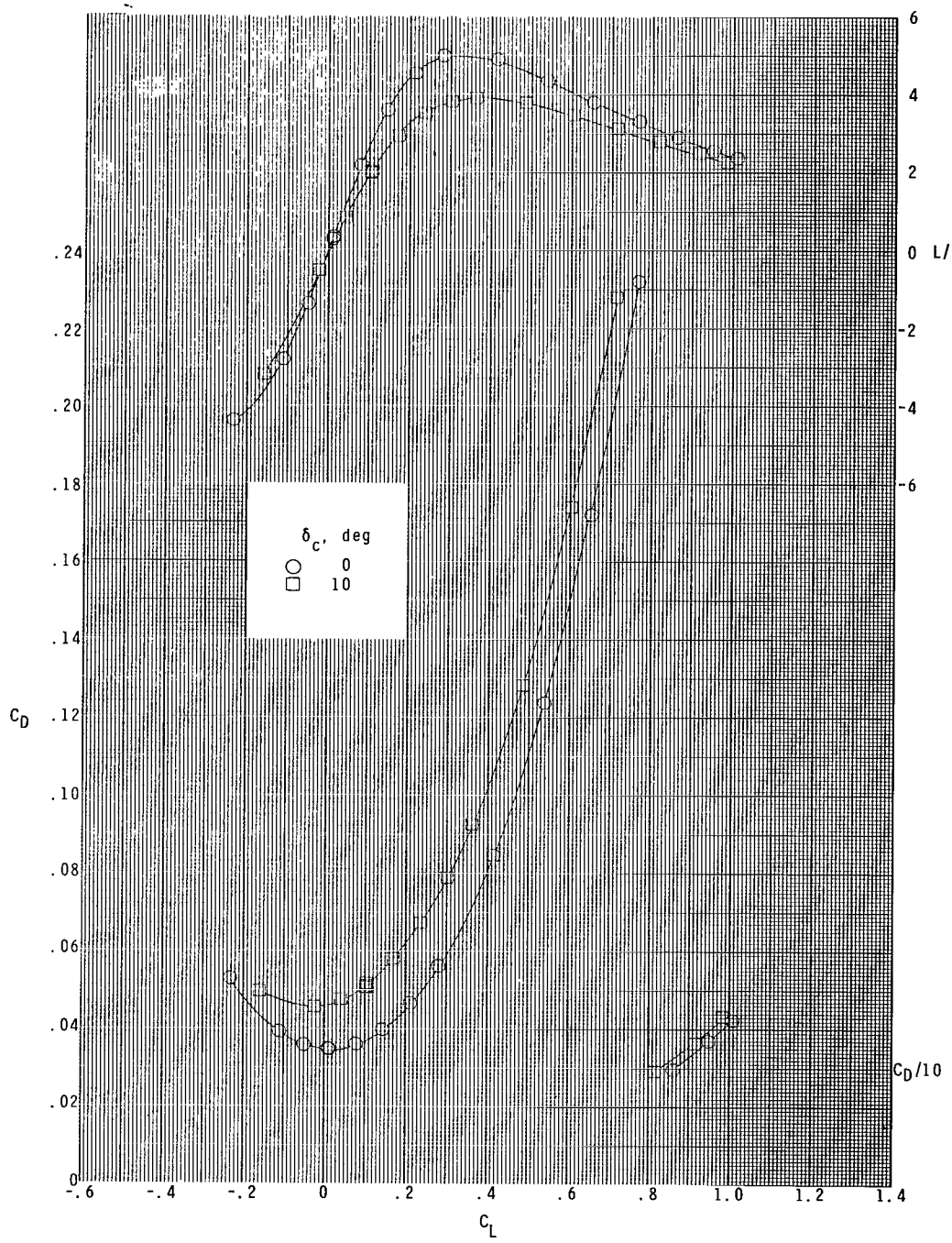

(a) Concluded.

Figure 9.- Continued.

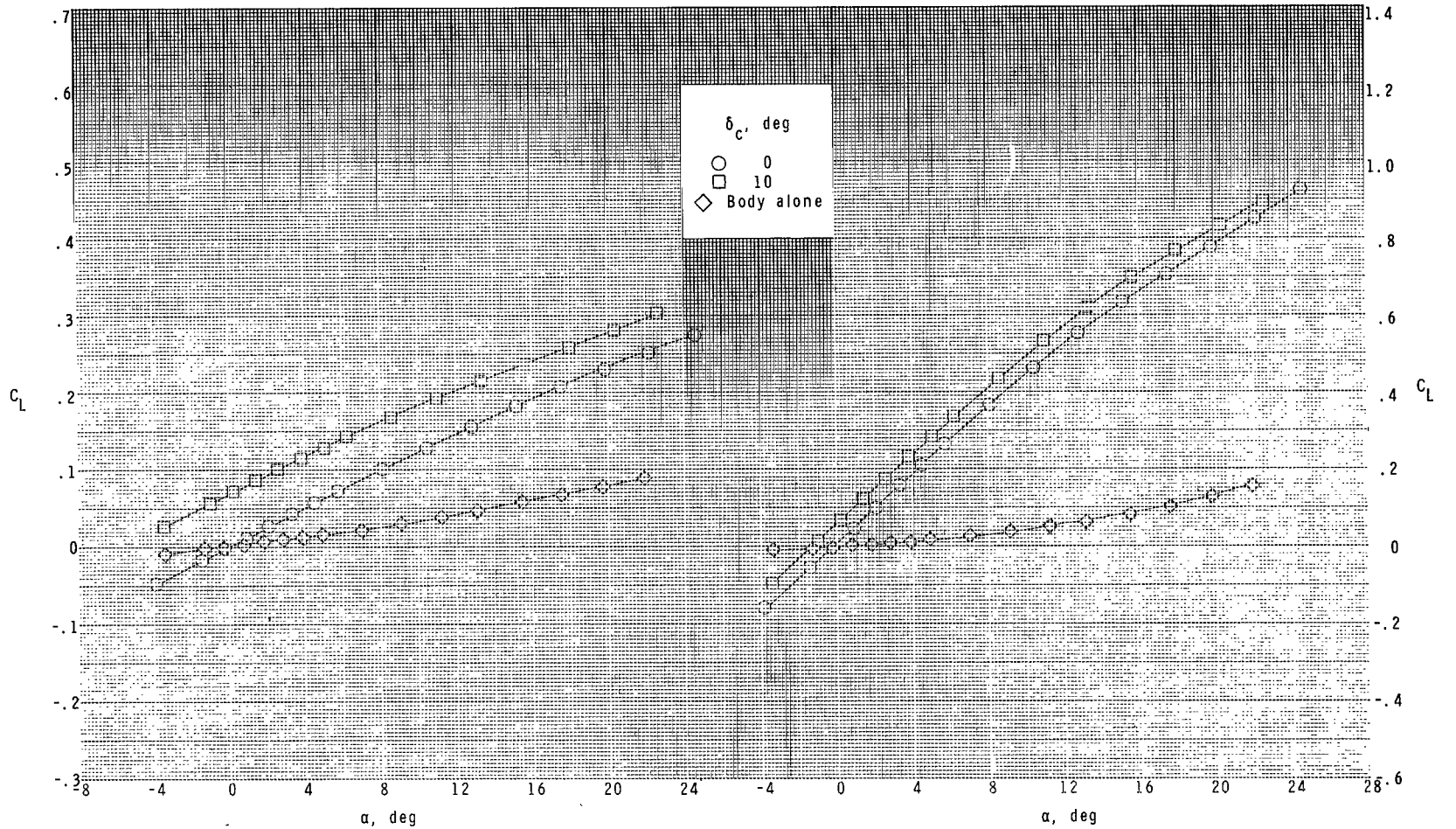

(b) M = 2.00.

Figure 9.- Continued.

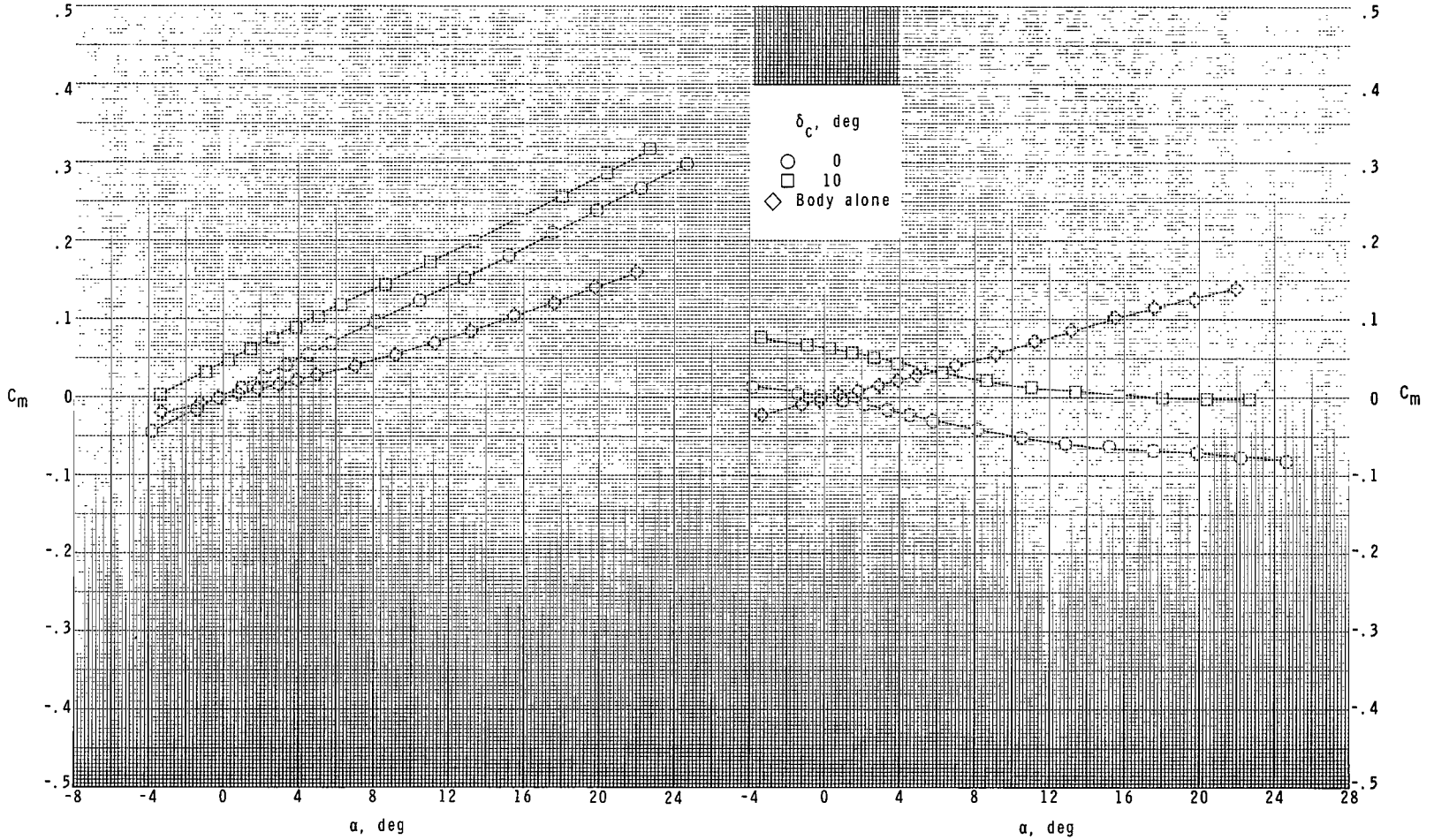

(b) Continued.

Figure 9.- Continued.

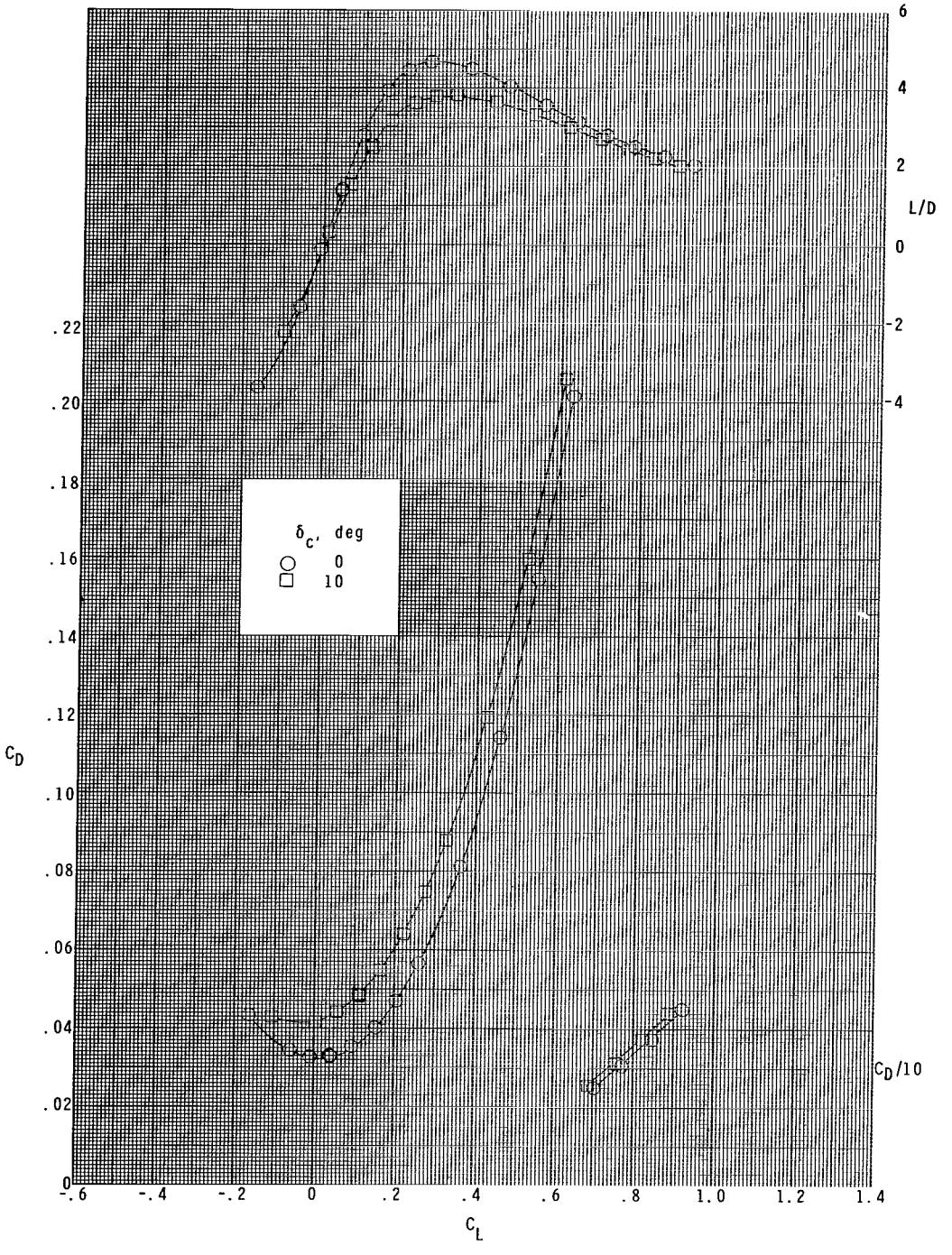

(b) Concluded.

Figure 9.- Continued.

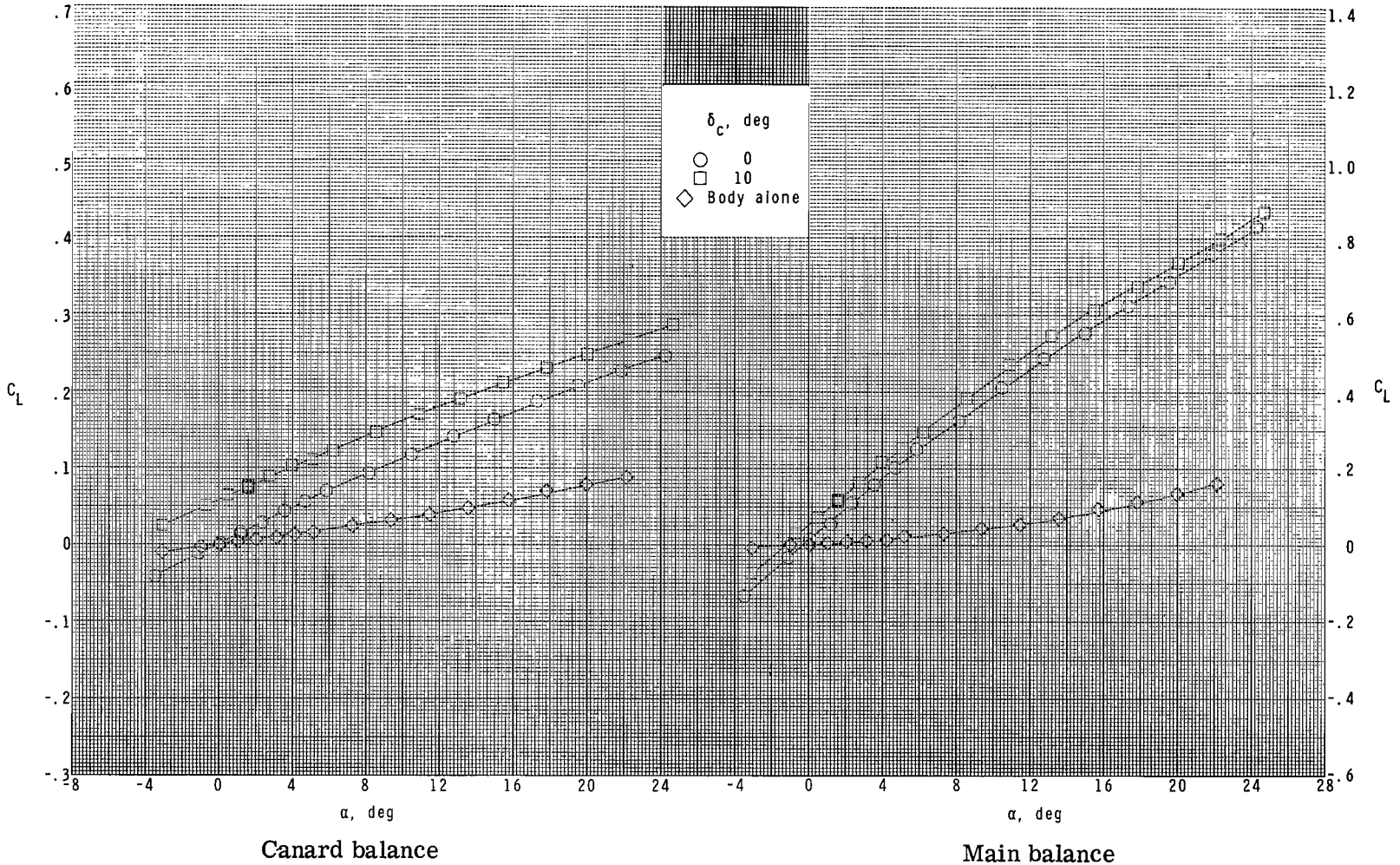

(c) M = 2.36.

Figure 9.- Continued.

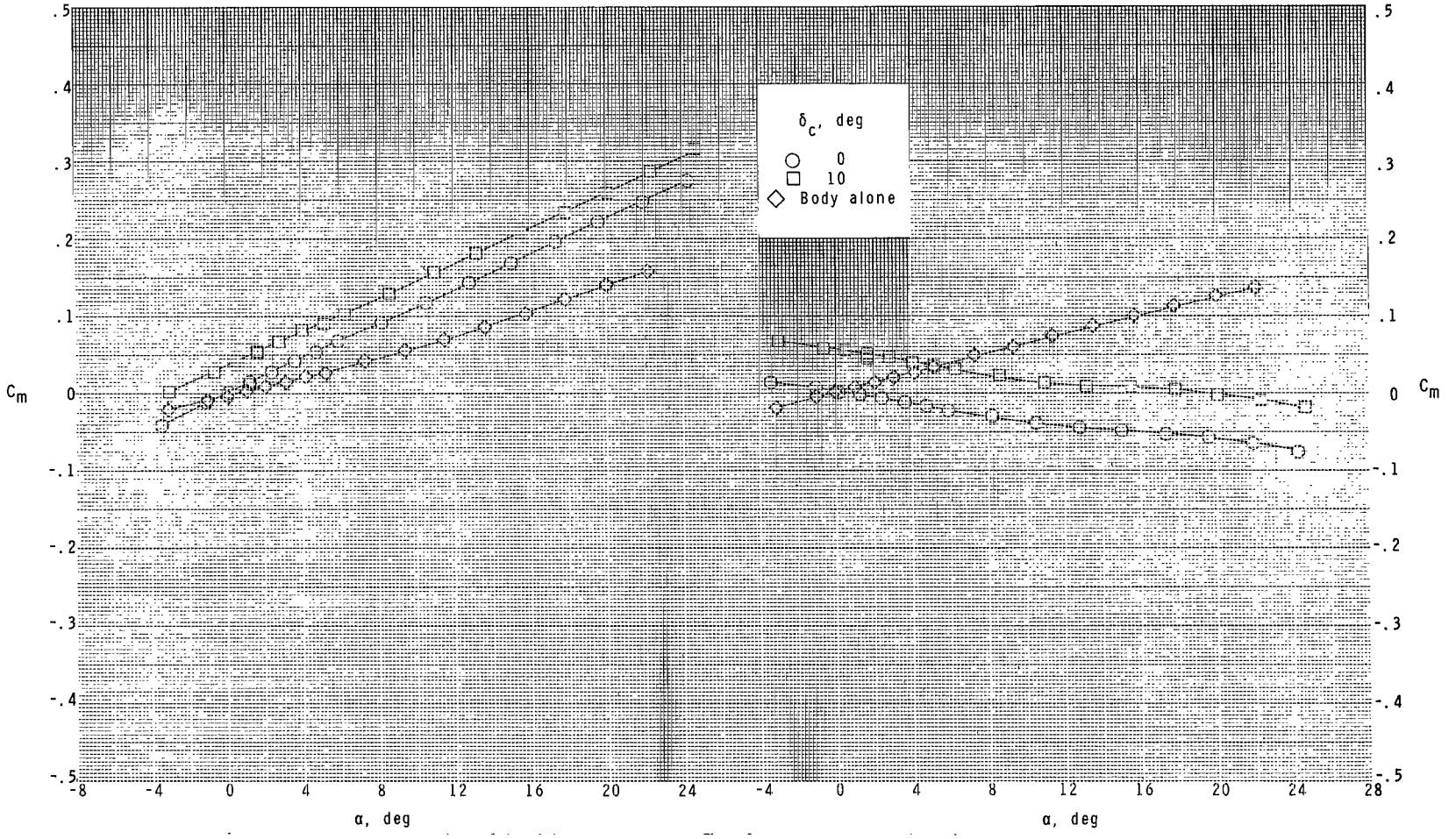

Canard balance

Main balance

(c) Continued.

Figure 9.- Continued.

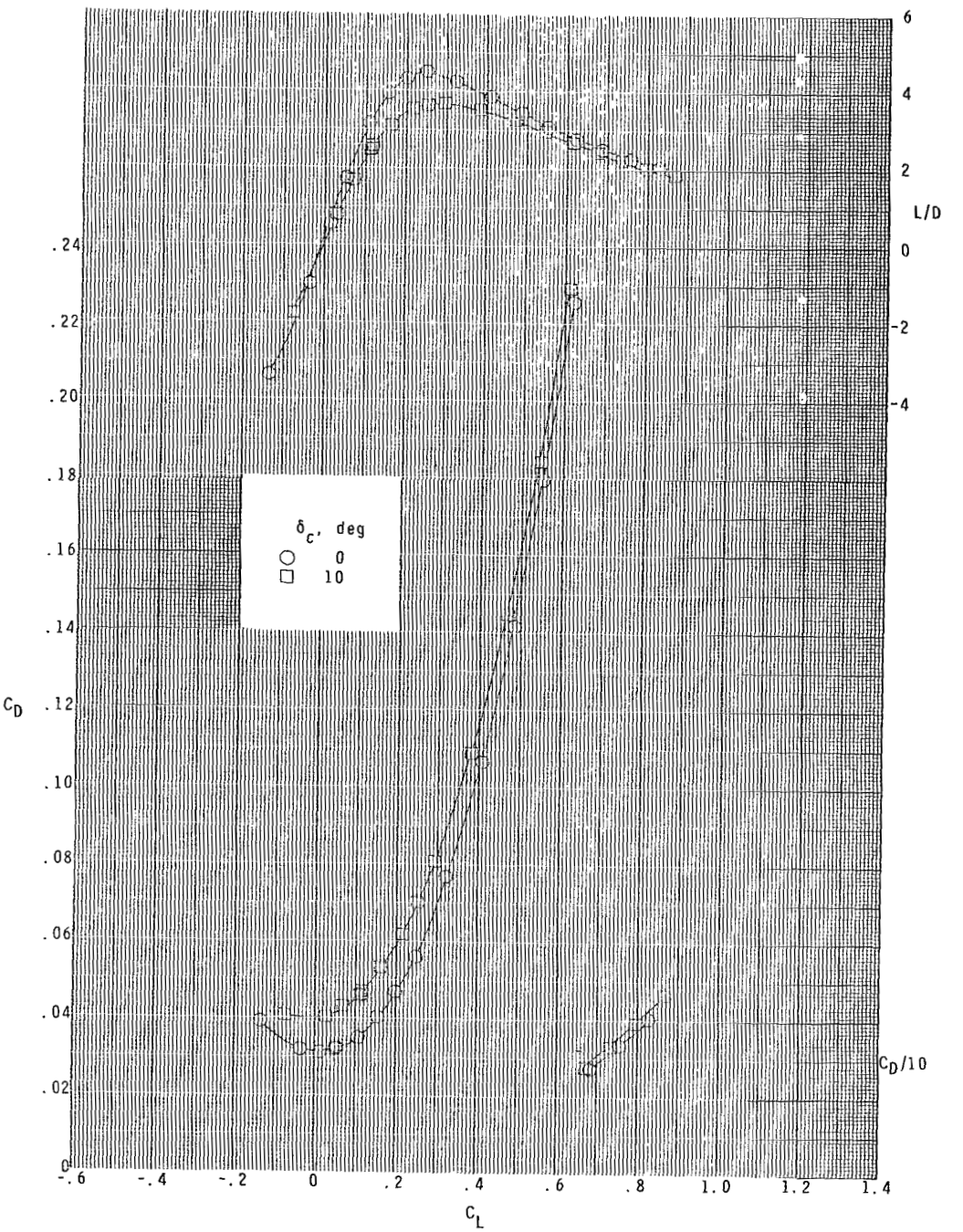

(c) Concluded.

Figure 9.- Continued.

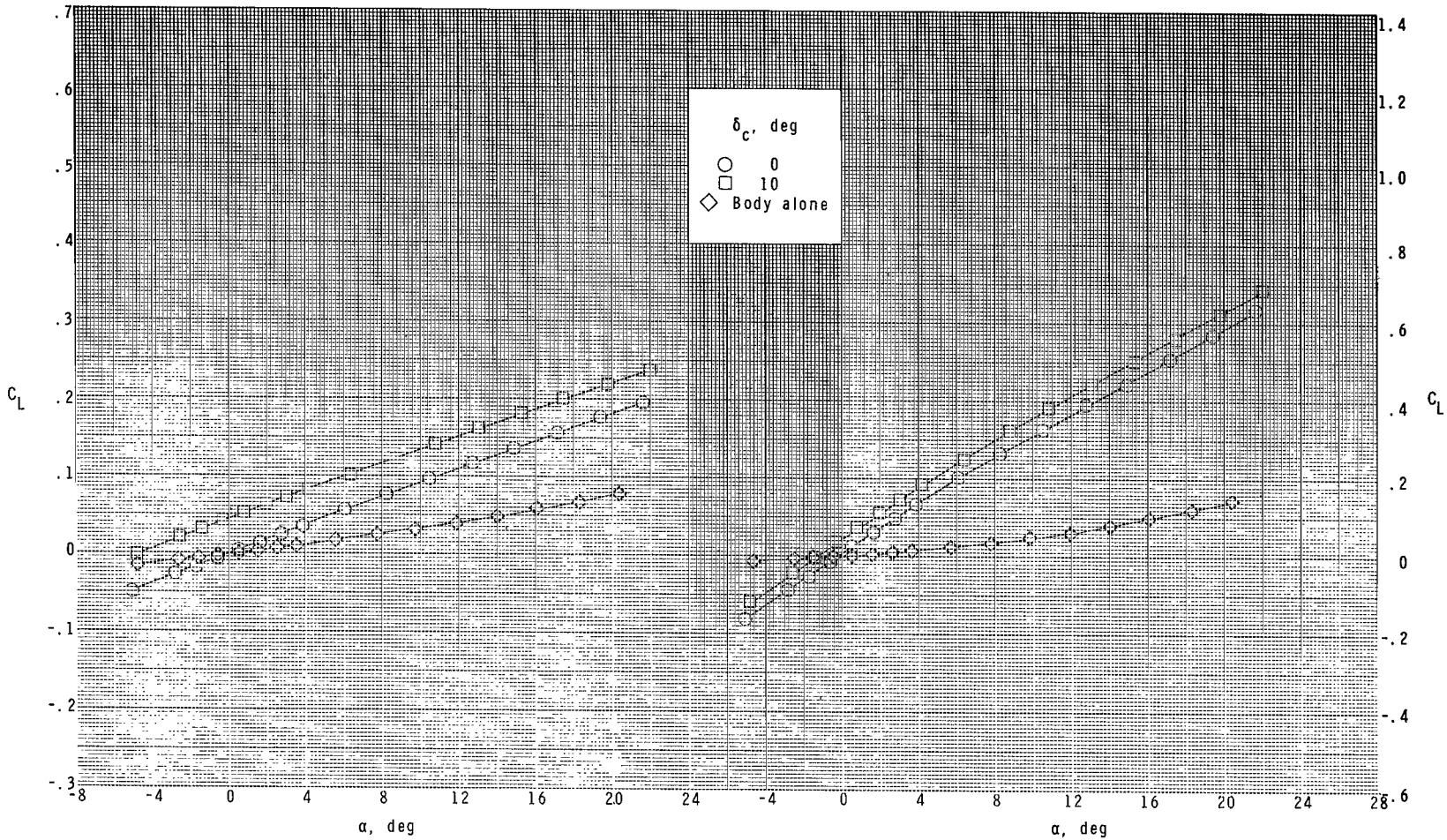

(d) M = 2.86.

Figure 9.- Continued.

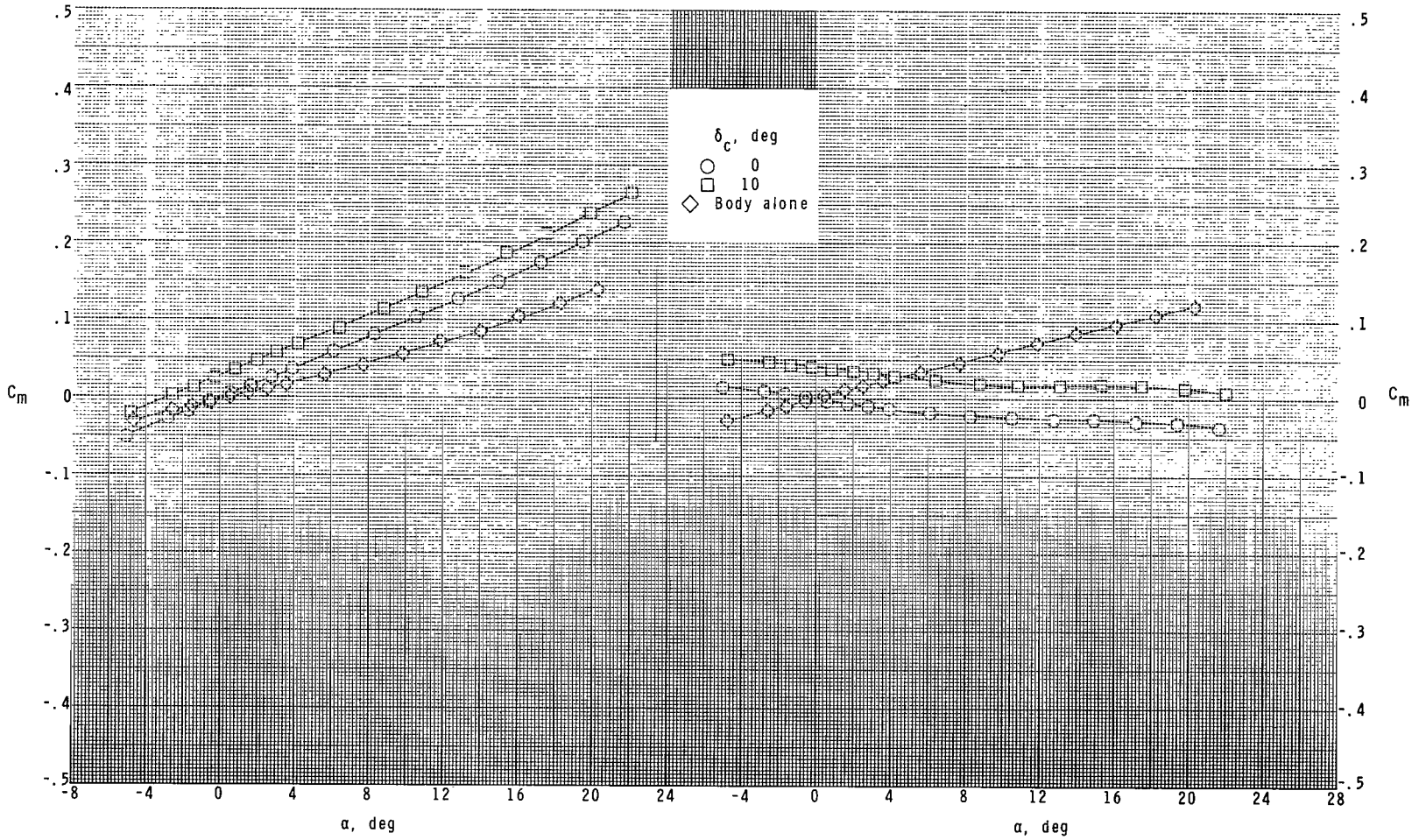

(d) Continued.

Figure 9.- Continued.

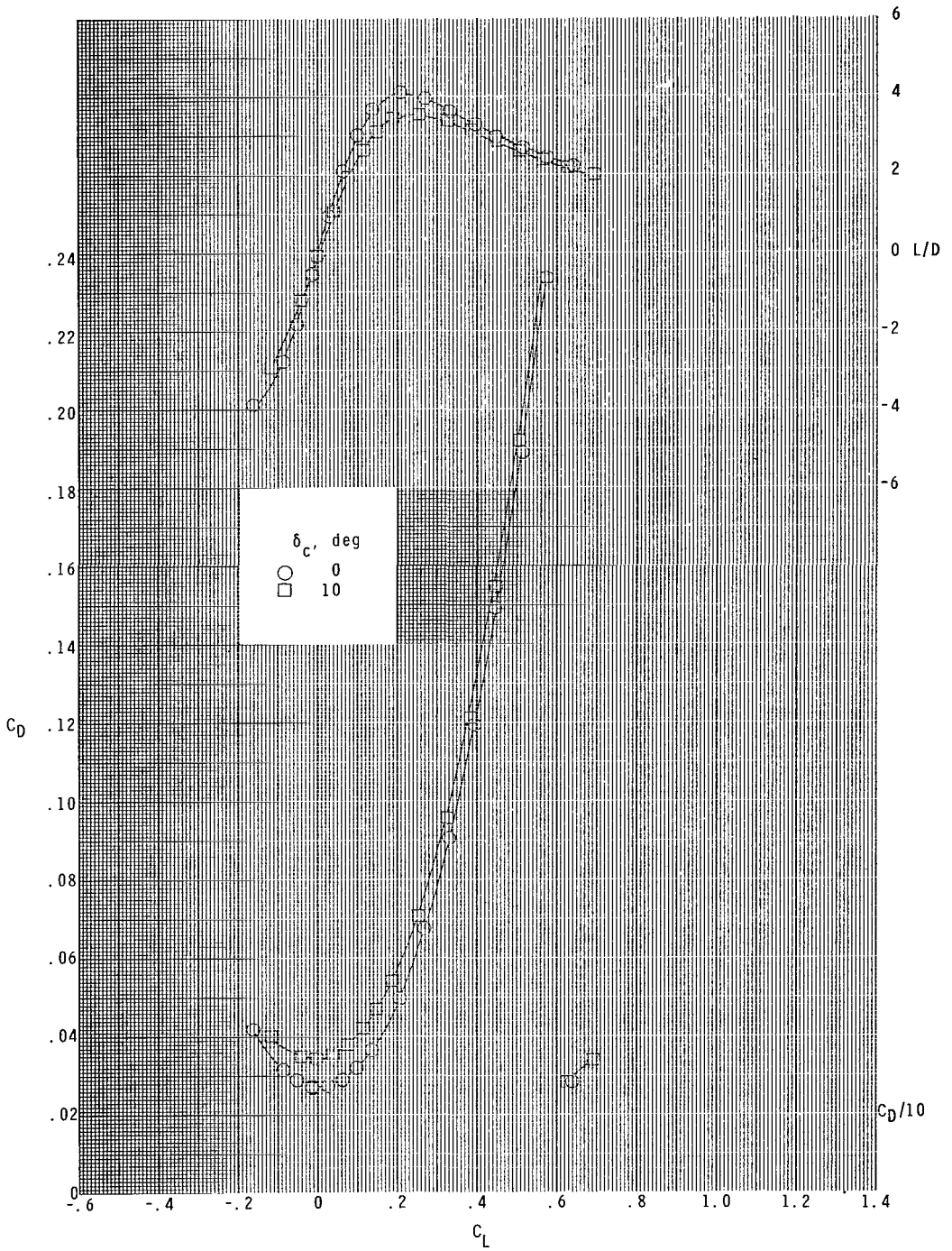

(d) Concluded.

Figure 9.- Concluded.

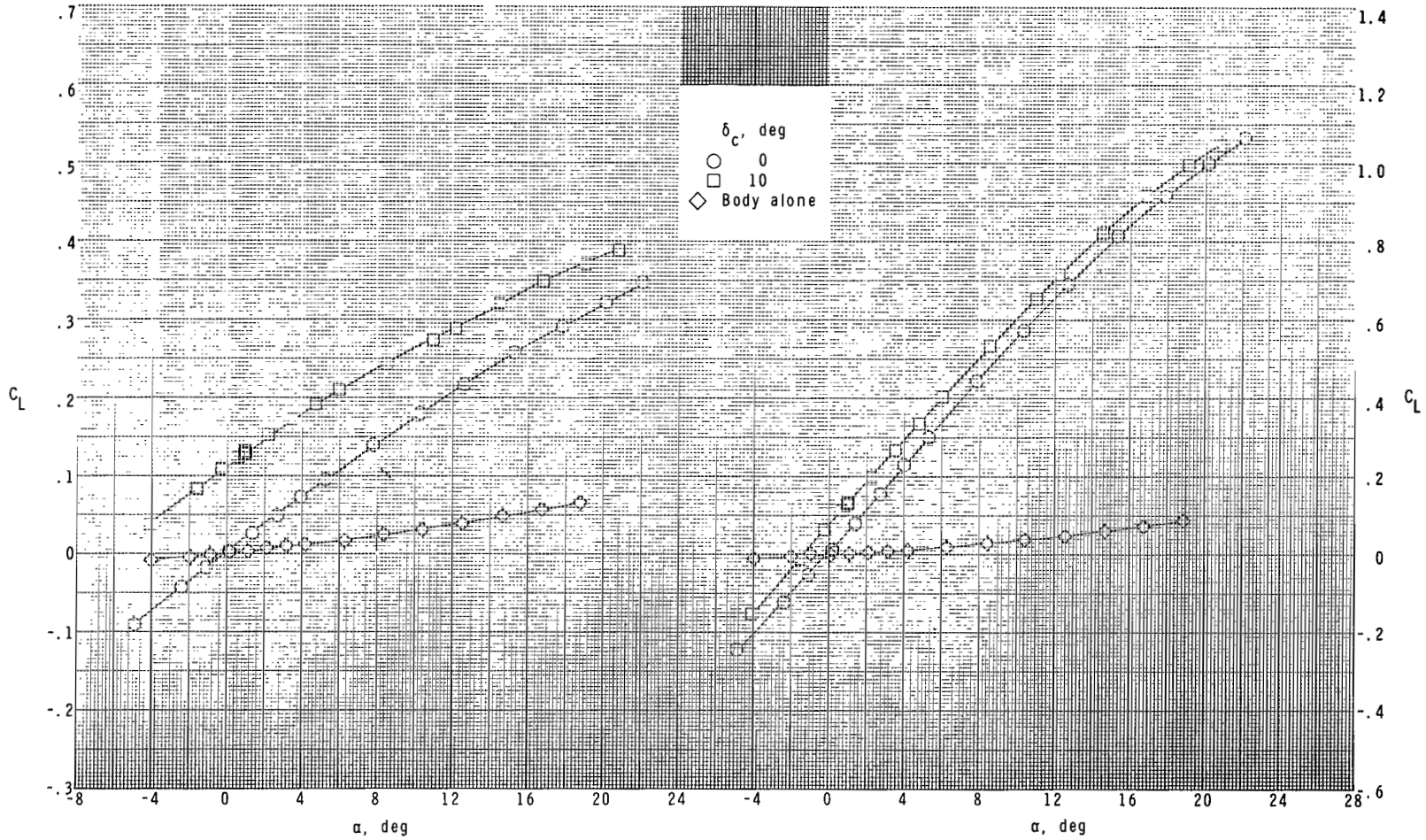

(a) M = 1.60.

Figure 10.- Longitudinal aerodynamic characteristics for $S_c/S_w = 0.300$ and $z/\bar{c} = 0.185$.

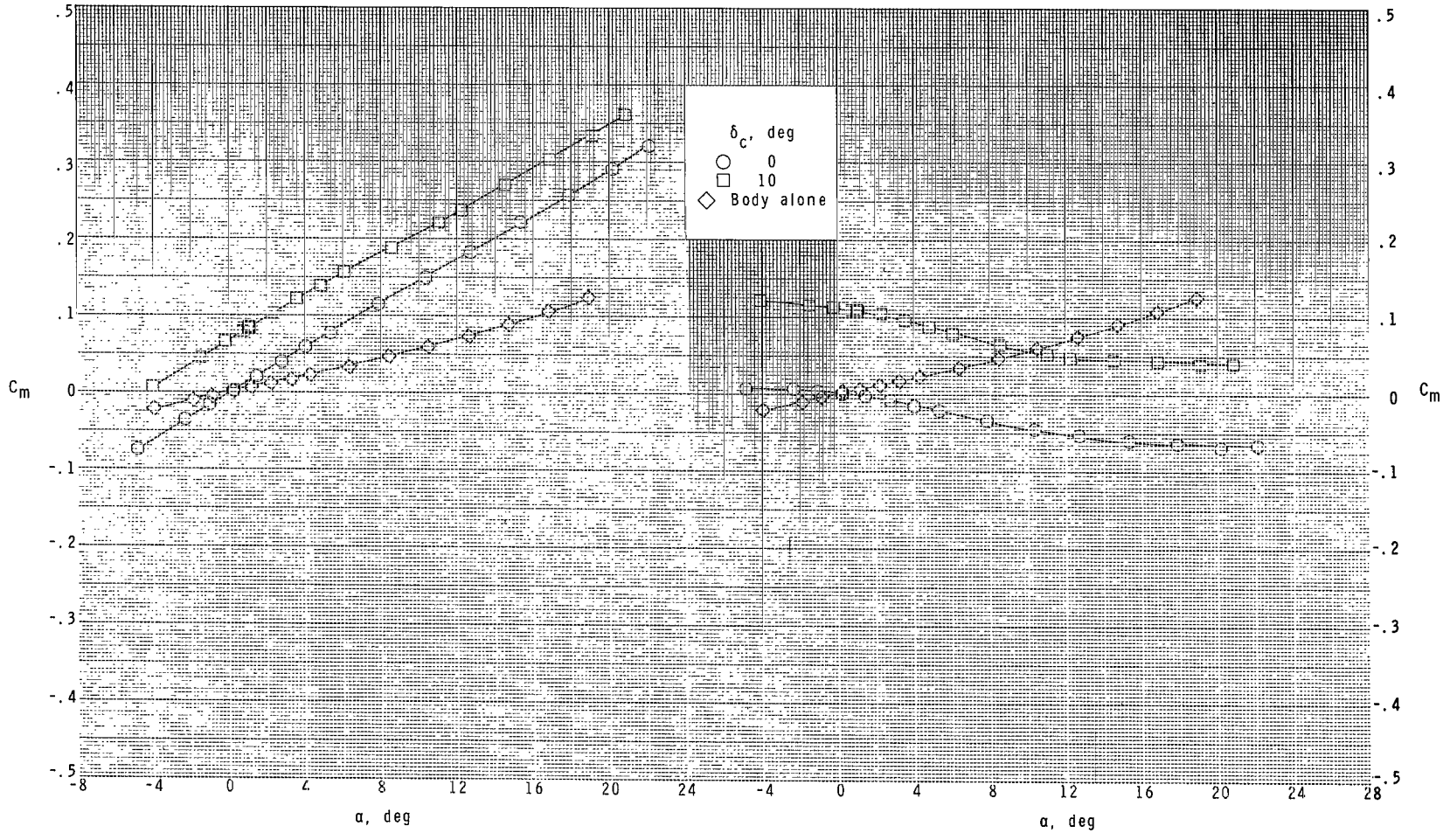

(a) Continued.

Figure 10.- Continued.

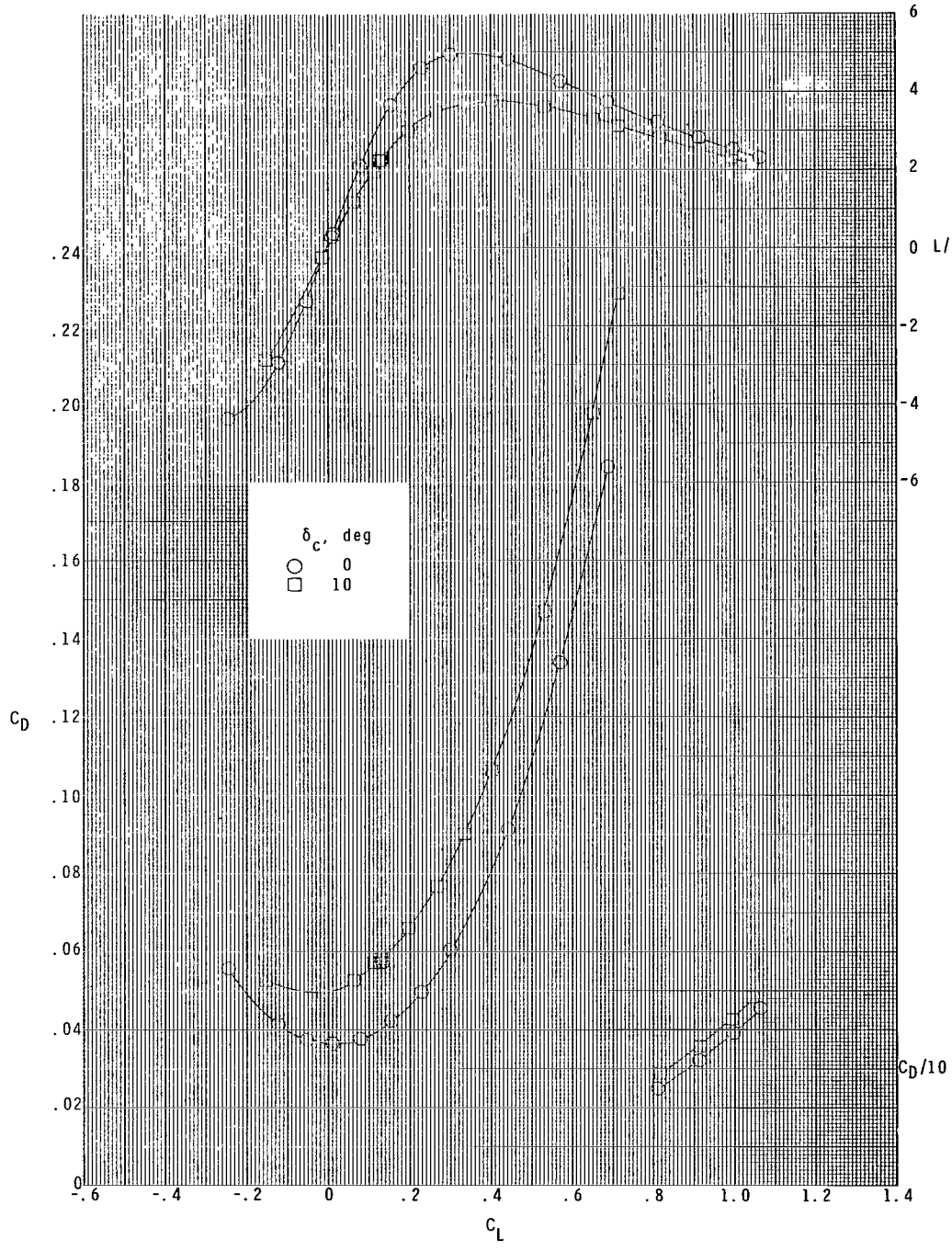

(a) Concluded.

Figure 10.- Continued.

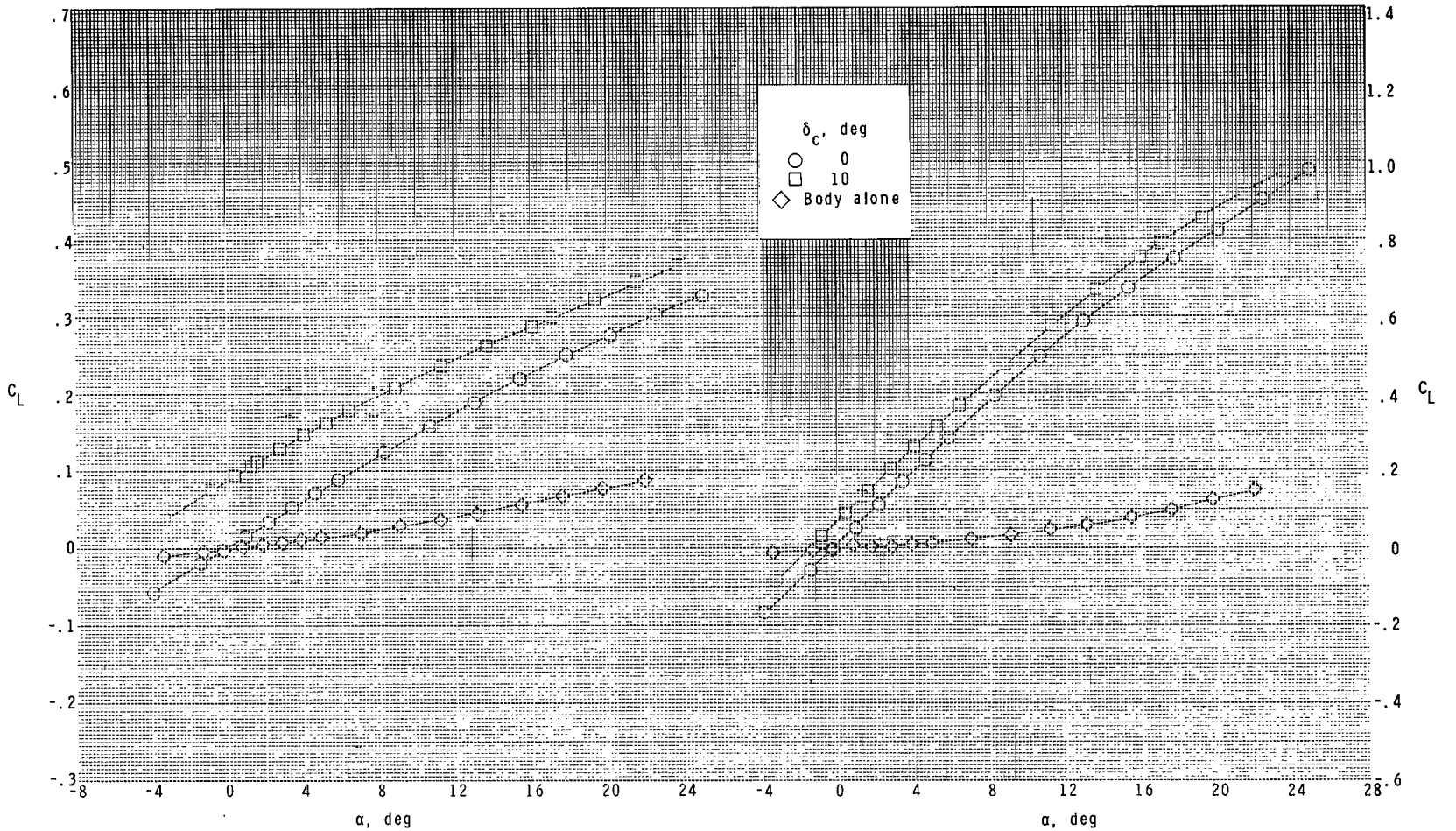

(b) M = 2.00.

Figure 10.- Continued.

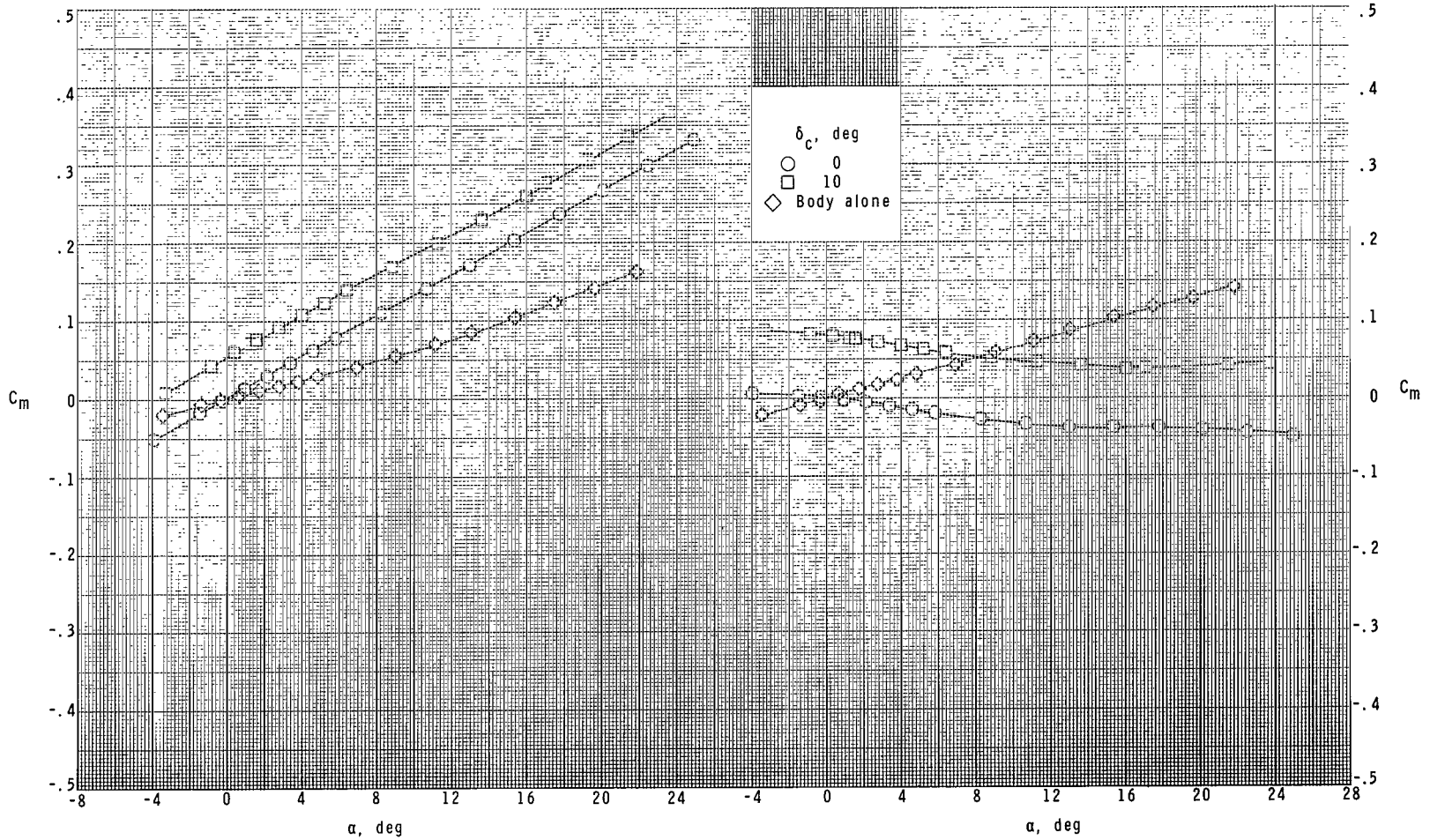

(b) Continued.

Figure 10.- Continued.

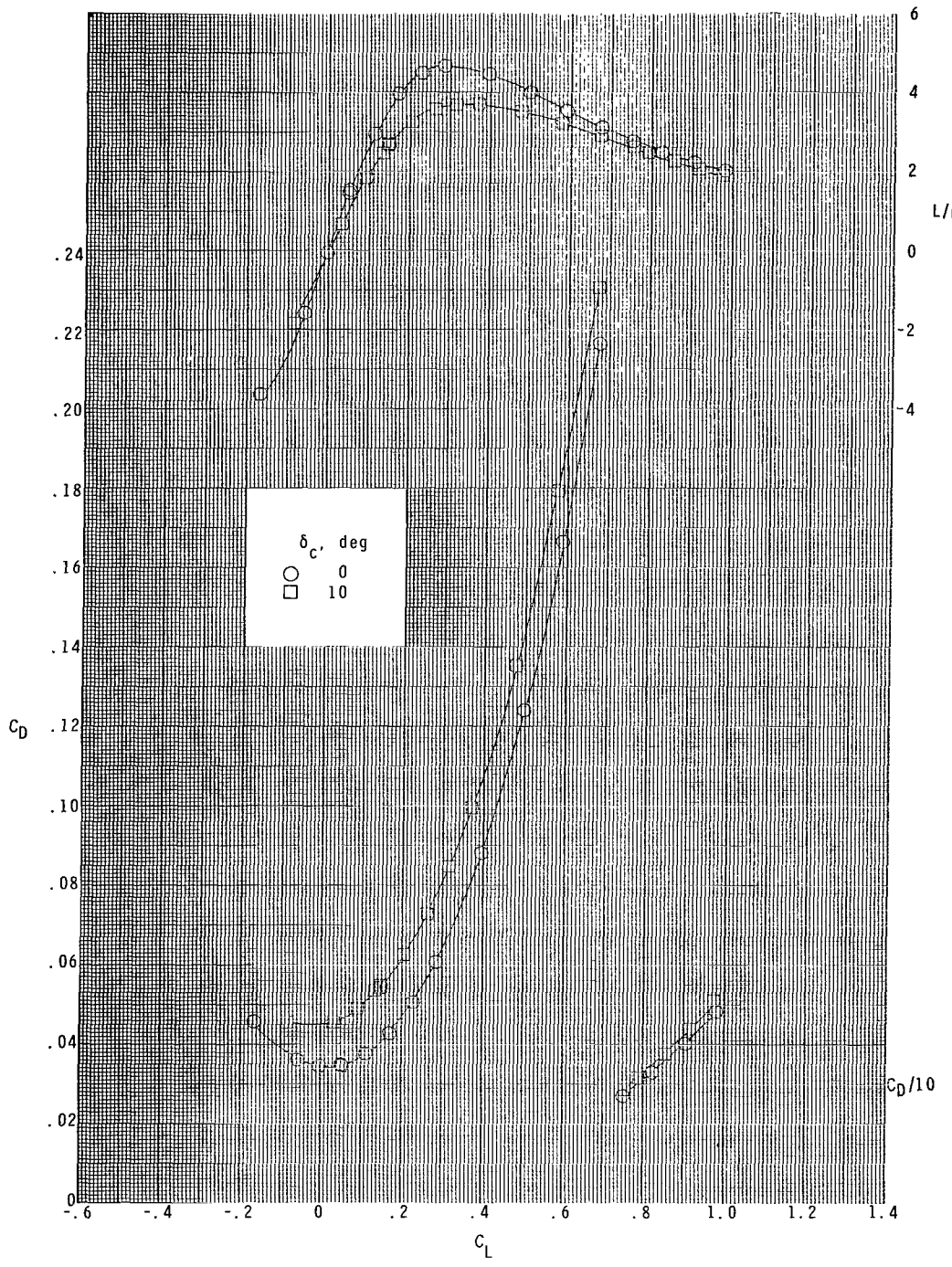

(b) Concluded.

Figure 10.- Continued.

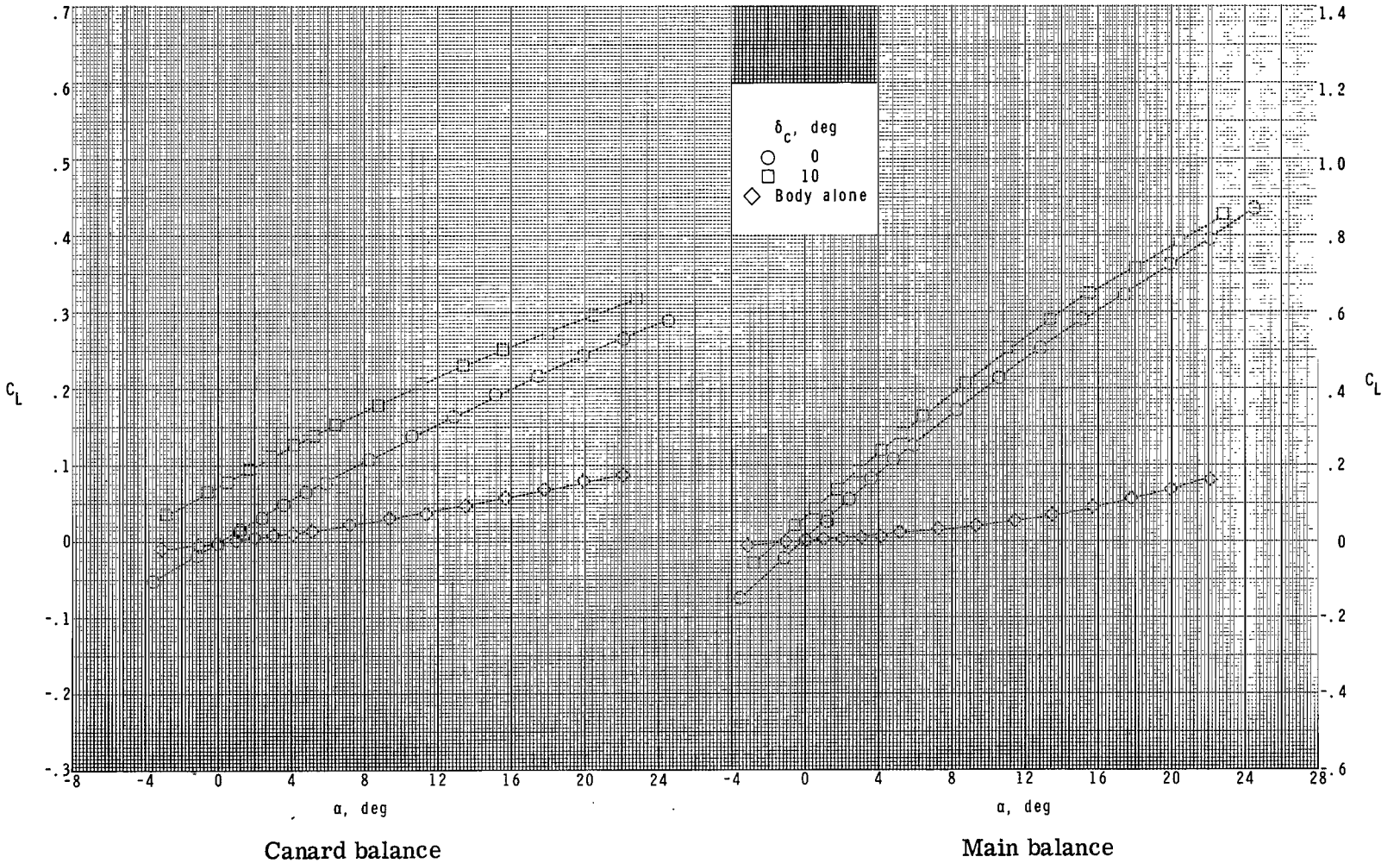

(c) M = 2.36.

Figure 10.- Continued.

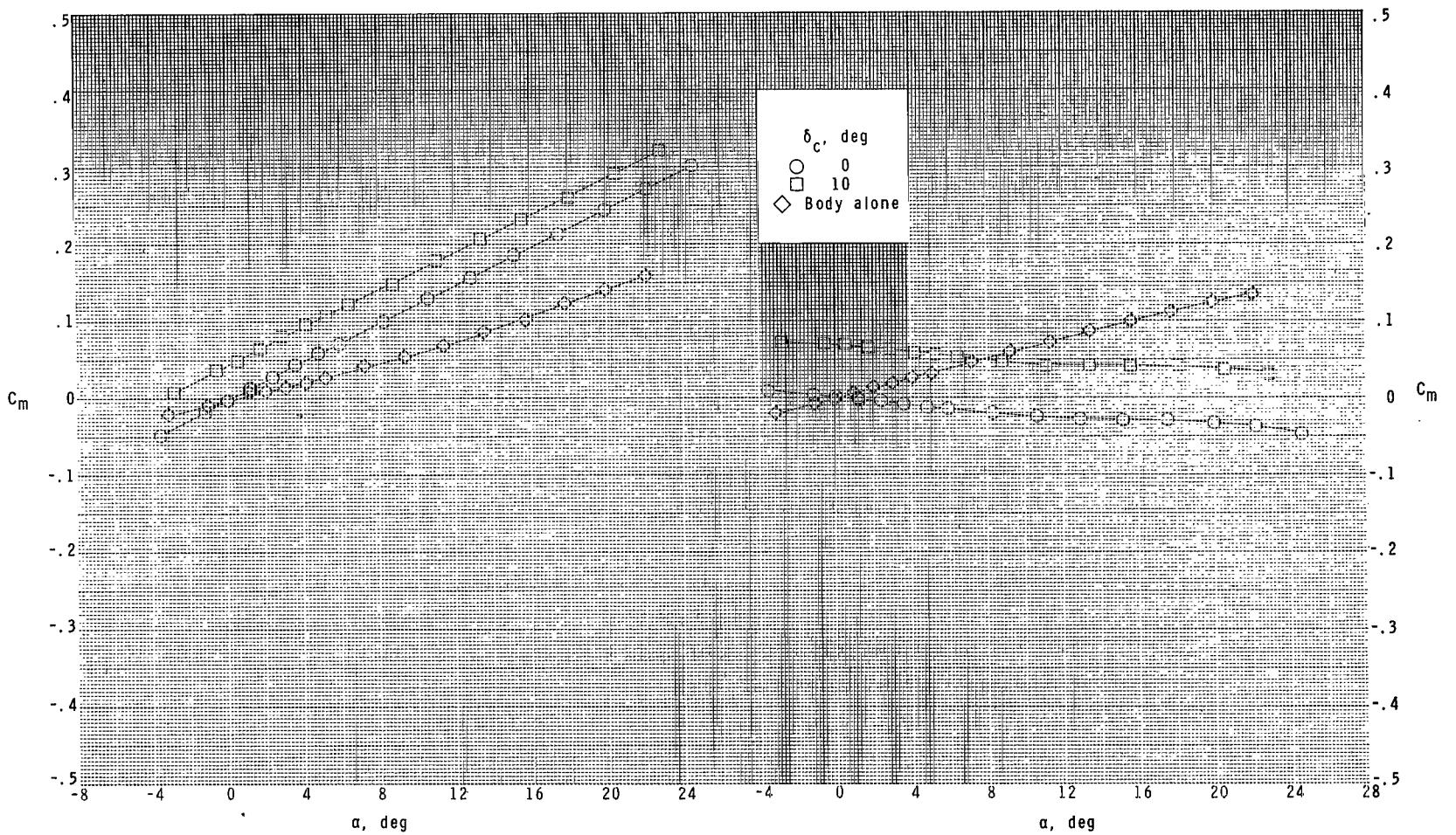

(c) Continued.

Figure 10.- Continued.

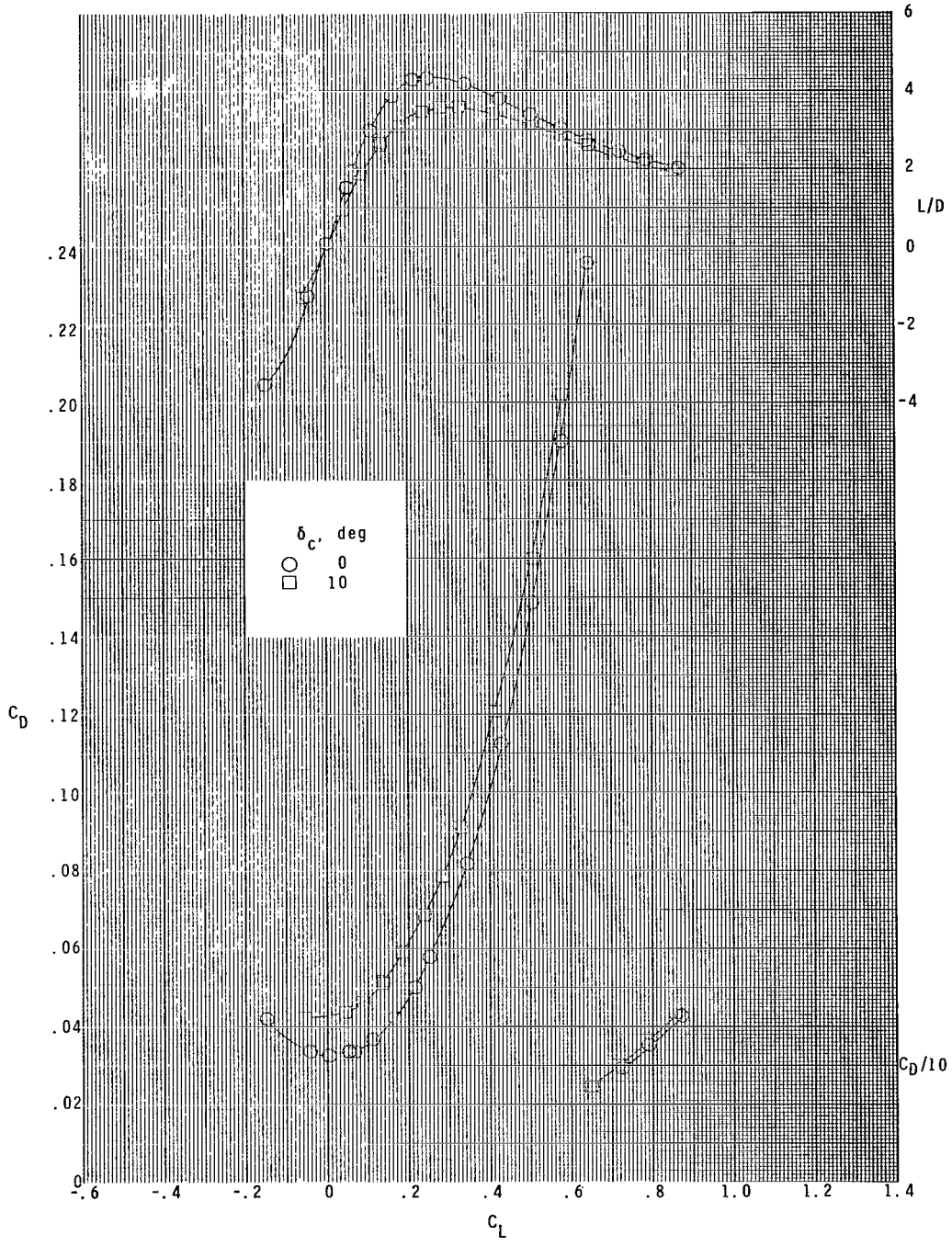

(c) Concluded.

Figure 10.- Continued.

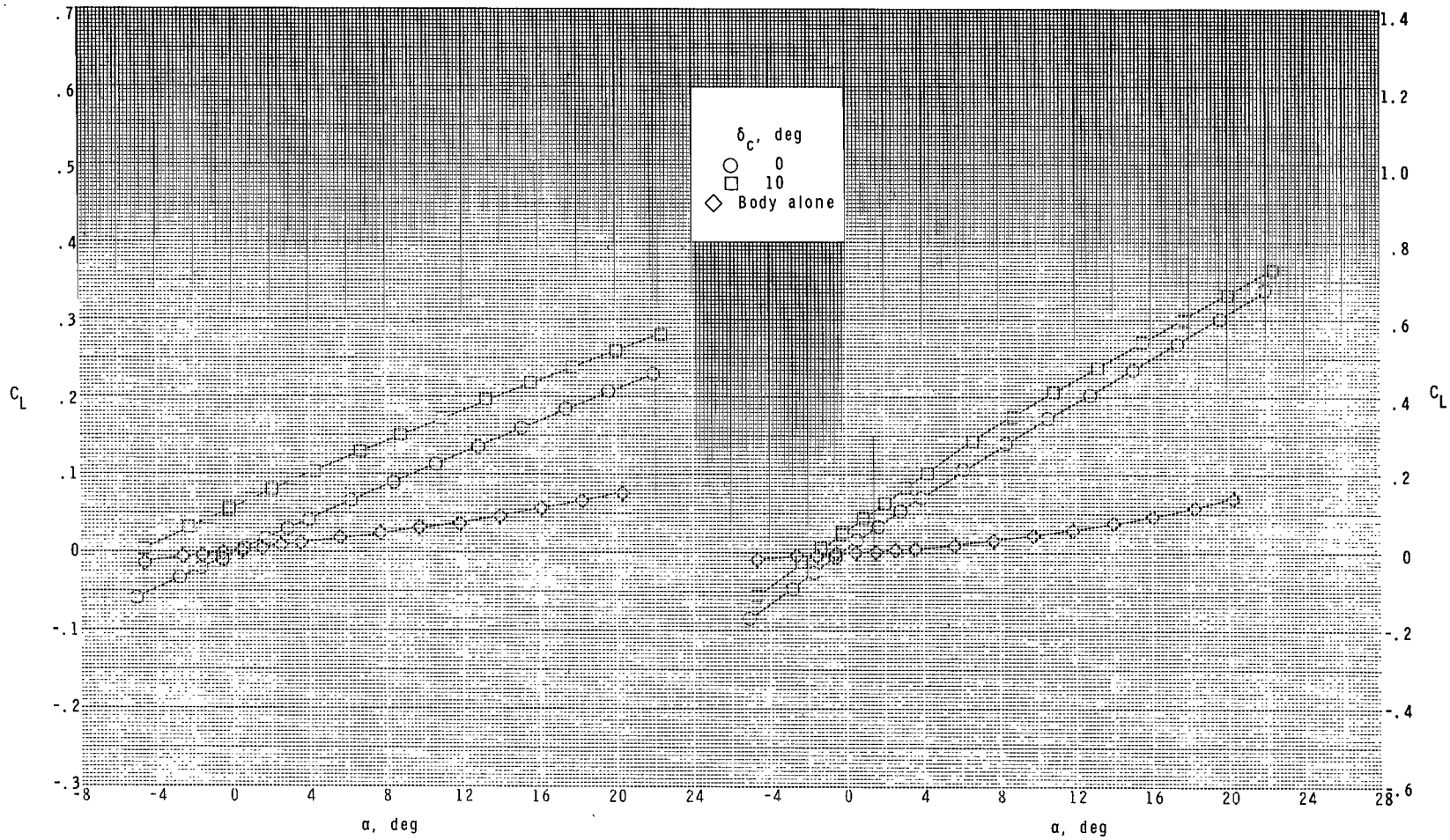

(d) M = 2.86.

Figure 10.- Continued.

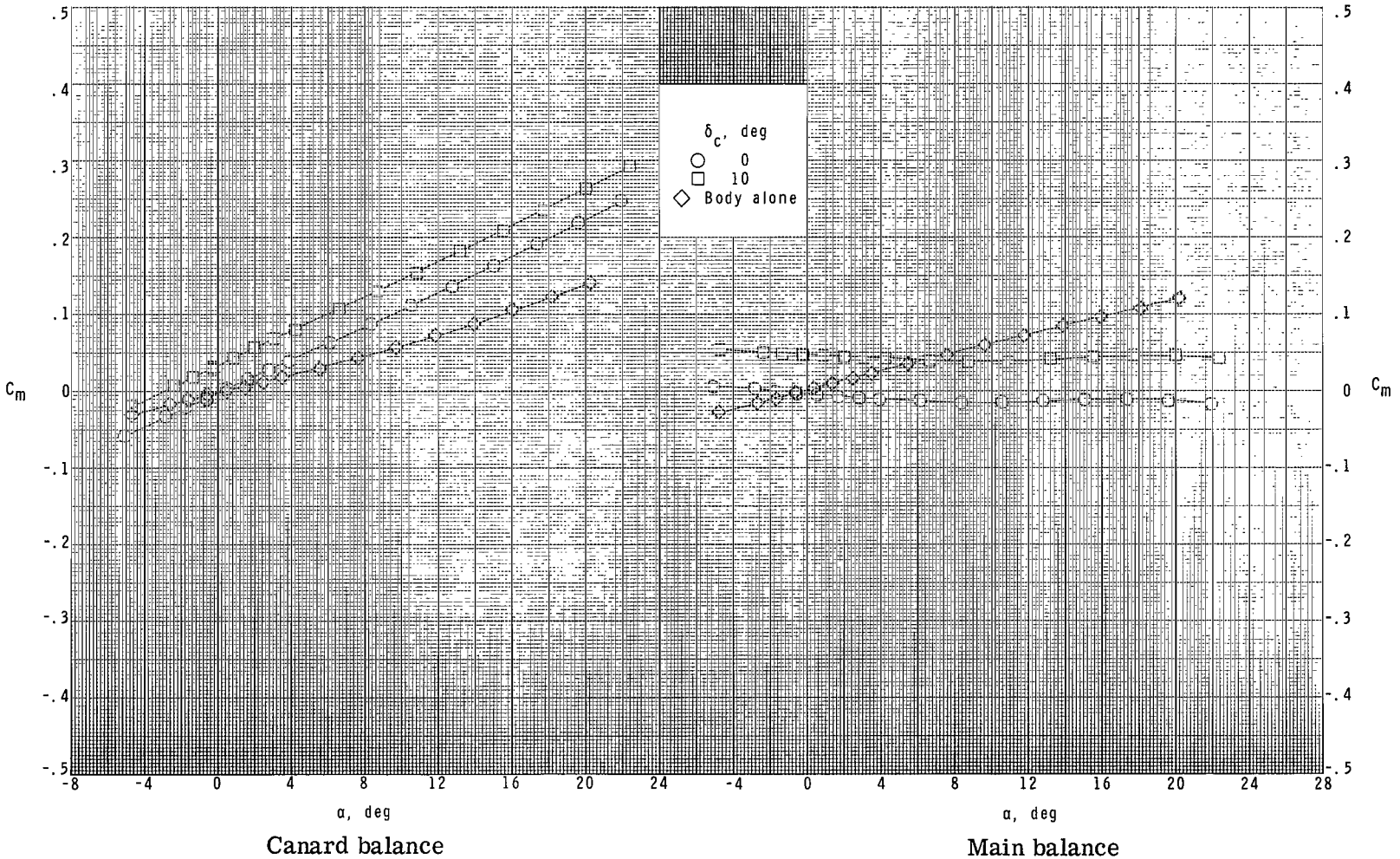

(d) Continued.

Figure 10.- Continued.

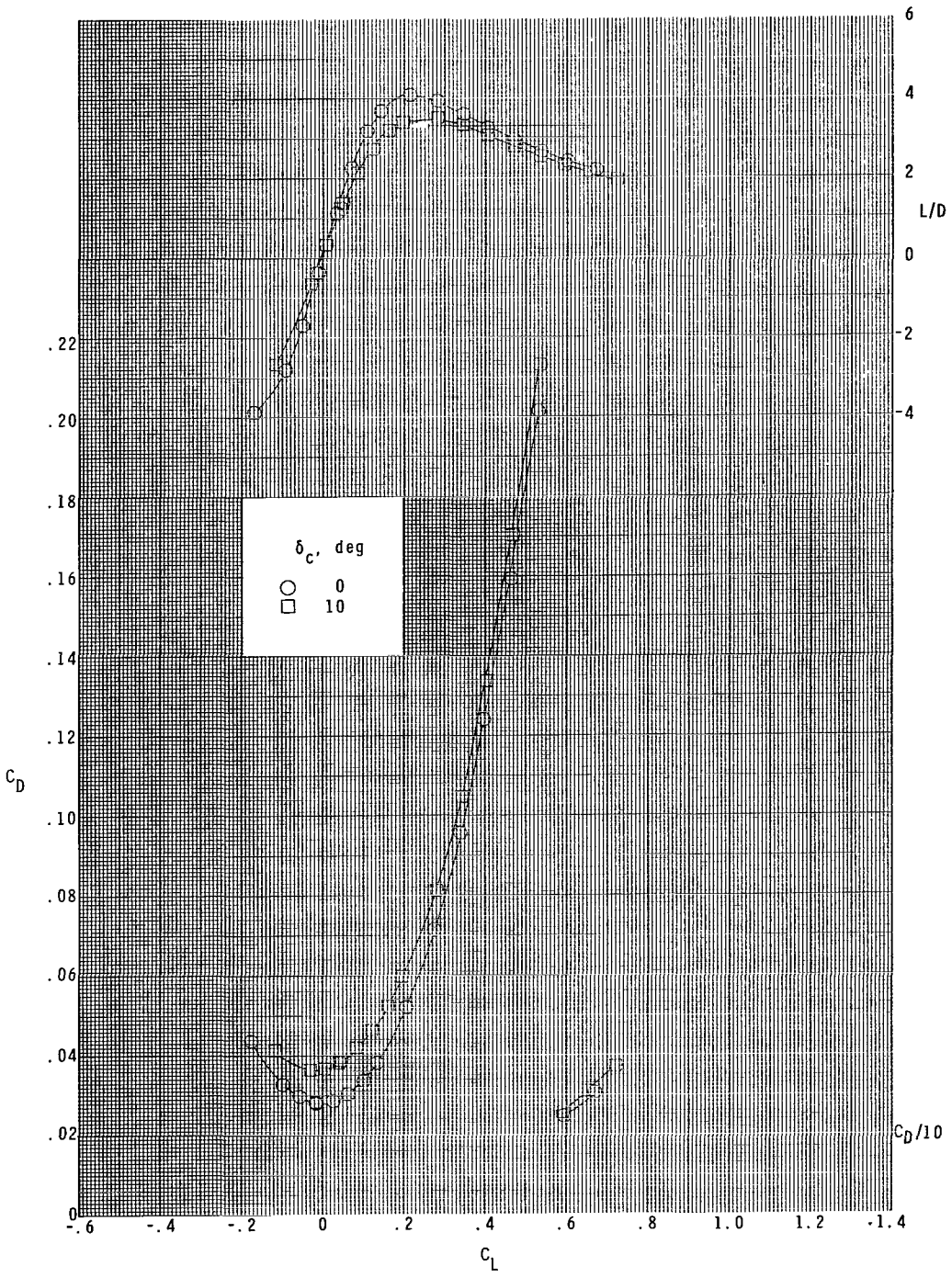

(d) Concluded.

Figure 10.- Concluded.

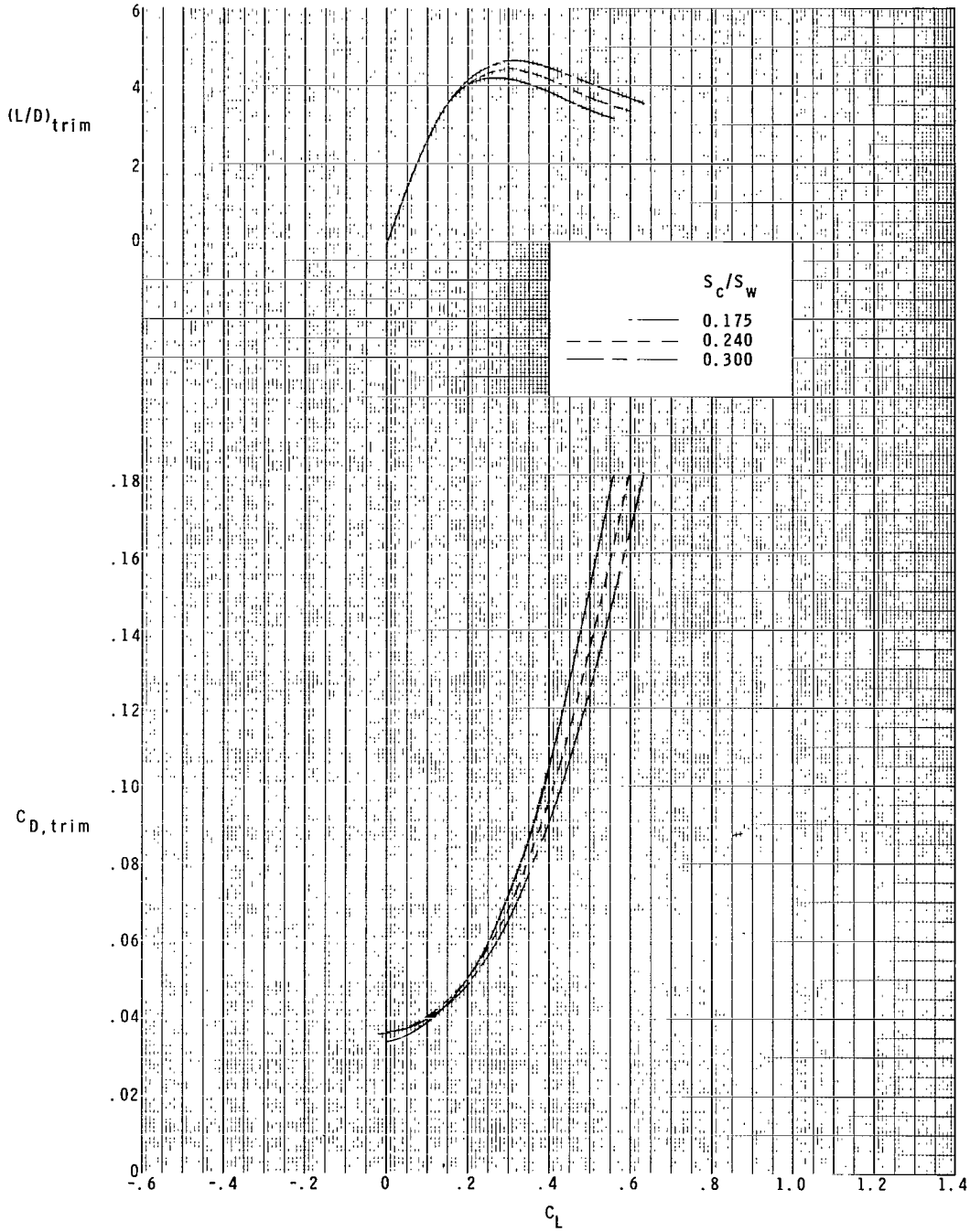

(a) All canards at $z/\overline{c} = 0.0$.

Figure 11.- Trimmed drag and lift-drag ratio for various values of S_c/S_w and $z/\overline{c}$ at M = 1.60.

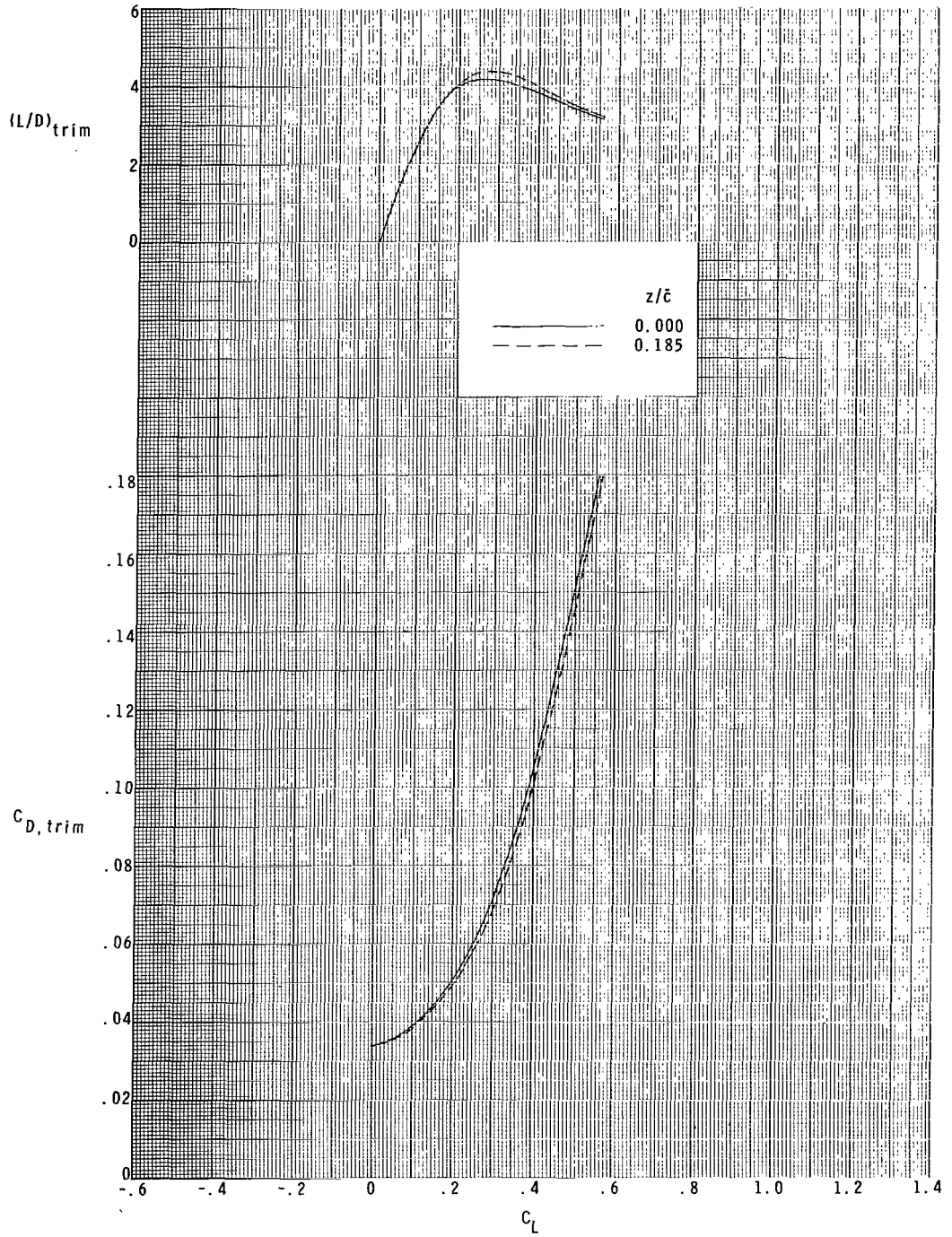

(b) $S_C/S_W = 0.175$.

Figure 11.- Continued.

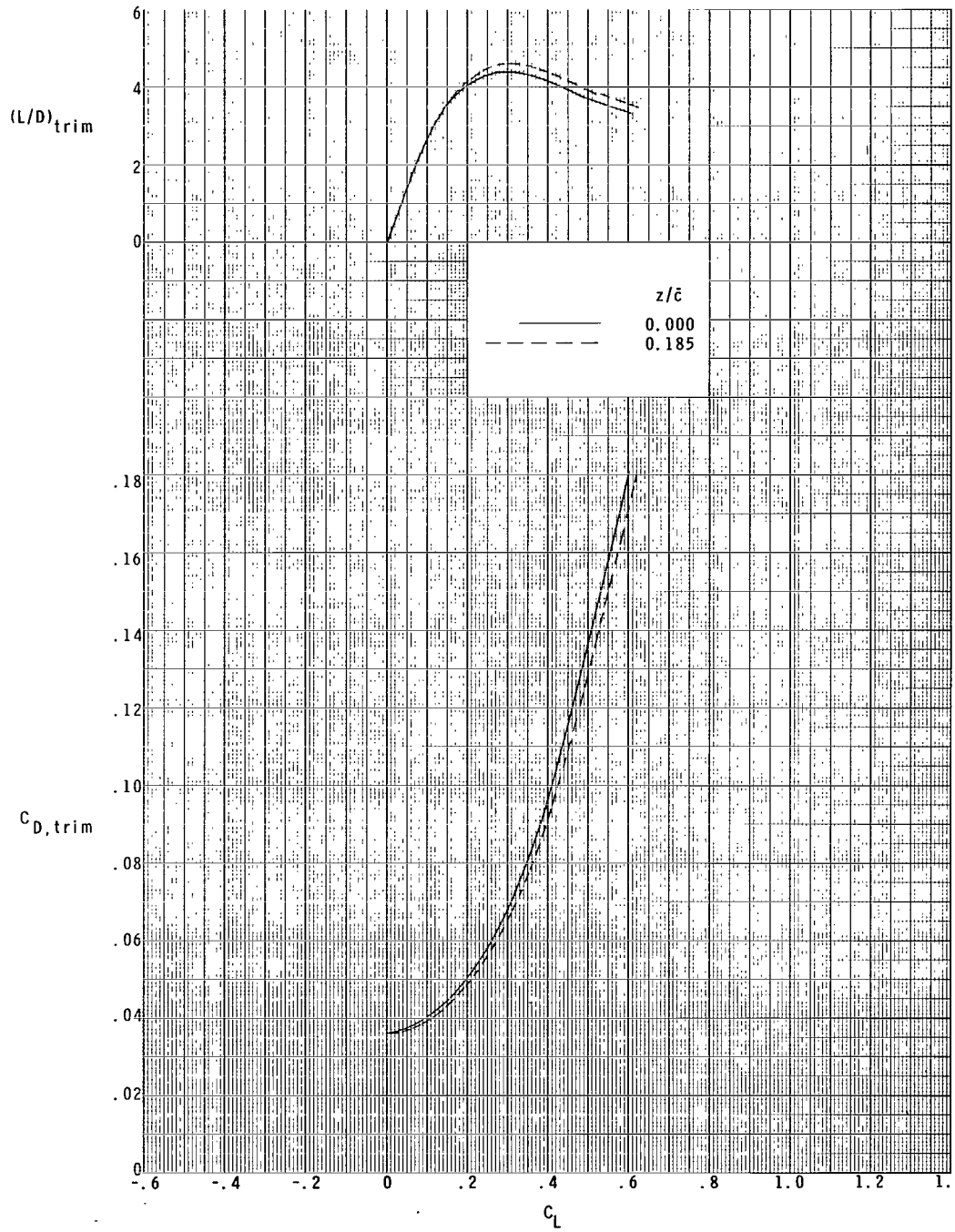

(c) $S_c/S_w = 0.240$.

Figure 11.- Continued.

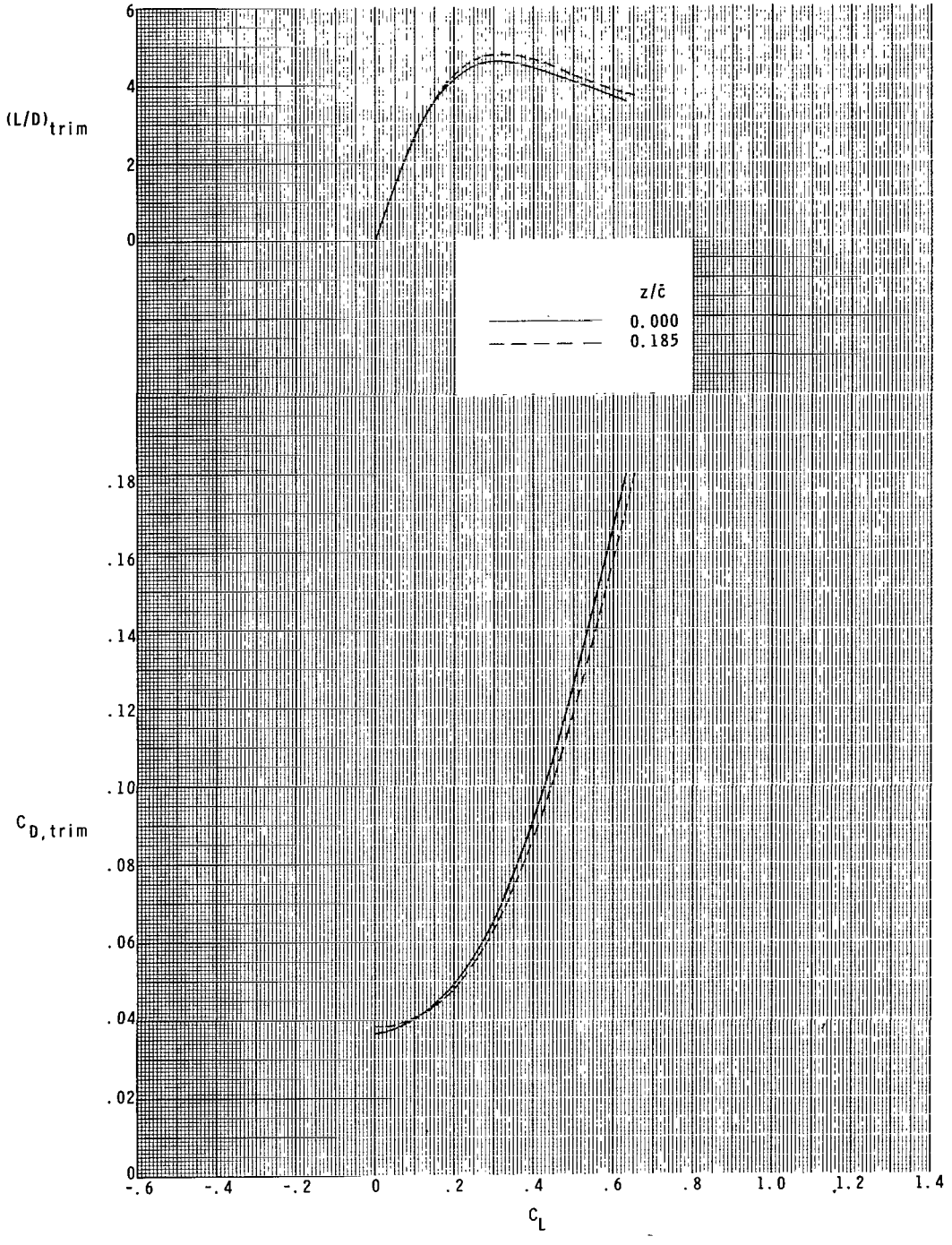

(d) $S_c/S_w = 0.300$.

Figure 11.- Concluded.

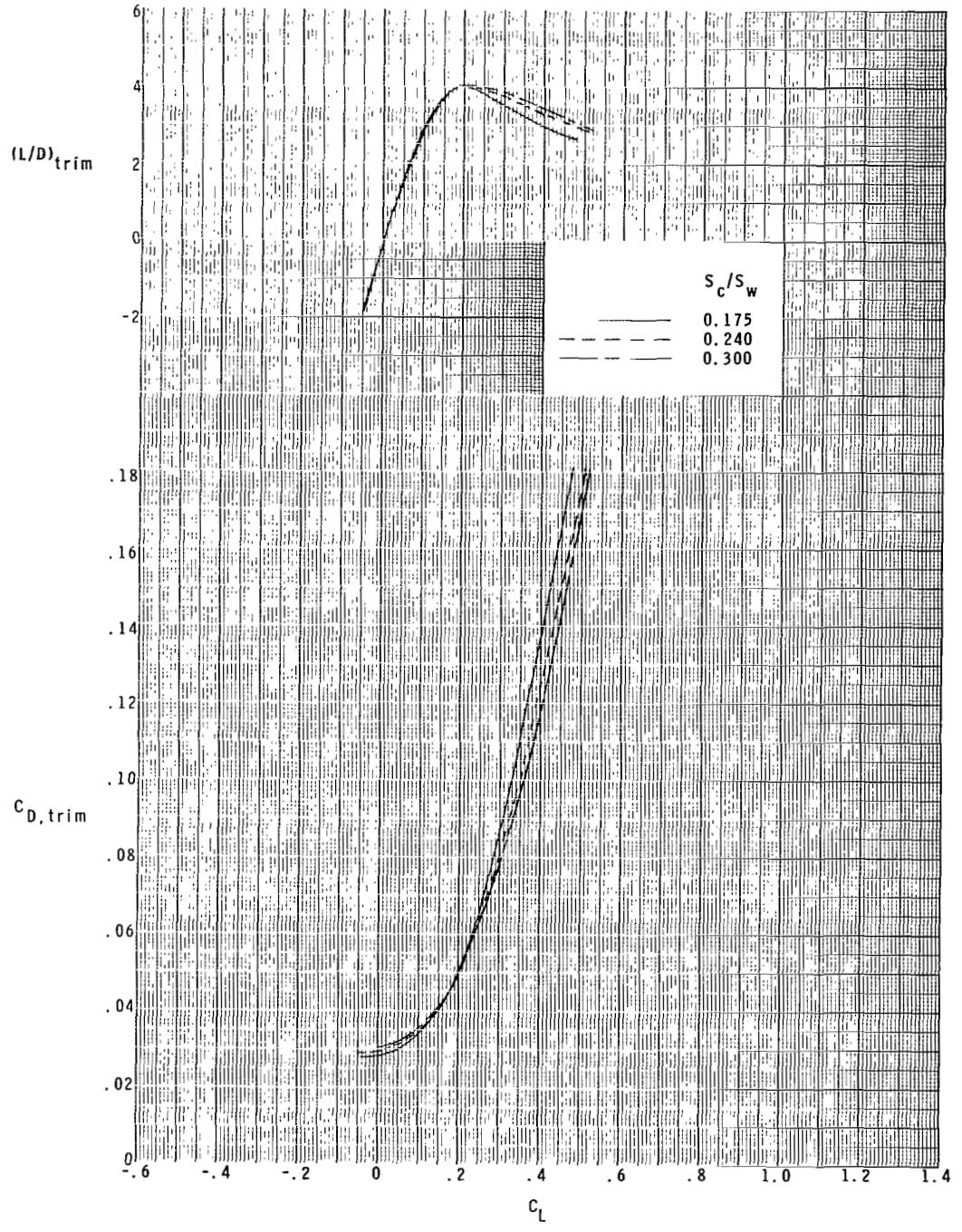

(a) All canards at $z/\bar{c} = 0.0$.

Figure 12.- Trimmed drag and lift-drag ratio for various values of S_c/S_w and $z/\bar{c}$ at $M = 2.86$.

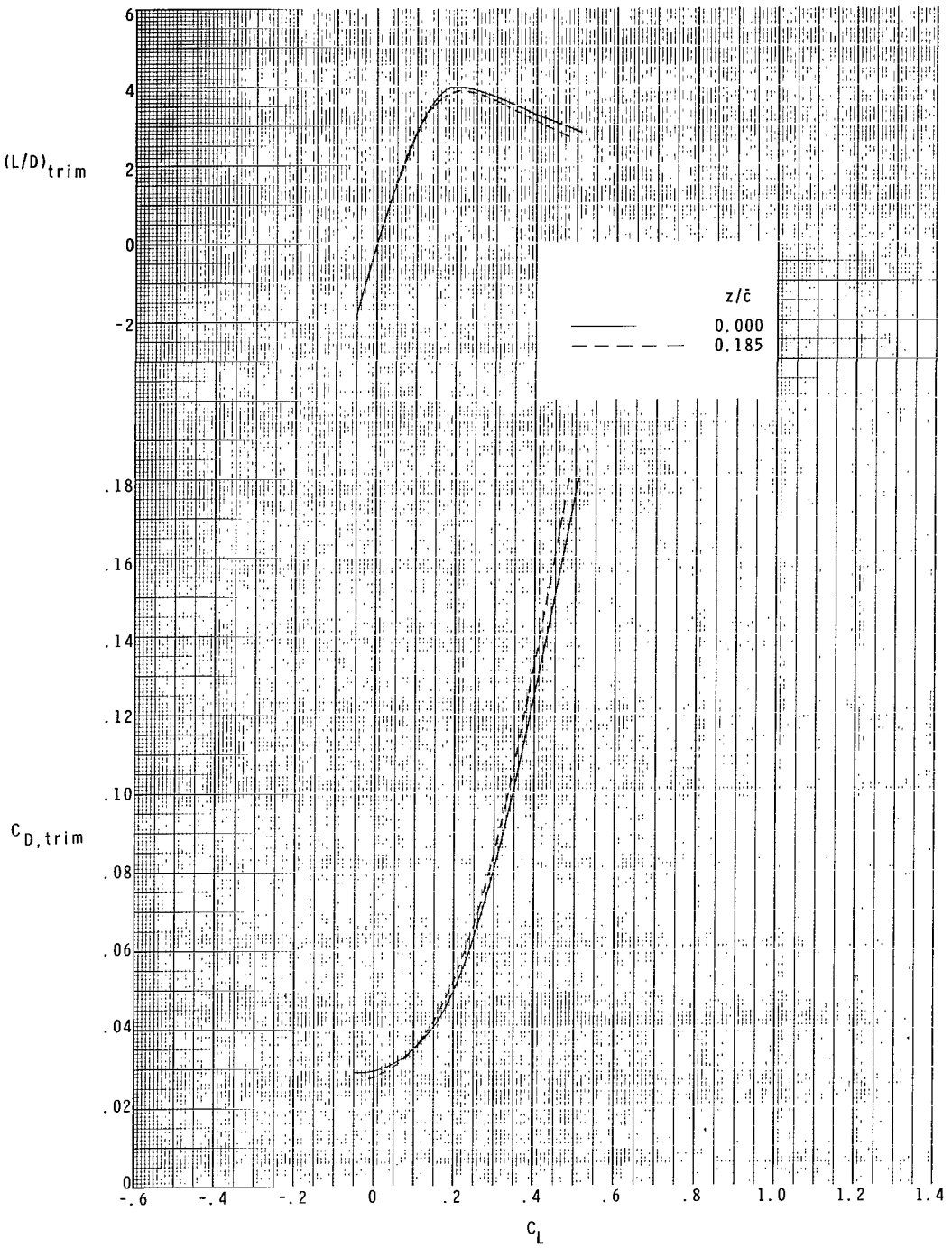

(b) $S_c/S_w = 0.240$.

Figure 12.- Continued.

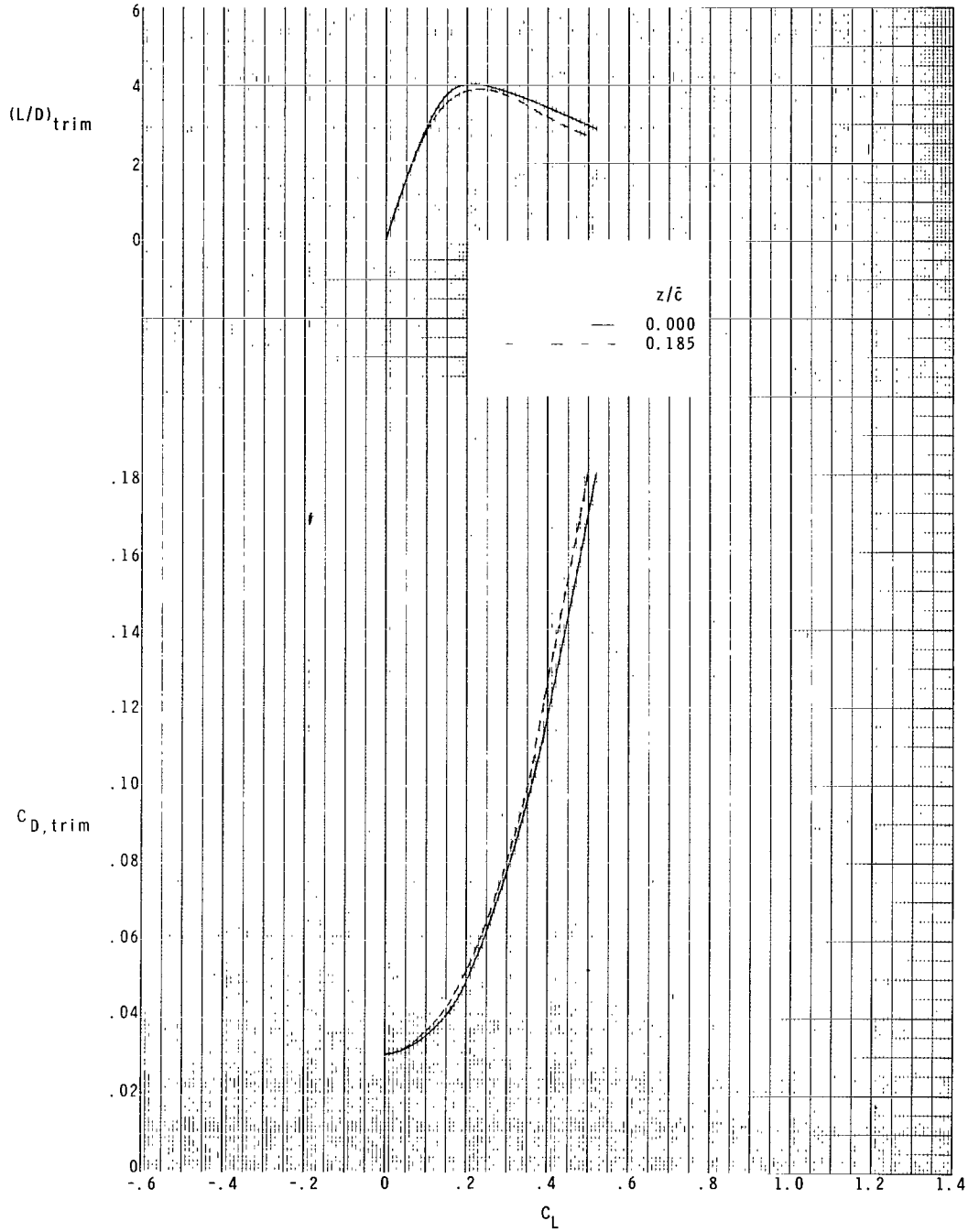

(c) $S_c/S_w = 0.300$.

Figure 12.- Concluded.

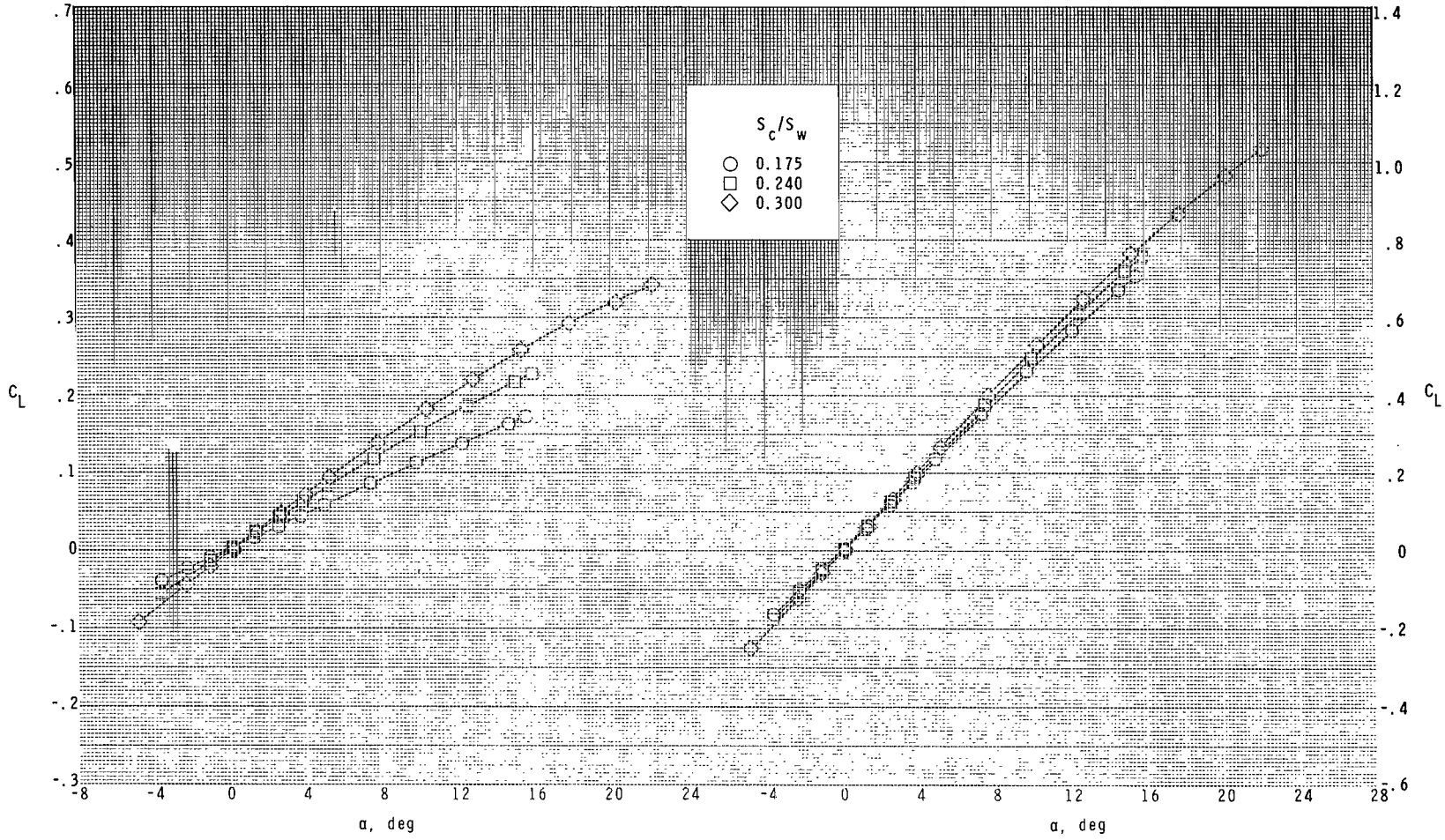

(a) $z/\bar{c} = 0.0$.

Figure 13.- Effect of canard size $(\delta_c = 0^o)$ and vertical position on lift and pitching moment of canard section and total configuration at M = 1.60.

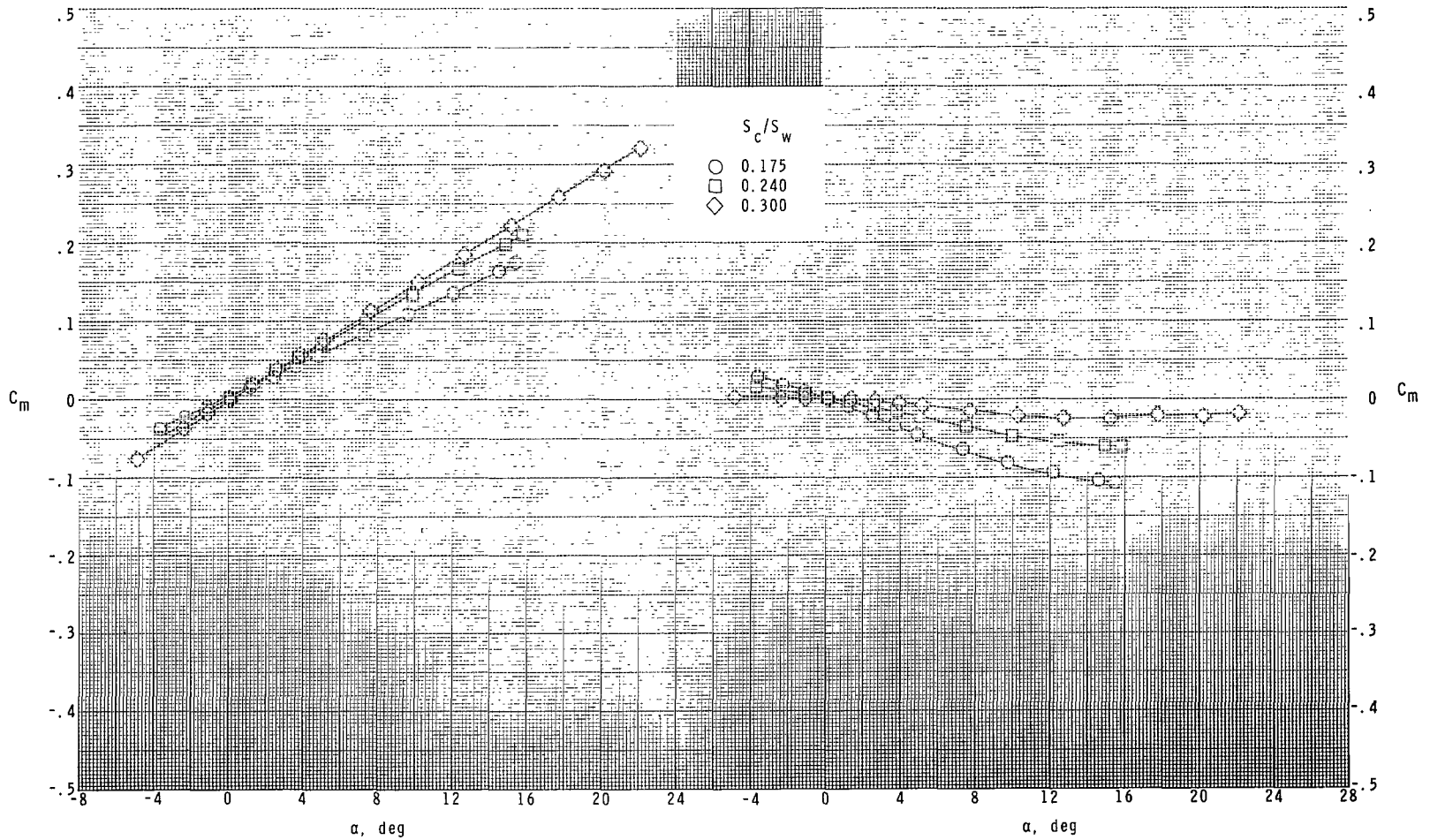

(a) Concluded.

Figure 13.- Continued.

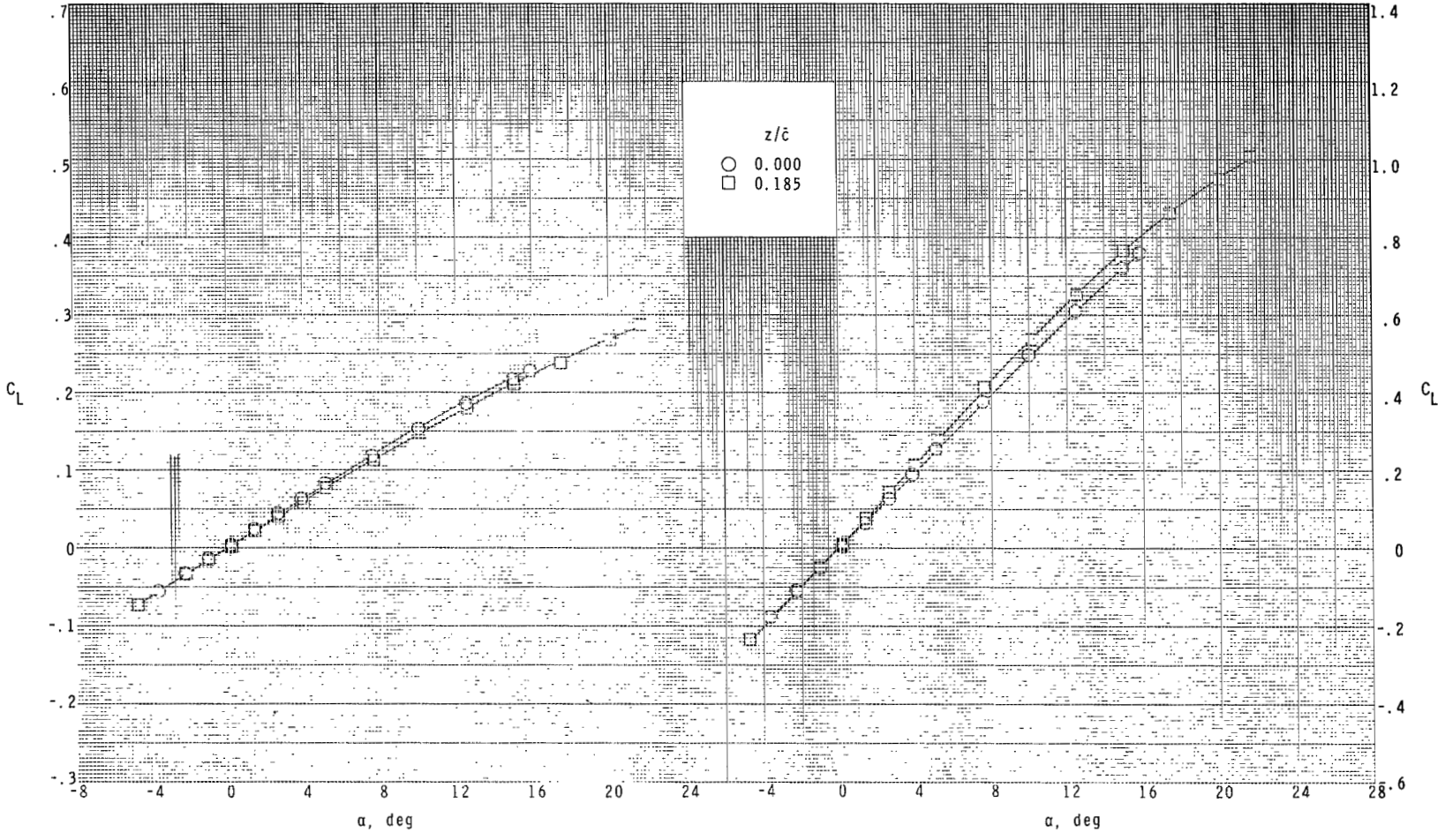

(b) $S_c/S_w = 0.240$.

Figure 13.- Continued.

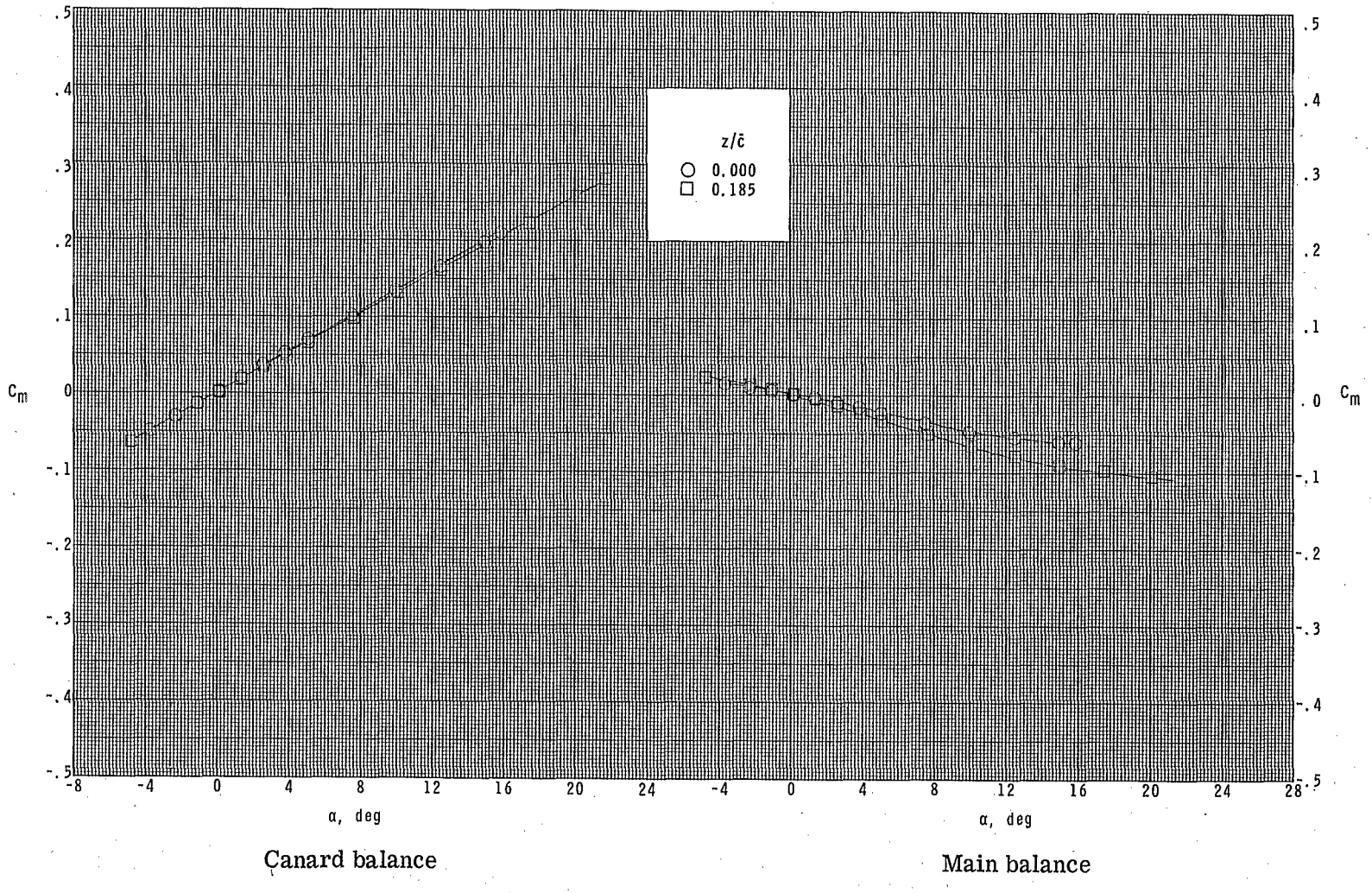

(b) Concluded.

Figure 13.- Continued.

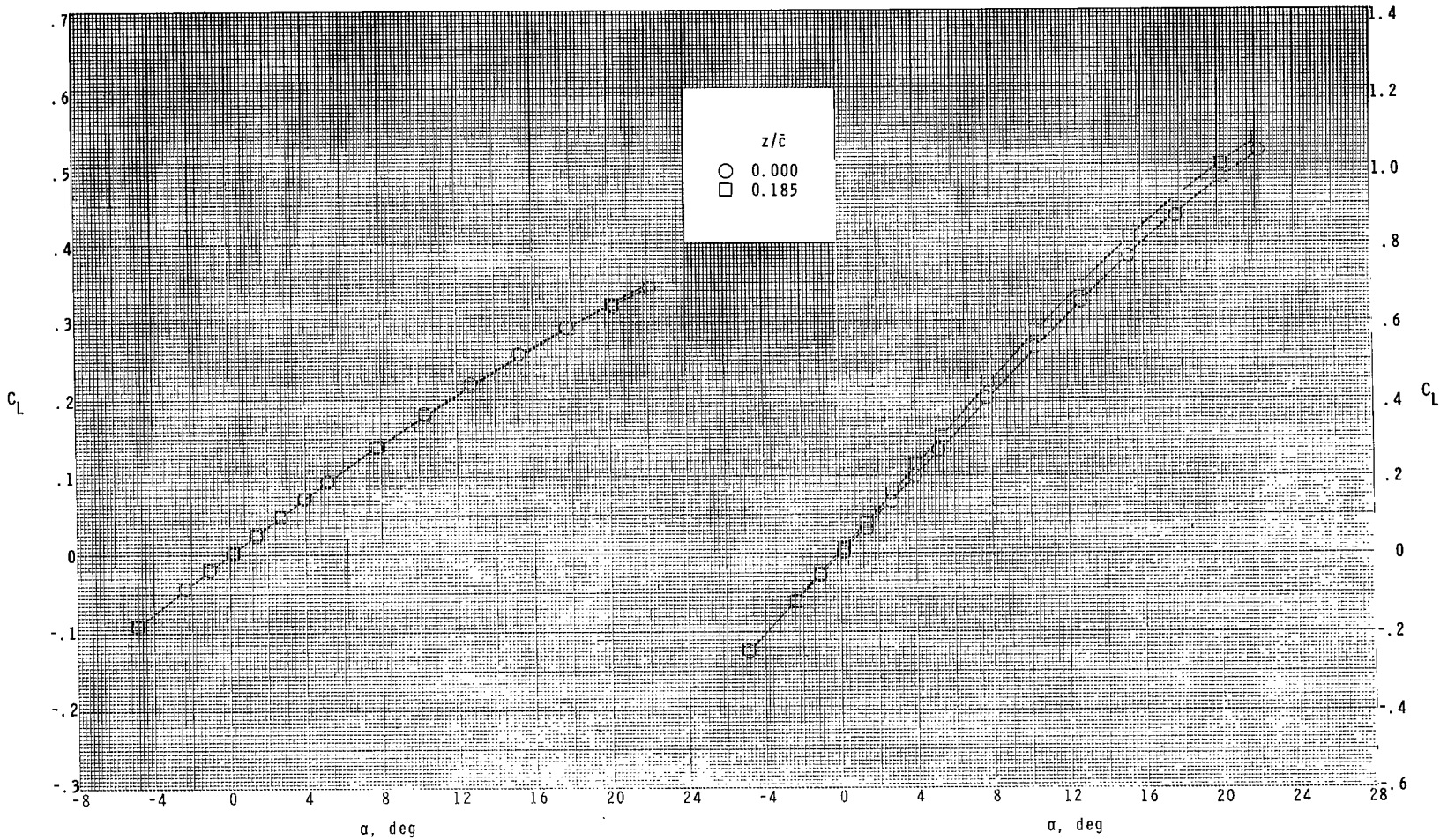

(c) $S_c/S_w = 0.300$.

Figure 13.- Continued.

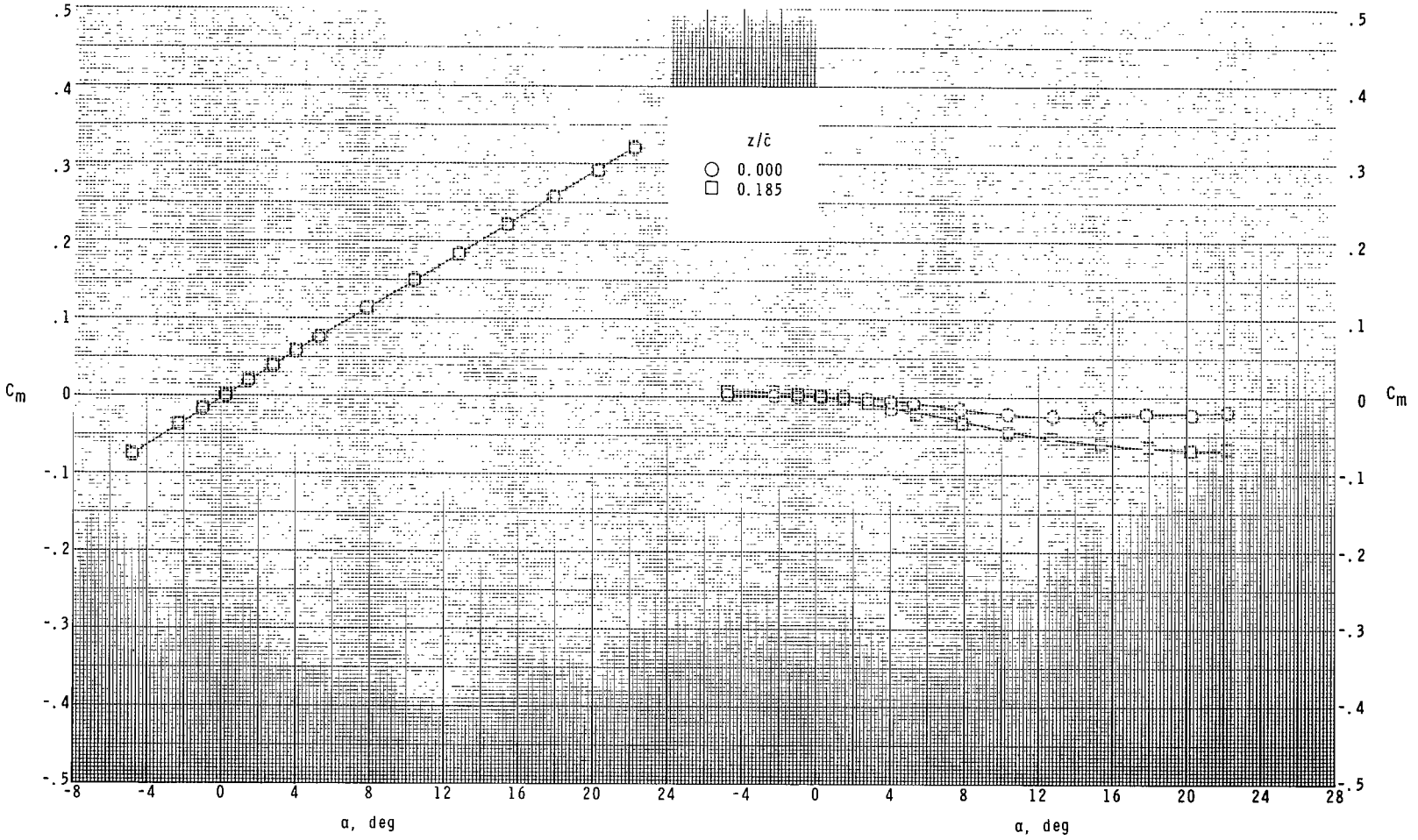

(c) Concluded.

Figure 13.- Concluded.

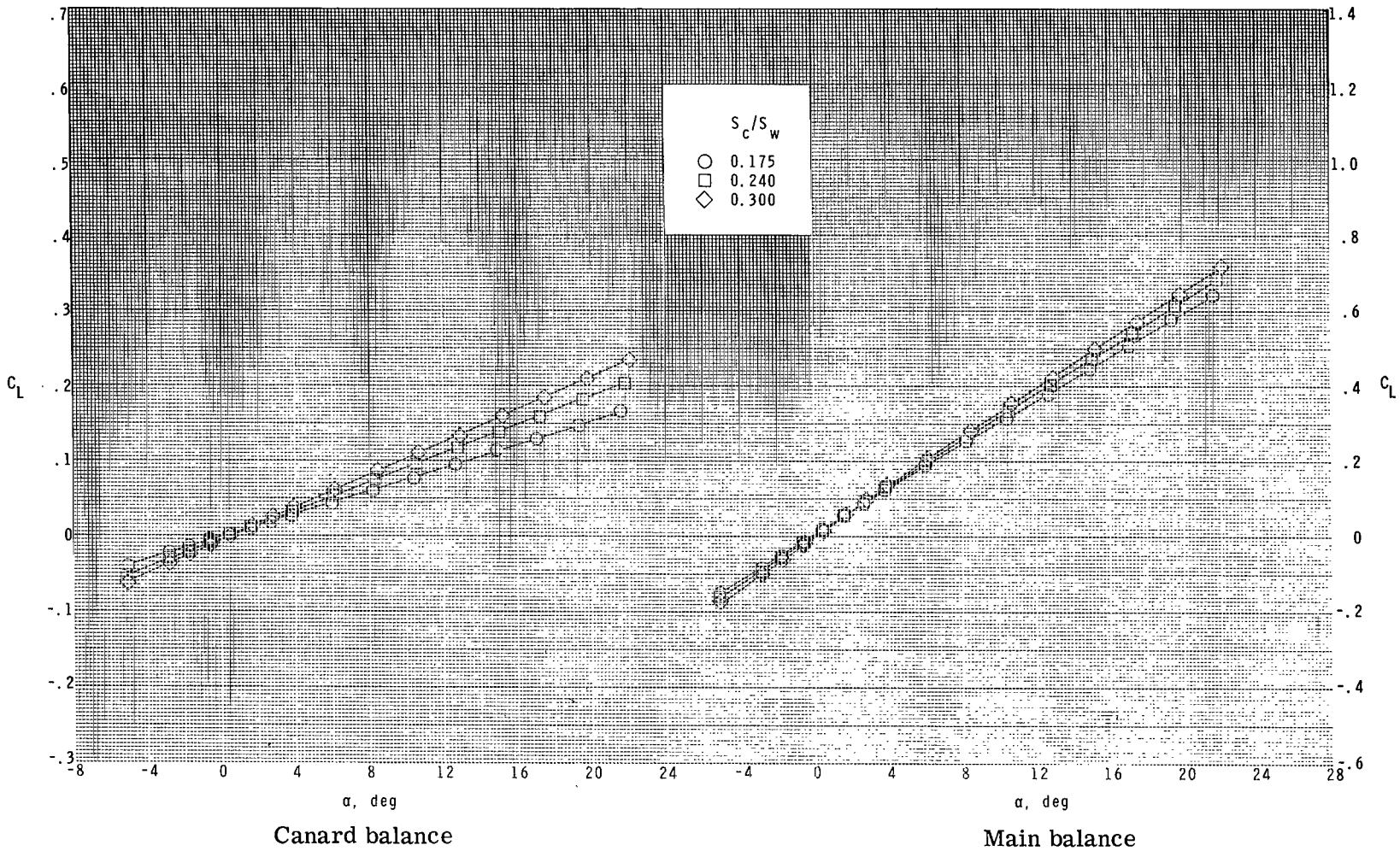

(a) $z/\bar{c} = 0.0$.

Figure 14.- Effect of canard size $(\delta_c = 0^o)$ and vertical position on lift and pitching moment of canard section and total configuration at M = 2.86.

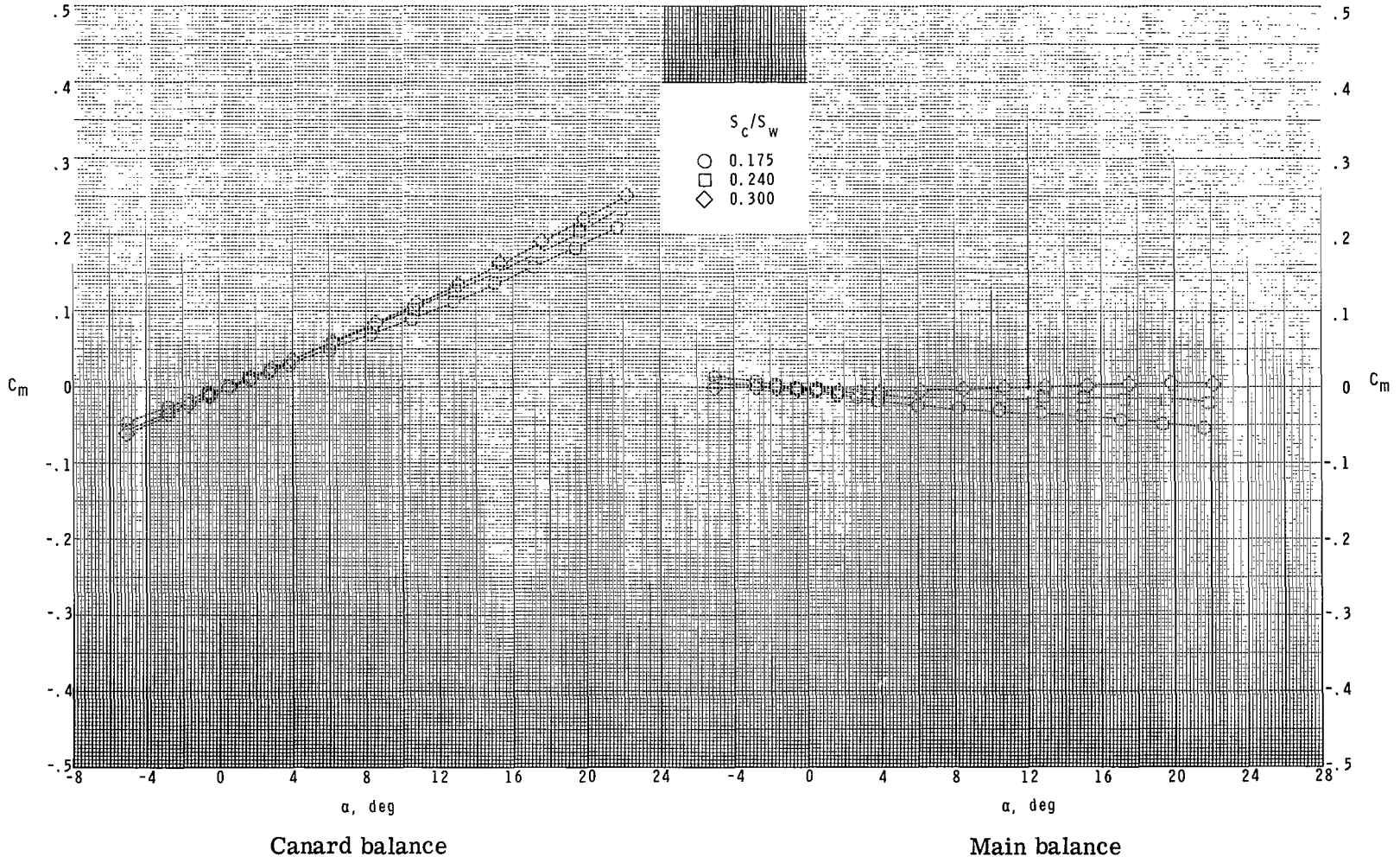

(a) Concluded.

Figure 14.- Continued.

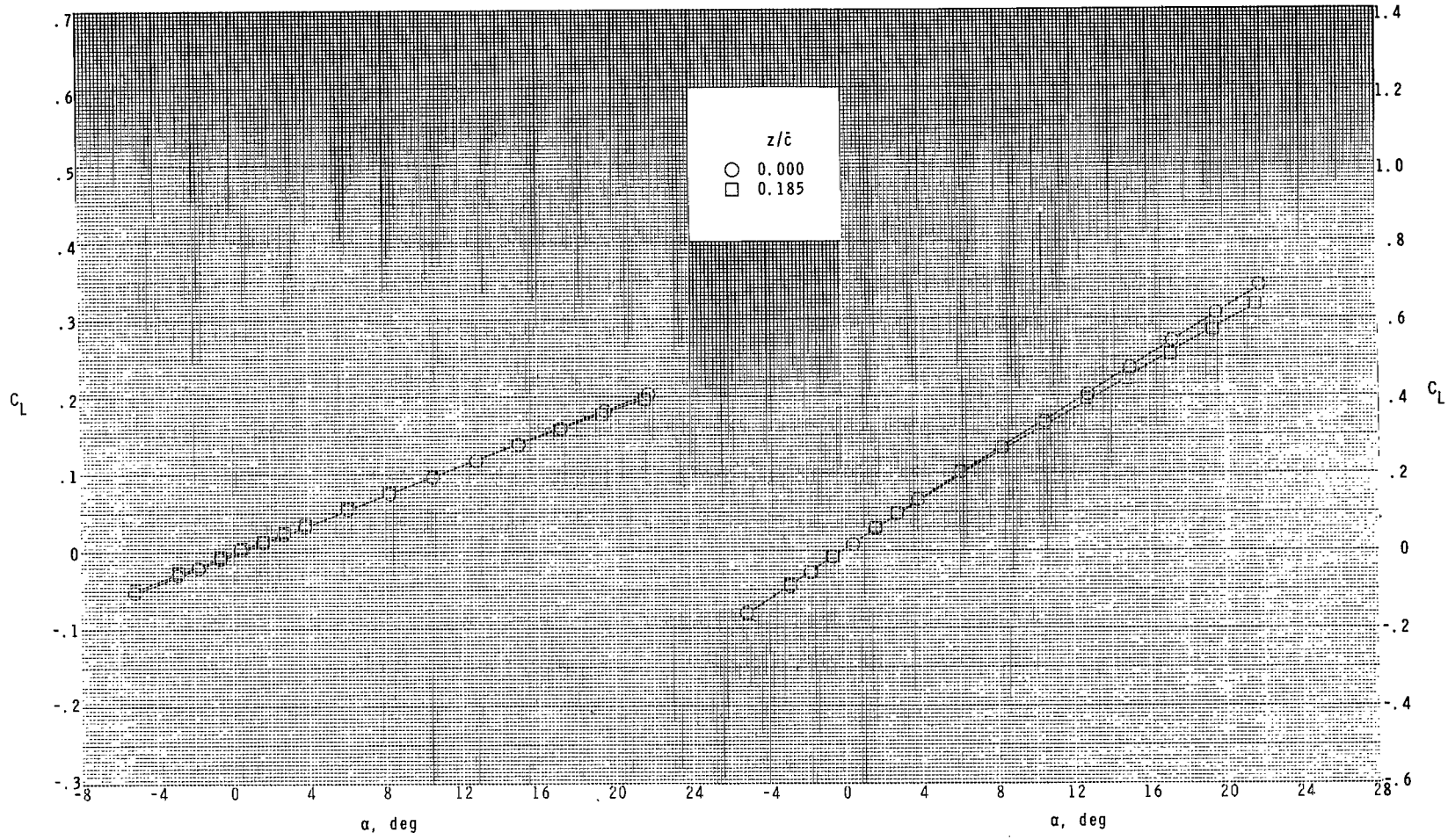

Canard balance

Main balance

(b) $S_c/S_w = 0.240$.

Figure 14.- Continued.

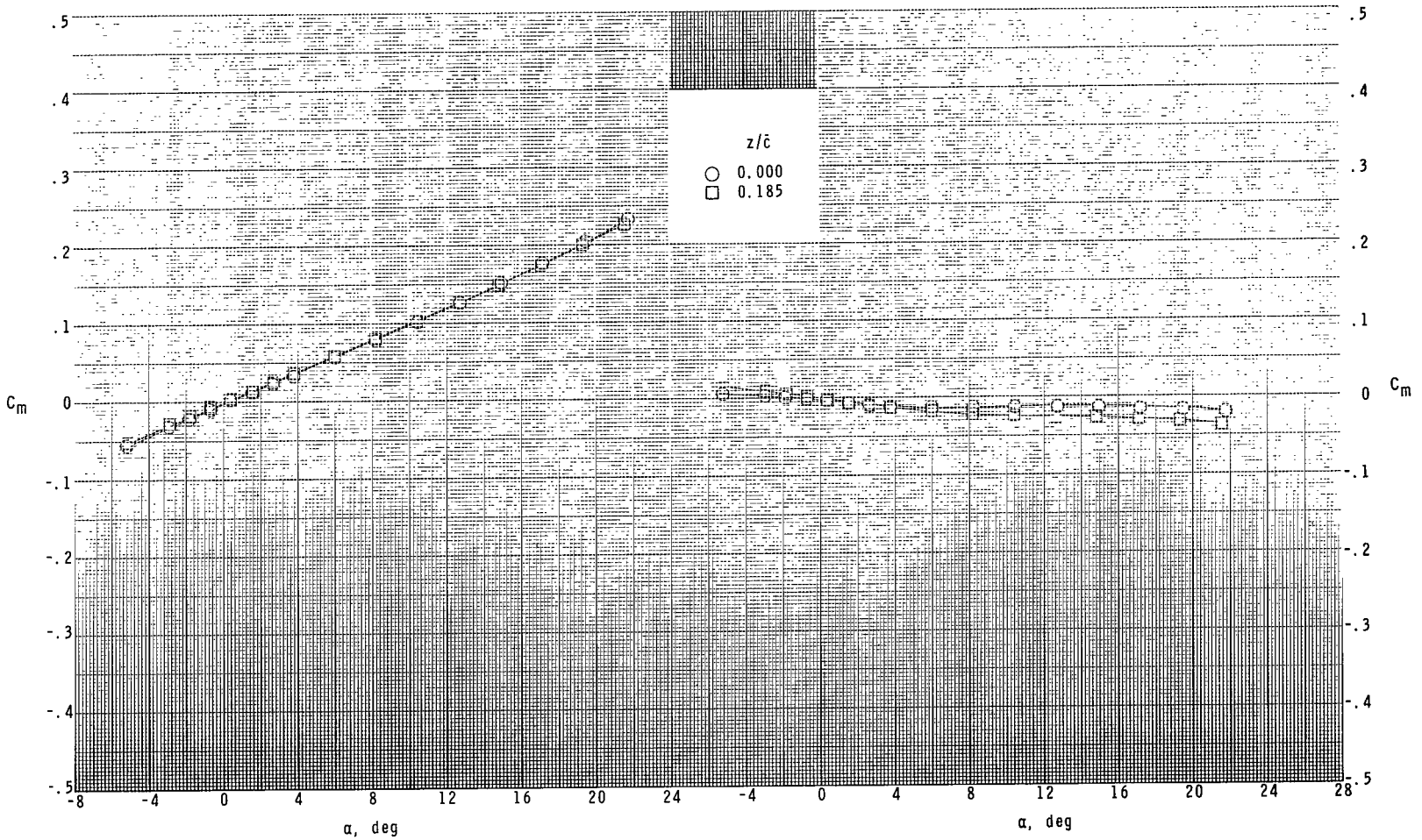

(b) Concluded.

Figure 14.- Continued.

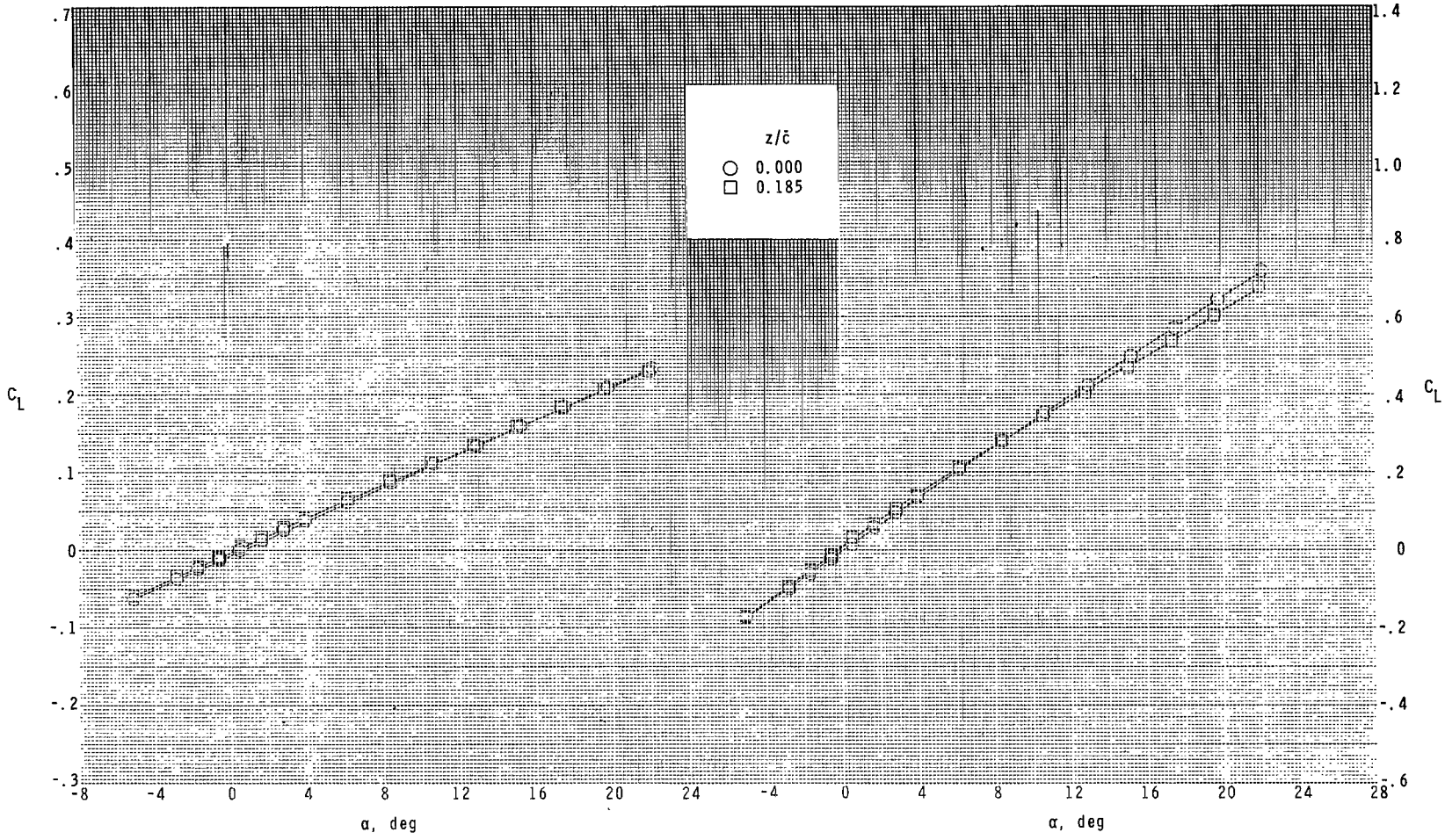

Canard balance

Main balance

(c) $S_C/S_W = 0.300$.

Figure 14.- Continued.

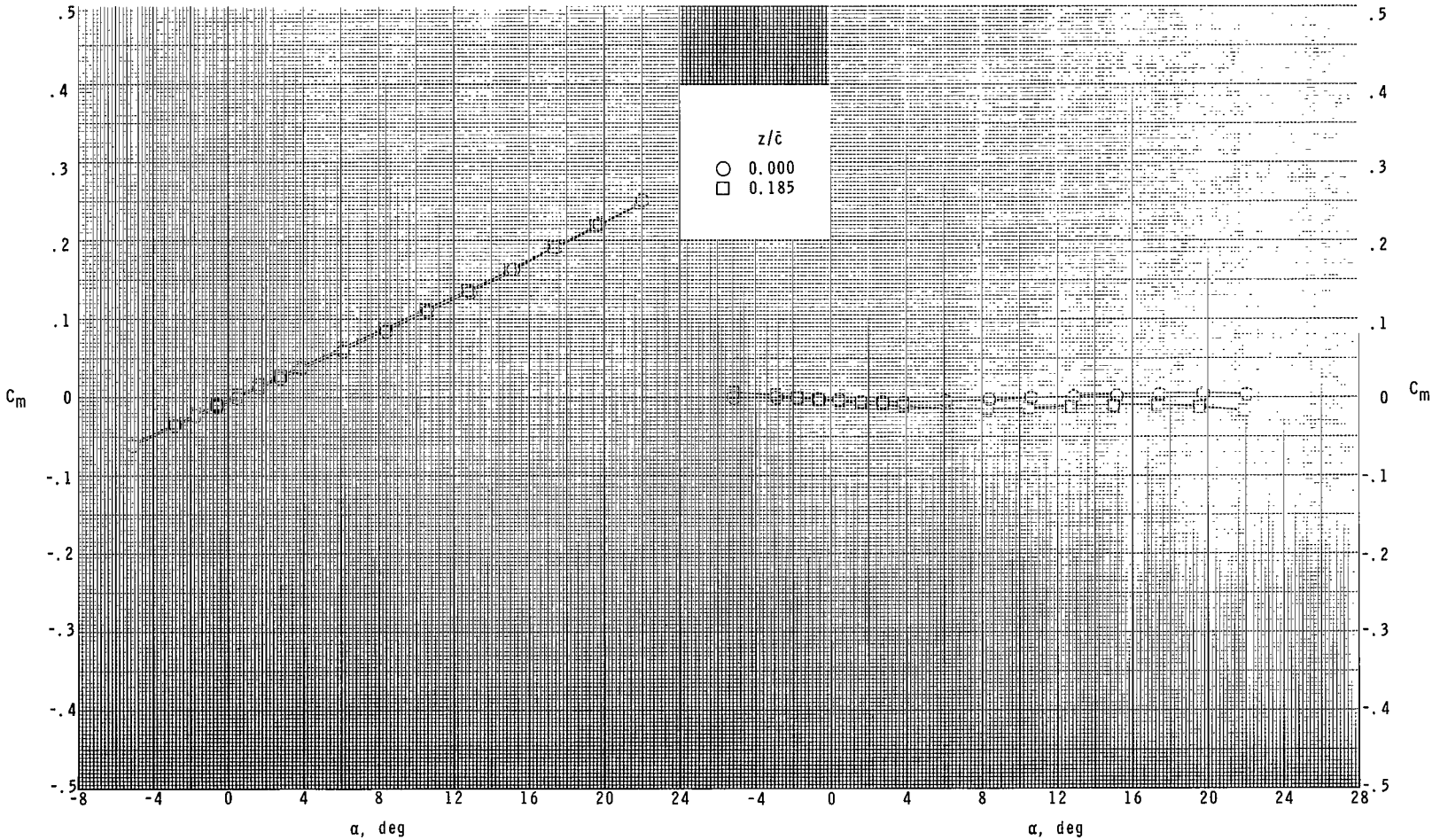

(c) Concluded.

Figure 14.- Concluded.

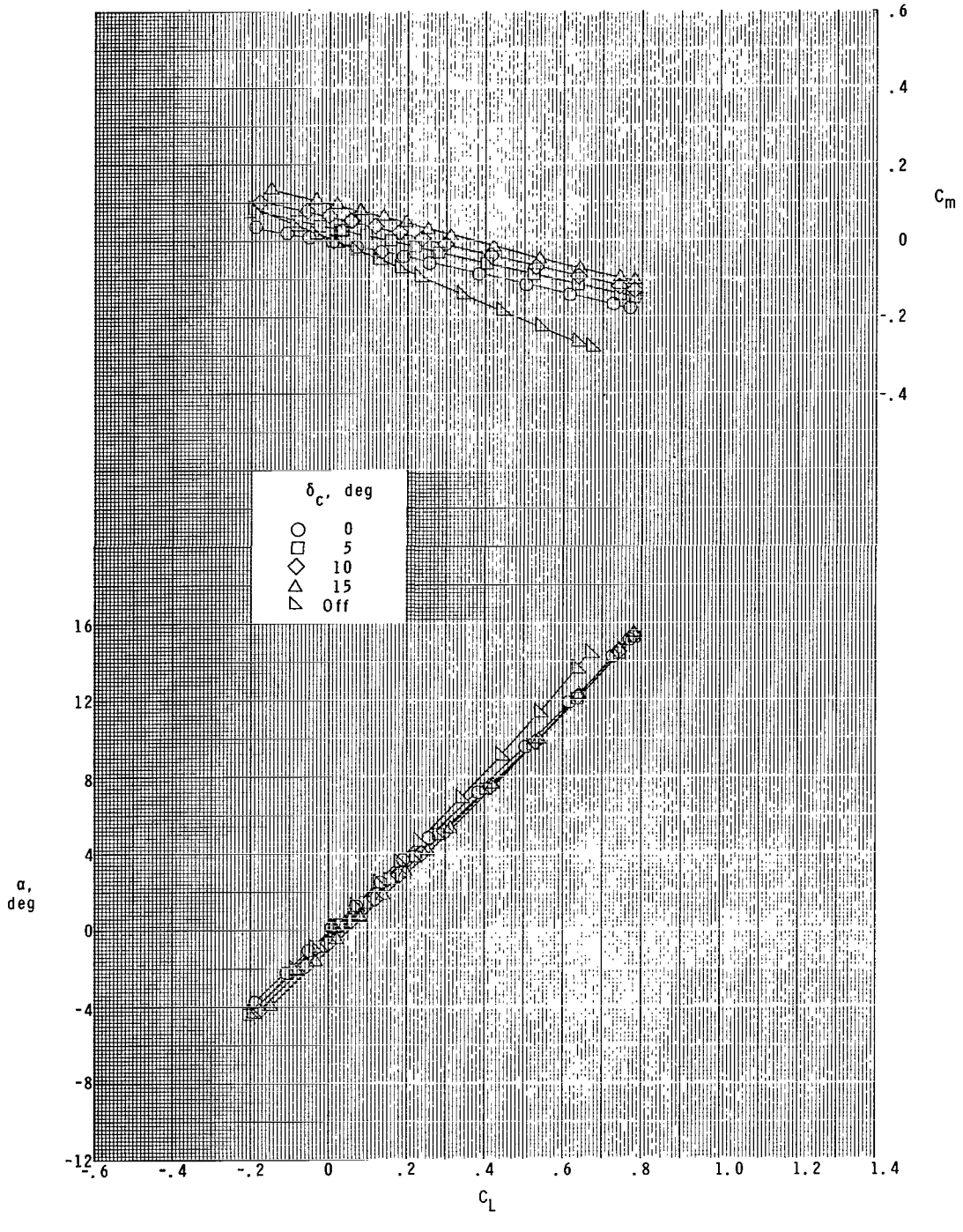

(a) M = 1.60.

Figure 15.- Longitudinal aerodynamic characteristics for 44° wing, $S_c/S_w = 0.175$, and $z/\bar{c} = 0.0$.

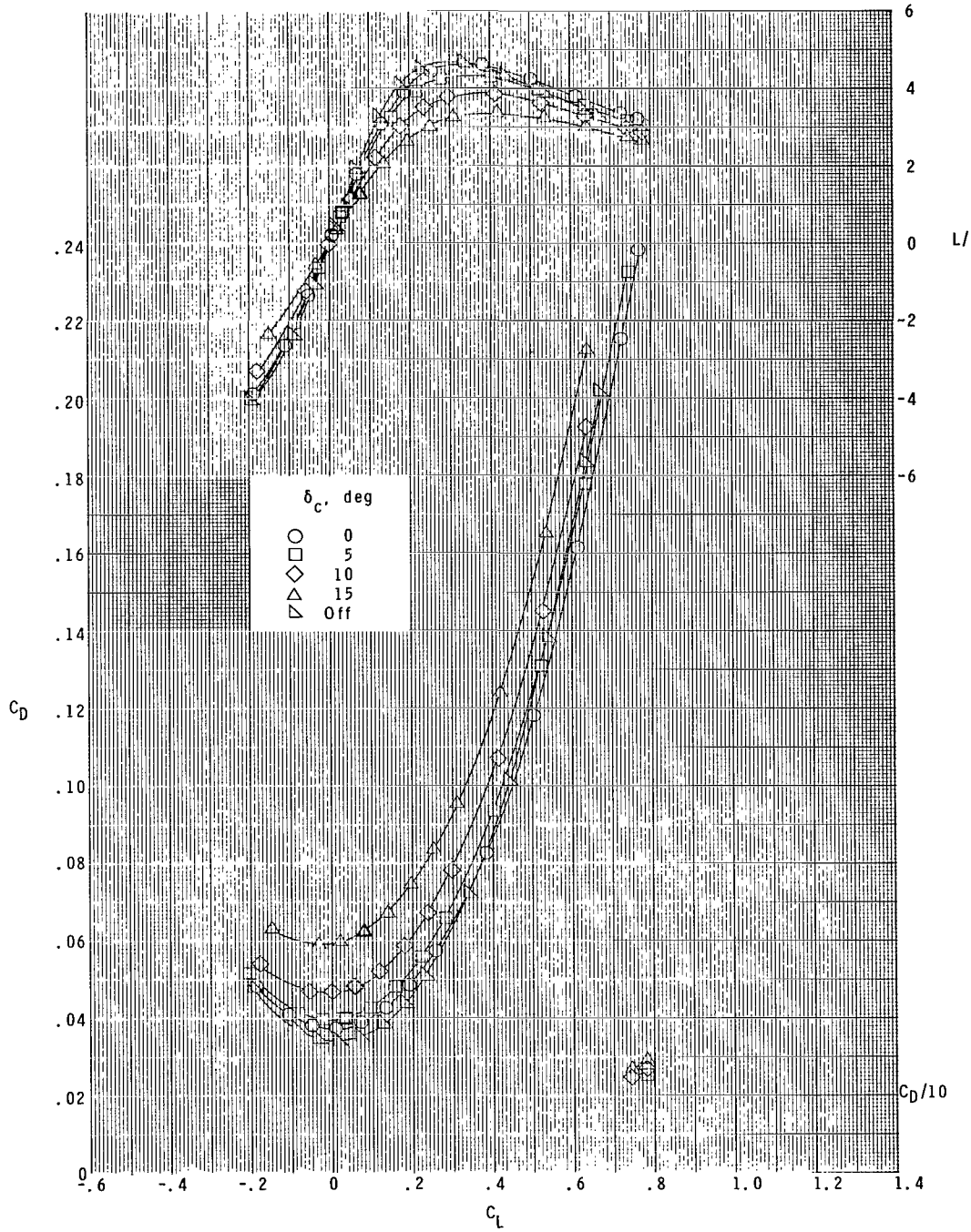

(a) Concluded.

Figure 15.- Continued.

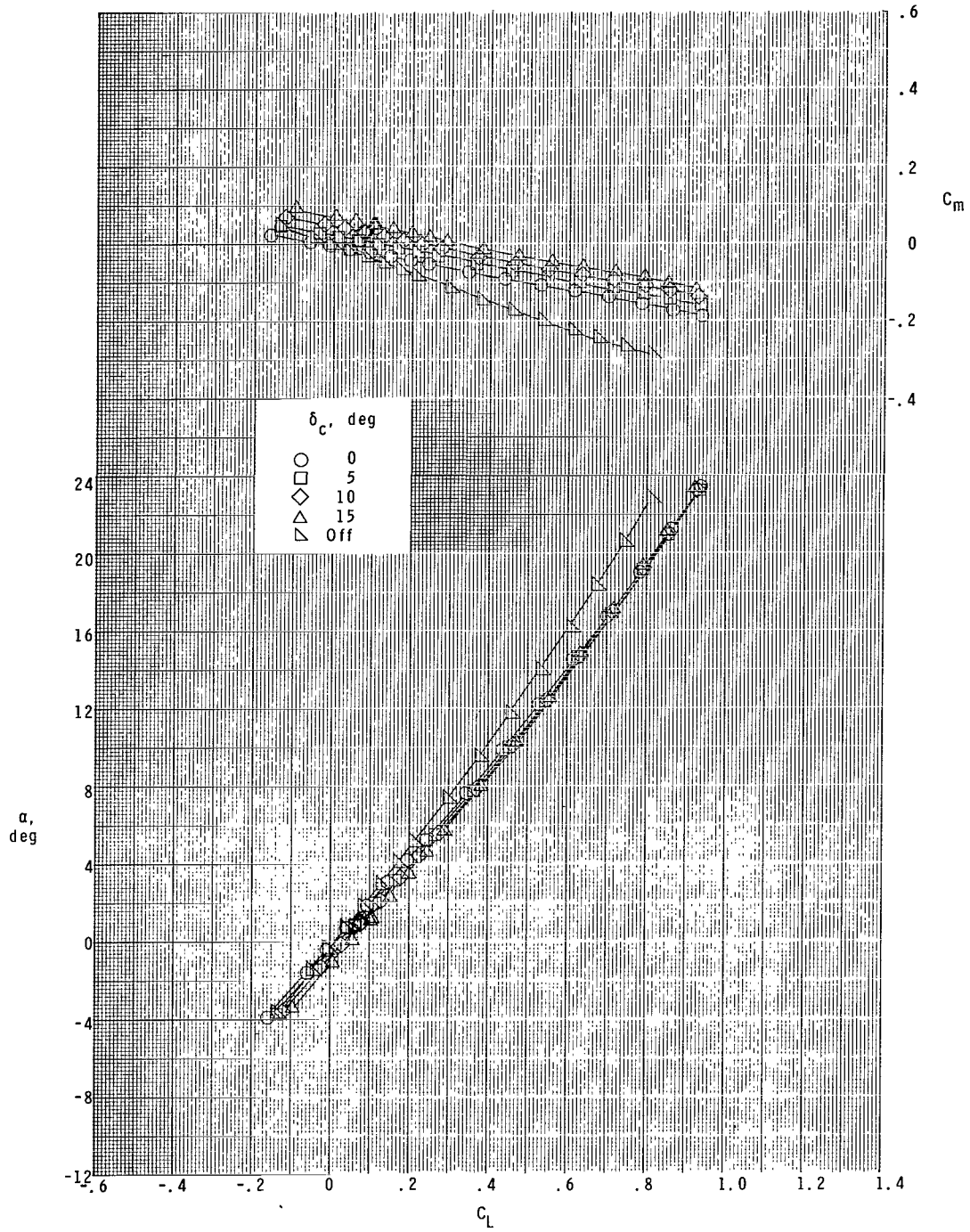

(b) M = 2.00.

Figure 15.- Continued.

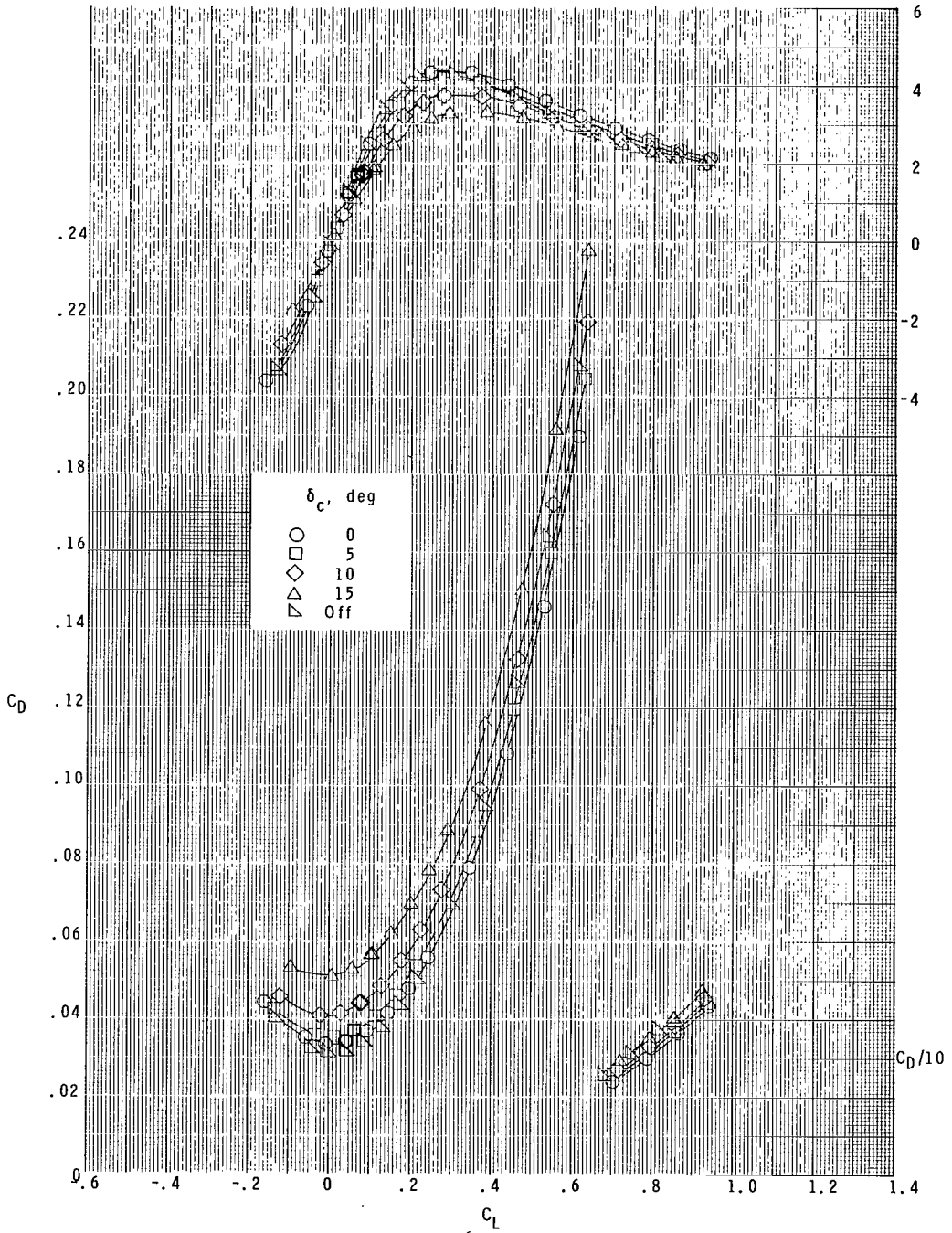

(b) Concluded.

Figure 15.- Concluded.

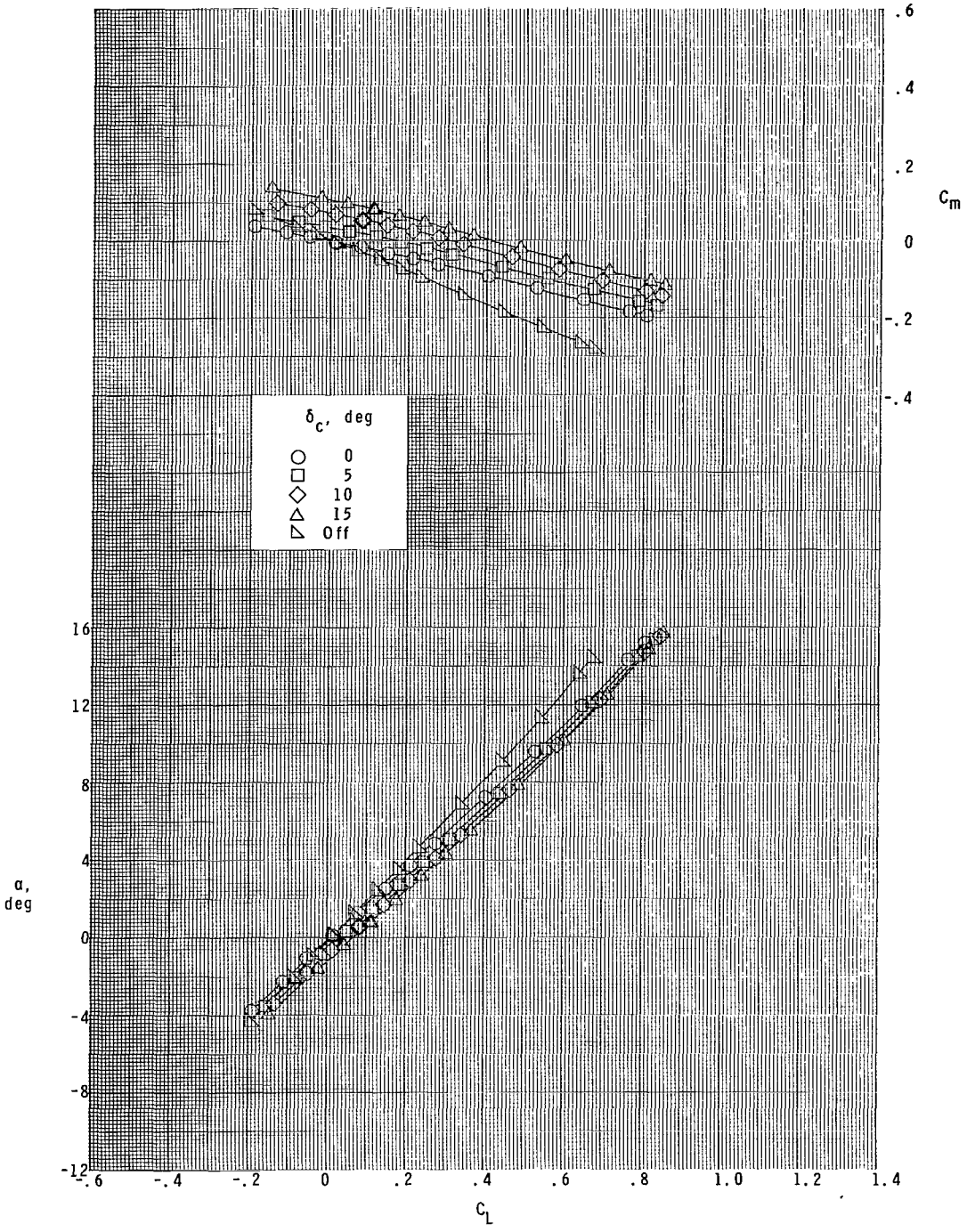

(a) M = 1.60.

Figure 16.- Longitudinal aerodynamic characteristics for 44° wing, $S_c/S_w = 0.175$, and $z/\bar{c} = 0.185$.

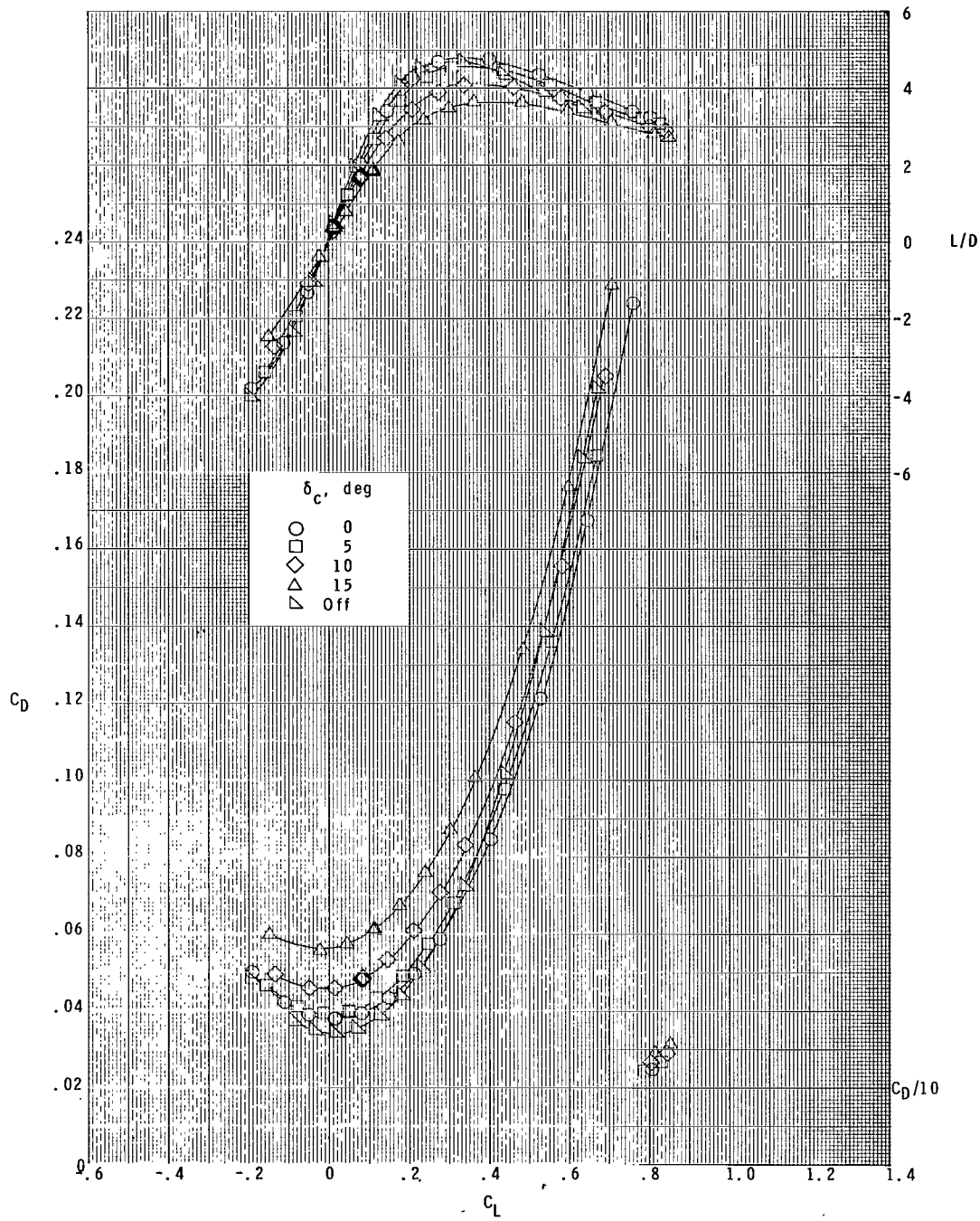

(a) Concluded.

Figure 16.- Continued.

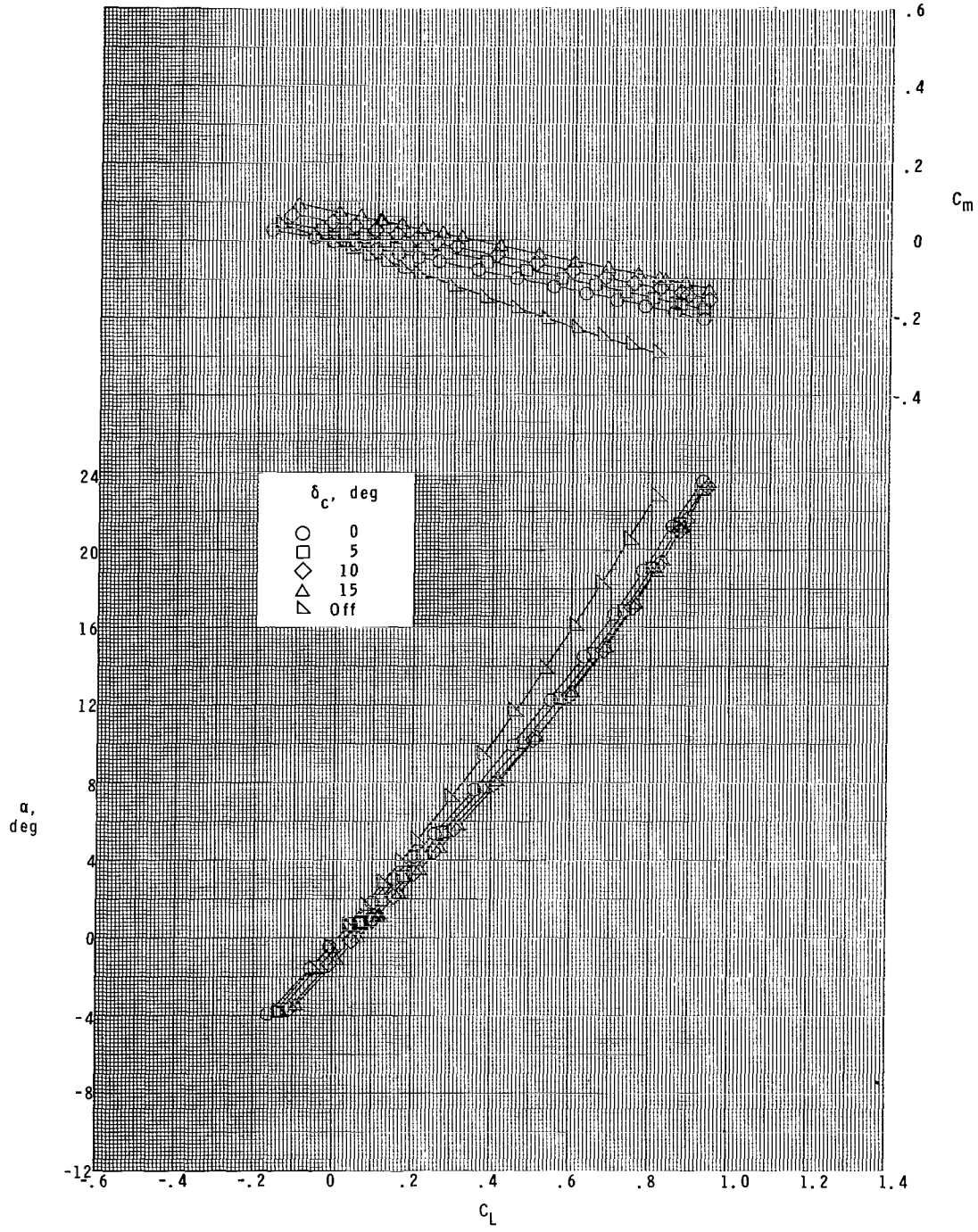

(b) M = 2.00.

Figure 16.- Continued.

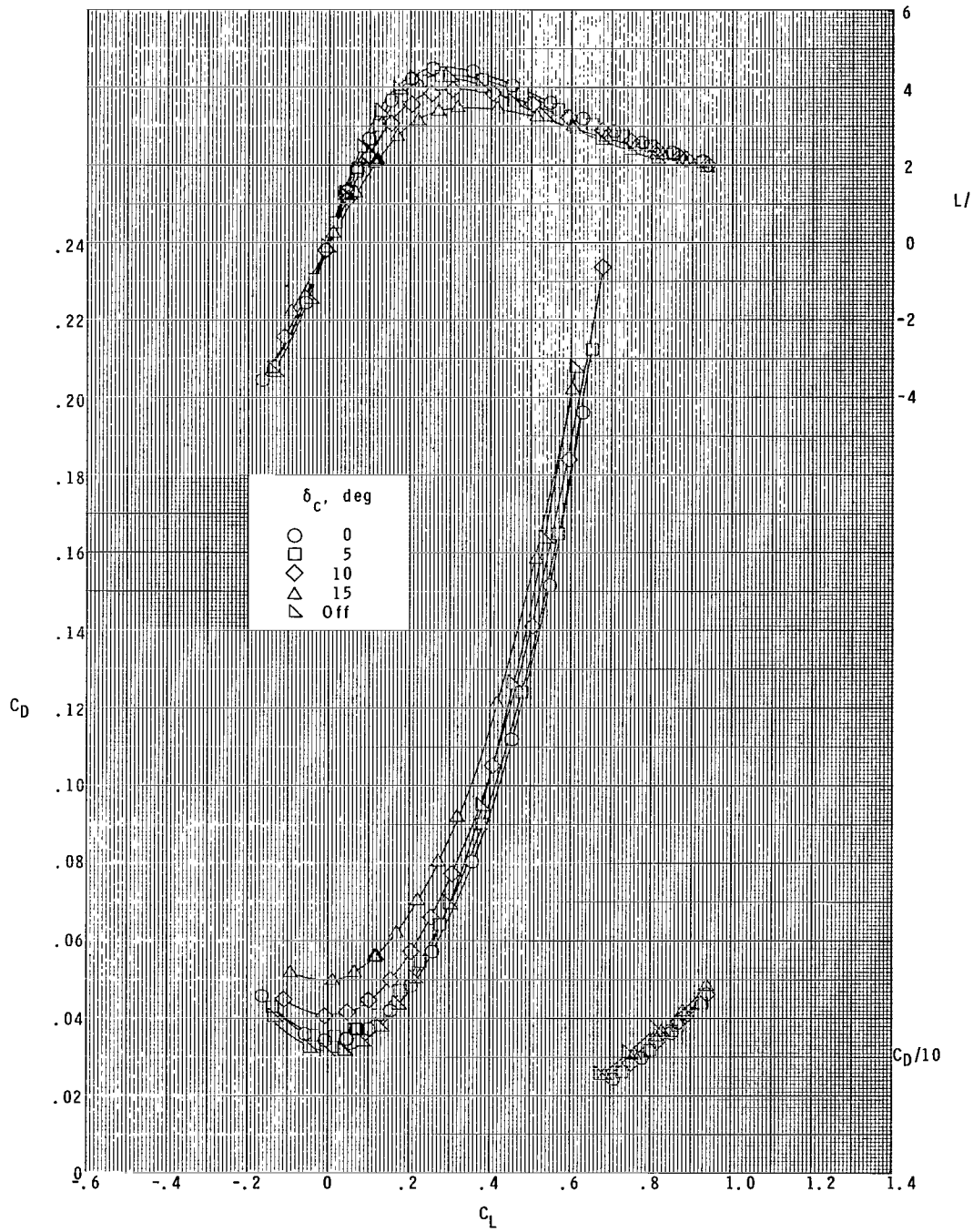

(b) Concluded.

Figure 16.- Concluded.

"The aeronautical and space activities of the United States shall be conducted so as to contribute . . . to the expansion of human knowledge of phenomena in the atmosphere and space. The Administration shall provide for the widest practicable and appropriate dissemination of information concerning its activities and the results thereof."

—NATIONAL AERONAUTICS AND SPACE ACT OF 1958

NASA SCIENTIFIC AND TECHNICAL PUBLICATIONS

TECHNICAL REPORTS: Scientific and technical information considered important, complete, and a lasting contribution to existing knowledge.

TECHNICAL NOTES: Information less broad in scope but nevertheless of importance as a contribution to existing knowledge.

TECHNICAL MEMORANDUMS: Information receiving limited distribution because of preliminary data, security classification, or other reasons.

CONTRACTOR REPORTS: Scientific and technical information generated under a NASA contract or grant and considered an important contribution to existing knowledge.

TECHNICAL TRANSLATIONS: Information published in a foreign language considered to merit NASA distribution in English.

SPECIAL PUBLICATIONS: Information derived from or of value to NASA activities. Publications include conference proceedings, monographs, data compilations, handbooks, sourcebooks, and special bibliographies.

TECHNOLOGY UTILIZATION PUBLICATIONS: Information on technology used by NASA that may be of particular interest in commercial and other non-aerospace applications. Publications include Tech Briefs, Technology Utilization Reports and Technology Surveys.

Details on the availability of these publications may be obtained from:

SCIENTIFIC AND TECHNICAL INFORMATION OFFICE

NATIONAL AERONAUTICS AND SPACE ADMINISTRATION

Washington, D.C. 20546